

Published in final edited form as:  
*J Org Chem.* 2011 June 3; 76(11): 4221–4259. doi:10.1021/jo2003693.

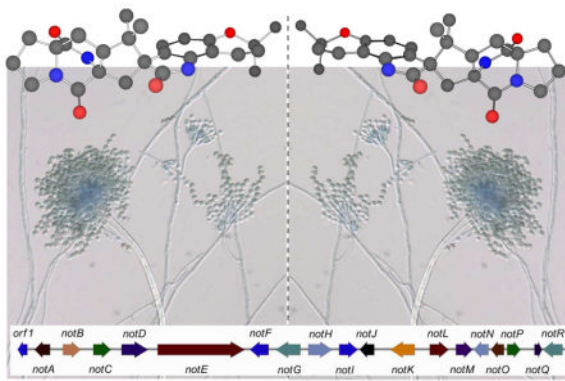
## Natural Products Synthesis: Enabling Tools to Penetrate Nature's Secrets of Biogenesis and Biomechanism†

**Robert M. Williams**

Department of Chemistry, Colorado State University, Fort Collins, Colorado 80523

Robert M. Williams: rmw@lamar.colostate.edu

### Abstract



Selected examples from our laboratory of how synthetic technology platforms developed for the total synthesis of several disparate families of natural products was harnessed to penetrate biomechanistic and/or biosynthetic queries is discussed. Unexpected discoveries of biomechanistic reactivity and/or penetrating the biogenesis of naturally occurring substances were made possible through access to substances available only through chemical synthesis. Hypothesis-driven total synthesis programs are emerging as very useful conceptual templates for penetrating and exploiting the inherent reactivity of biologically active natural substances. In many instances, new enabling synthetic technologies were required to be developed. The examples demonstrate the often un-tapped richness of complex molecule synthesis to provide powerful tools to understand, manipulate and exploit Nature's vast and creative palette of secondary metabolites.

### Introduction

Natural products have constituted a resplendent source of chemical value to medicine, both modern and traditional, as well as providing a seemingly limitless supply of challenging structures for the synthetic chemist. Natural products have been one of the main drivers for the development of modern asymmetric methodology and has been used as a testing ground for ever more innovative strategies and concepts for complex molecule synthesis. Many practitioners of the art of total synthesis have limited their often breath-taking conquest of a natural product, to assembly of the single natural substance itself and have rarely harnessed the power of the total synthesis technology platform they have labored to develop, for penetrating the mode of action of biologically natural products and/or the biogenesis of the

†This paper is dedicated to Professor Ei-ichi Negishi, Professor Yoshito Kishi and the late Professor R.B. Woodward for their extraordinarily high standards of scientific excellence and for invaluable mentoring.

natural compound or the larger family of natural agents to which it belongs. Our laboratory has long held an interest in how biologically active natural substances exert their effects in living systems and also how Nature constructs these beautiful and complex materials. In this Perspective, we will show examples selected from our laboratory, of how total synthesis platforms can be exploited to penetrate some of Nature's closely guarded secrets of molecular construction and molecular action.

### I. Bicyclomycin

Our first foray into natural products total synthesis was the *Streptomyces* sp. metabolite bicyclomycin (bicozamycin).<sup>1</sup> We devised an electrophilic glycine species (**1**) that was used to address the installation of the branched isoleucine bridge constituting the bicyclo[4.2.2]diazadecane ring system.<sup>2</sup> Conversion of lactone **3** into the bicyclic substrate **4** was followed by regioselective bridgehead carbanion oxidation and double diastereodifferentiating aldol condensation. The overall synthesis constituted just twelve steps from commercially available glycine anhydride.

Bicyclomycin represented a structurally new class of antimicrobial agent and its mechanism of action was later elucidated by Widger and co-workers in an extensive series of publications to act on the ATP-dependent motor protein Rho.<sup>3</sup>

At the time, it was known that the *exo*-methylene moiety was essential for antimicrobial activity<sup>[ref]</sup> and we wondered whether the *exo*-methylene and adjacent carbinolamine could participate in the formation of a highly electrophilic pyruvamide system (**10**, Scheme 2).

Iseki and co-workers at Fujisawa first demonstrated that thiols added irreversibly to the *exo*-methylene moiety to provide the thiol-addition species **11** with the bicyclo[4.2.2] core structure intact;<sup>4</sup> a process whose mechanism was first proposed and studied by our laboratory.<sup>5</sup> Kohn and co-workers subsequently discovered that, depending on the pH of the medium, different thiol-addition products were produced including an interesting Claisen rearrangement product **13**.<sup>6</sup> Based on the interesting and novel chemical (and later, biochemical) reactivity of bicyclomycin that was emerging, we wondered if the bridging ether oxygen atom was obligatory for antimicrobial activity or was a spectator atom (Figure 1).

This turned out to be the first instance where we attempted to harness the total synthesis technology platform we had developed to construct the natural product, to prepare a single analog ("carba"bicyclomycin).<sup>7</sup> The objective was to answer the question concerning the relevance of the bridging ether oxygen atom as, two of the three thiol-addition structures discovered by Kohn, et al.,<sup>6</sup> require participation of that oxygen atom. As shown in Scheme 3, we developed a rather unique solution to constructing the bicyclo[4.2.2] ring structure by deploying a 2,3-Wittig ring-contraction (**15** to **16**). Bridgehead carbanion generation from **17** and double-diastereodifferentiating aldol condensation and deprotection, furnished "carba"bicyclomycin. While still reactive with respect to thiolate addition to the *exo*-methylene moiety, this compound turned out to lack antimicrobial activity and clearly indicated the structural requirement for the bridging oxygen atom.<sup>8</sup> This type of interrogation became a major thematic paradigm in our laboratory to the present time. In other words, we sought to extract maximum value from developing a total synthesis platform by exploiting that powerful synthetic technology to prepare mechanistically-inspired analogs as mechanistic probes.

### II. Prenylated Indole Alkaloids

An out-growth of attempts to make more reactive latent Michael-type acceptors based on the bicyclomycin structure, we had prepared the bicyclo[2.2.2]diazaoctane system **23** via the

intramolecular enolate-epoxide ring-opening reaction shown in Scheme 4.<sup>9</sup> We were aware of the existence of the brevianamides, isolated by Arthur Birch in the late 1960's,<sup>10</sup> and decided to devise methodology to construct the bicyclo[2.2.2]diazaoctane core of the brevianamides. The first foray, was a non-stereocontrolled intramolecular Michael addition on system **25**,<sup>11</sup> which led us to develop a stereocontrolled intramolecular S<sub>N</sub>2' cyclization reaction (Scheme 5) that culminated in the first asymmetric synthesis of brevianamide B;<sup>12</sup> a minor metabolite of *Penicillium brevicompactum*.

Right around the time we initiated studies on the synthesis of brevianamides A and B, new members of what has become an enormous family of prenylated indole alkaloids from various genera of fungi, the structures of the paraherquamides<sup>13</sup> and marcfortines<sup>14</sup> were published. A “unified” retrosynthesis was devised to accommodate the differences in relative stereochemistry at the bridging isoprene-derived stereogenic center between the brevianamides and paraherquamides. The goal was to selectively access the two possible reactive rotamers (*endo* and *exo*) for the intramolecular S<sub>N</sub>2' cyclization reaction. This process would install an isopropenyl residue that could then participate in an olefin-cation cyclization to give the generalized 2,3-disubstituted indole. Chemo-selective oxidation of 2,3-disubstituted indoles was well known in the literature to furnish either the *spiro*-ψ-indoxyl of the brevianamides or the *spiro*-oxindole of the paraherquamides.

The brevianamide project turned out to be a fortuitous choice, as we stumbled on a surprising discovery regarding the absolute stereochemistry of this natural product, which in turn led us into the larger field of secondary metabolite biosynthesis.

It was found that the diastereofacial selectivity of the intramolecular S<sub>N</sub>2' cyclization reaction could be exquisitely controlled to provide the *syn*-relative stereochemistry (paraherquamides) by running the reaction in a poorly coordinating solvent such as benzene, which we suggested proceeded *via* a closed transition state shown in Scheme 6.<sup>12</sup> The diastereoselectivity could be reversed to favor the corresponding *anti*- stereochemistry, by the addition of a “mismatched” crown ether and selectivities as high as 10:1 favoring the anti-isomer were observed.

The asymmetric synthesis of (−)-brevianamide B was completed by this approach as summarized in Scheme 7. The intramolecular S<sub>N</sub>2' reaction proved effective in delivering the desired *anti*-diastereomer in up to a 4.9:1 ratio. The planned olefin-cation cyclization worked smoothly and the peracid oxidation of the 2,3-disubstituted indole was entirely diastereoselective giving a single 3-(S)-hydroxindolenine that rearranged smoothly to the corresponding *spiro*-indoxyl. We encountered significant difficulty in removing the *N*-*para*-methoxybenzyl group and eventually found that formation of the dipole-stabilized benzylic carbanion, generated through treatment with excess *t*-butyl lithium and quenching with molecular oxygen, effected the removal of this difficult to cleave protecting residue.

When the synthesis was completed, attempts to obtain an authentic sample of (−)-brevianamide B from Prof. Birch and other labs that had isolated the natural compound, were fruitless. On the other hand, the major metabolite, (+)-brevianamide A, whose absolute configuration was established by X-ray crystallographic analysis,<sup>10i</sup> was made available. Prof. Birch had reported the semi-synthetic conversion of brevianamide A into brevianamide B by a redox process which we followed to obtain an authentic sample of (−)-brevianamide B.<sup>[10c]</sup>

The semi-synthetic and totally synthetic samples of (−)-brevianamide B proved identical by all spectroscopic methods and had *the same sign and magnitude of optical rotation* revealing that these substances possessed the same absolute configuration. Due to the initial difficulty we encountered in locating a sample of brevianamide B, our laboratory endeavored to

acquire cultures of *Penicillium brevicompactum* which were grown and harvested to provide natural brevianamide A (the major metabolite) and a small amount of natural brevianamide B. Much to our surprise, the absolute configuration of the natural brevianamide B turned out to be the (+)-enantiomer, and was thus antipodal to the semi-synthetic material. This clearly revealed that Nature had constructed these two diastereomeric natural substances in two enantiomorphic forms (Scheme 8). This discovery was quite fascinating to us and drew us to ponder how the two pseudo-enantiomeric brevianamides arose in Nature. We also learned a very powerful lesson from this exercise: namely, that had we not endeavored to isolate the natural compound ourselves, directly from the producing organism, we would have never stumbled on the puzzling absolute stereochemical differences between brevianamides A and B. This accidental discovery drew us irresistibly into learning the origin of this enantio-divergent biogenesis.

In 1970, Porter and Sammes were the first to speculate on the biogenetic origin of the bicyclo[2.2.2]diazaoctane ring system of brevianamides A and B, wherein the intramolecular Diels-Alder reaction of the reverse-prenylated indole-derived azadiene was invoked (Figure 2).<sup>15</sup> Interestingly, Birch later proposed an alternative biogenesis invoking the intermediacy of an epidithiapiperazinedione species.<sup>16</sup>

Birch then carried out radio-labeled precursor incorporation experiments in *Penicillium brevicompactum* and demonstrated that *cyclo-L-Trp-L-Pro* (brevianamide F) was incorporated intact into brevianamide A.<sup>17</sup> Based on this important result, he suggested that brevianamide F was reverse-prenylated to deoxybrevianamide E, which in turn was oxidized and cyclized to give brevianamides A and B.

Combining the results from Birch and considering the Sammes IMDA biogenetic proposal,<sup>15</sup> we suggested the modified biogenetic pathway shown in Scheme 9, wherein the azadiene species is *achiral*, which should give rise (in the absence of enzyme mediation) to a *racemic* Diels-Alder product. Inferring the presence of an *R*-selective indole oxidase, the presumed racemic intermediate would be converted into two optically pure, diastereomeric 3*R*hydroxyindolenines, suffering a Pinacol-type rearrangement that would give the observed natural substances (−)-brevianamide A and (+)-brevianamide B. As our synthesis passed through the presumed hexacyclic Diels-Alder adduct **42**, our total synthesis platform provided us with the tools to probe this interesting stereochemical puzzle. To interrogate this biogenetic pathway, we had to (ironically) adapt our asymmetric synthesis to prepare isotopically labeled, *racemic* cycloadduct **42** and determine if this was a biosynthetic precursor to the brevianamides. This was accomplished and the requisite racemic, authentic <sup>13</sup>C-labeled cycloadduct **42** was used as a reference standard to screen culture extracts for the presence of this species and was also deployed in a precursor incorporation experiment.

Despite how soundly our proposal appeared on paper in terms of accommodating the relative and absolute stereochemistry of these substances, this compound did not incorporate into either brevianamide A or B and we were also unable to detect even a trace of this substance as a natural metabolite (Figure 3).

If hexacycle **42** was not on the pathway to the brevianamides, then what alternative structure was? We then turned our attention to preparing an earlier intermediate, first suggested by Birch,<sup>17</sup> namely deoxybrevianamide E, in radio-labeled form in order to determine if this was indeed the second stage after brevianamide F. We found that synthetic, tritium-labeled deoxybrevianamide E was incorporated in significant radiochemical yield into brevianamide A, B and E in cultures of *P. brevicompactum* (Scheme 10).<sup>18</sup> The presence of brevianamide E suggested that the oxidation of the indole to either the incipient 3-hydroxyindolenine or

the *spiro*-indoxyl, might precede the formation of the bicyclo[2.2.2]diazaoctance ring system. We found that tritium-labeled deoxybrevianamide E, when fed to cultures of *P. brevicompactum* did not incorporate into either brevianamide A or B, revealing that this was a shunt (dead-end) metabolite. We speculated that deoxybrevianamide E was stereoselectively oxidized to the 3-*R*-hydroxyindolenine that could suffer three fates: (1) irreversible ring closure to brevianamide E; (2) Pinacol-type rearrangement to indoxyl **46**; and (3) a second oxidation to an azadiene species followed by IMDA to form the core bicyclo[2.2.2]ring system and final Pinacol-type rearrangement to produce the brevianamides. This alternative biogenetic hypothesis could also account for the observed relative and absolute stereochemistries of brevianamides A and B, and assumed that after setting the *R*-stereogenic center at the stage of hydroxyindolenine **45**, would suffer IMDA cyclization from two of the four possible diastereomeric transition states.

This new biogenetic hypothesis has proven very elusive to secure additional experimental corroboration. We tried in earnest, to prepare the indoxyl **46**, but this compound appears to be unstable, spontaneously suffering a retro-Michael reaction giving the dehydroalanine piperazinedione and the prenylated indoxyl. Some insight into this process was obtained from our collaborator, Prof. Domingo at the University of Valencia, where he performed *ab initio* calculations on the four diastereomeric transition state structures for the putative IMDA reaction of azadiene **47**.<sup>19</sup> This IMDA reaction was found to be controlled by frontier molecular orbitals HOMO<sub>(dieneophile)/LUMO<sub>(azadiene)</sub></sub>. All four diastereomeric transition structures were examined and it was found that the lowest<sub>(rel.)</sub> energy transition structure is TSA which leads to brevianamide A (see Table 1). The next highest energy transition structure is TSB, which lies approximately 6~7 kcal/mol above TSA and leads to brevianamide B. An intramolecular H-bond was found in TSA between the indoxyl N-H and the tryptophyl carbonyl group accounting for a large fraction of the relative stabilization energy. After TSB, the next highest energy transition structures are TSA' and TSB', which would lead to C-19-*epi*-brevianamide A and C-19-*epi*-brevianamide B, respectively. Our lab previously described the total synthesis of C-19-*epi*-brevianamide A and using this authentic specimen, were unable to detect this substance as a metabolite of *Penicillium brevicompactum*.

This theoretical study therefore predicts that the relative distribution of brevianamides A and B from *Penicillium brevicompactum* is a direct manifestation of the relative energies of the four diastereomeric transition structures: brevianamide A is the major metabolite, brevianamide B is a minor metabolite and neither of the C-19-*epi*- structures are found. While this provided some indirect and possibly provocative evidence for biosynthetic events following the hydroxylation of deoxybrevianamide E, it has been less than satisfying in terms of providing insight into the proposed biosynthetic IMDA reaction. We then turned our attention to attempting to validate the azadiene-IMDA construction in the laboratory.

As shown in Scheme 12, we enjoyed early success in generating a protected, yet functional analog of a putative azadiene by the DDQ oxidation of **48** in modest yield. Tautomerization of **49** to the azadiene **50** could be followed easily by nmr, with the IMDA cyclization occurring at or below room temperature providing a ~2:1 ratio of *syn:anti* diastereomers. These were readily separated and were converted into *d, l*-brevianamide B and the corresponding C-19-*epi*-brevianamide B in a few steps.

This study demonstrated that the core 6 ring system common to this family might indeed arise by an intramolecular Diels-Alder cyclization from a pre-formed dioxopiperazine that subsequently undergoes oxidation to an azadiene species. It is significant that the diastereofacial bias of the Diels-Alder cyclization was not strongly affected by solvent. The same ratio of *syn:anti* diastereomers (~2:1) was obtained in THF as in aqueous methanol. As

will be seen below, improved versions of this IMDA reaction were later developed in the context of preparing more complex members of this family of prenylated indole alkaloids.

Before moving to our very recent work on the biomimetic total synthesis and biosynthesis of these substances, the diastereofacially selective intramolecular  $S_N2'$  reaction first developed for the synthesis of brevianamide B (Scheme 7), was successfully applied to the asymmetric total syntheses of (+)-paraherquamide B,<sup>21</sup> (-)-paraherquamide A<sup>22</sup> and stephacidin A.<sup>23</sup> A few key elements of the paraherquamide B and A syntheses are illustrated in Schemes 13 and 14, respectively. A fortuitous feature of the closed transition state manifold for the intramolecular  $S_N2'$  reaction, was the predilection for the *syn*-diastereomer, which is the natural relative stereochemistry for virtually all of the metabolites discovered after the brevianamides. This powerful methodology allowed for the stereocontrolled asymmetric synthesis of three representative members of this family.

Both the paraherquamide A and B syntheses required the construction of the dioxepin ring system, in which the final enol ether alkene was installed in the very last stage of the synthesis. In both instances, the dehydration of the hindered neopentyl-like alcohol was dehydrated with  $(PhO)_3PMeI$  and all other dehydrating reagents examined failed.

The most modern application of the intramolecular  $S_N2'$  cyclization strategy, was to the asymmetric total synthesis of stephacidin A as shown in Scheme 15.<sup>23</sup> For this synthesis, we also developed an improved synthesis of the Seebach<sup>24</sup> asymmetric allylation of proline by employing chloral to make the proline enolate alkylation precursor; a process that has been published as an *Org. Synth.* procedure.<sup>25</sup> This synthesis required seventeen steps overall and proceeded in 5% overall yield from S-proline. As in the other instances, the intramolecular  $S_N2'$  cyclization was completely diastereoselective for the desired *syn*-isomer. Employing modern cross-methathesis methodology<sup>26</sup> to install the enal and several microwave-mediated steps, resulted in a highly efficient synthesis of (-)-stephacidin A following the Wacker-type cyclization of the intramolecular  $S_N2'$  cyclization product.

We also endeavored to transform our totally synthetic (-)-stephacidin A into synthetic (+)-stephacidin B following the elegant path described by Baran for the conversion of stephacidin A into (-)-avravillamide<sup>27</sup> and the subsequent efficient dimerization of (-)-avravillamide to (+)-stephacidin B, first proposed by Qian-Cutrone<sup>28</sup> and then elegantly validated by Myers.<sup>29</sup>

At the same time that we were investigating the asymmetric synthesis of (-)-stephacidin A, we had devised a new and very effective method to generate the azadiene species implicated in the IMDA construction of the stephacids and the more recently discovered notoamides.<sup>30</sup> As shown in Scheme 16, we discovered that  $\beta$ -hydroxyproline derivatives, could be readily dehydrated under Mitsunobu conditions to install the unsaturation in the proline residue, required for the IMDA process.<sup>31</sup>

Significantly, treatment of **74** under Mitsunobu conditions in warm dichloromethane, resulted in the direct production of *D, L*-stephacidin A in a ~2.4:1 ratio with C-6-*epi*-stephacidin A. This was our first success at generating the free (OH) *achiral* azadiene species **75**, that we have implicated as a possible biosynthetic intermediate to stephacidin A. Like other IMDA reactions similar to this one, a preponderance of the desired *syn*-isomer was produced in about a 2.4:1 ratio. We also found that a Davis oxaziridine-based oxidation of stephacidin A directly produced the *spiro*-oxindole natural product notoamide B. This conversion experimentally validates our proposal that stephacidin A serves as the immediate biosynthetic precursor to notoamide B. The biomimetic synthesis of stephacidin A as shown in Scheme 16, has provided us with the tools to prepare double  $^{13}C$ -labeled stephacidin A that we have recently used to further validate the bioconversion of stephacidin

A into notoamide B when this synthetic, racemic labeled precursor was fed to cultures of *Aspergillus versicolor*.<sup>32</sup>

This efficient IMDA strategy has been recently applied in our laboratory to concise, biomimetic total syntheses of *D, L*-malbrancheamide, and *D, L*-malbrancheamide B (Scheme 17),<sup>33</sup> *D, L*-marcfortine C (Scheme 18),<sup>34</sup> *D, L*-brevianamide B,<sup>31b</sup> *D, L*-versicolamide B<sup>30c</sup> and both (+)- and (-)-versicolamide B (Scheme 19).<sup>35</sup> The marcfortine C synthesis required fifteen steps from commercially available 6-hydroxyindole and proceeded in 3.7% overall yield.

In the case of the versicolamide synthesis, the optically pure oxindole species **81** (plus a minor diastereomer) was generated through oxaziridine oxidation. With that quaternary stereogenic center set, the Mitsunobu-based dehydration followed by base-mediated tautomerization and IMDA cyclization, furnished (+)-versicolamide B (and a diastereomer in a 1.4:1 ratio). In this instance, the IMDA cyclization reaction was entirely anti-selective; a situation that was predicted based on theory by Domingo and co-workers.<sup>19b</sup>

The *ab initio* calculations performed by Domingo, et al., revealed that for the *spiro*-6 ring formation, similar to that deployed in the biomimetic stephacidin A synthesis (Scheme 16, top), the *syn*-transition state is slightly favored by a little over 1 kcal/mol.<sup>19b</sup> Our experimental results on many different substrates, validates this prediction.

On the other hand, the corresponding *spiro*-5 mode of IMDA cyclization, such as that deployed in the versicolamide B synthesis (Scheme 19) was predicted to be favored by 4~7 kcal/mol. Again, our experimental observations fully support these theoretical predictions.

Many of these total synthesis platforms, have been extensively utilized by our laboratory to prepare isotopically-labeled probe molecules to interrogate individual biosynthetic steps. For instance, the malbrancheamide synthesis was “put to work” through the preparation of double <sup>13</sup>C-labeled pre-malbrancheamide, and was used to demonstrate that the halogenation of the indole ring occurs step-wise after the formation of the bicyclo[2.2.2]diazaoctane core (Scheme 21).<sup>33b</sup> We observed that double <sup>13</sup>C-labeled premalbrancheamide was converted into malbrancheamide B with 5.5% isotopic incorporation. This result established that the dioxopiperazine is reduced to the mono-oxopiperazine of pre-malbrancheamide before the halogenase steps and further, that the initial site of halogenation is at the electronically preferred 6-position of the indole.

A particularly exciting discovery occurred in 2008 when Prof. James Gloer, at the University of Iowa, isolated (+)- versicolamide B from cultures of *Aspergillus versicolor* NRRL 35600.<sup>30c</sup> He had also isolated (-)-stephacidin A and (+)-notoamide B from the same organism. It was immediately recognized that, the (-)-stephacidin A produced by this organism, was the *antipode* of the same substance originally isolated by Qian-Cutrone, et al., at Bristol-Myers Squibb from *Aspergillus ochraceus* WC76466.<sup>28a,36</sup> Later, Tsukamoto and co-workers isolated (+)-stephacidin A and (-)-notoamide B from cultures of a marine-derived *Aspergillus* sp. obtained from the common mussel *Mytilus edulis*, which was collected off Noto Peninsula in the Sea of Japan (and thus the name “notoamides”).<sup>30</sup> Very interestingly, Tsukamoto and coworkers then isolated the antipodal (-)-notoamide B from the marine-derived *Aspergillus* sp.<sup>30e</sup> Based on this, we proposed a “unified” biogenesis of the two distinct antipodal families as shown in Scheme 22. We speculated that the possible key precursor, was notoamide E, a metabolite we had inadvertently synthesized before Prof. Tsukamoto was able to identify this substance as a natural metabolite in her marine-derived *Aspergillus* sp.<sup>30d</sup>

In this biogenetic scheme, we envisioned that notoamide E, would be oxidized by two-electrons and tautomerized to the *achiral* azadiene species **75**. Please note that this is the *same* azadiene species we generated in Scheme 16, in the context of the biomimetic synthesis of *D, L*-stephacidin A. Each organism then, would have an enzyme (that we speculate is the oxidase) that would preferentially bind this species in one of four possible transition state conformers, mediating the face-selective IMDA reaction to give the respective (+)- or (-)-stephacidin A enantiomers.

We have already validated the laboratory as well as the biosynthetic transformation of double  $^{13}\text{C}$ -labeled stephacidin A into notoamide B as mentioned above.<sup>32</sup> The remaining mystery then, was the origin of versicolamide B, which has the rare *anti*-stereochemistry at C-6 (stephacidin numbering). Does this come from the as yet, undetected minor IMDA product C-6-*epi*-stephacidin A? Or, does versicolamide B arise from a distinct channel that would have to be stereochemically parallel, in an antipodal sense, in the separate species of the *Aspergillus* fungi that produce the observed natural (+)- and (-)-enantiomers?

We were in an excellent position to test this biogenetic hypothesis through the synthesis of double  $^{13}\text{C}$ -labeled notoamide E. Much to our chagrin, doubly-labeled notoamide E was found to incorporate into notoamides C, 3-*epi*-C and D (Scheme 23) in both *Aspergillus versicolor* and the marine-derived *Aspergillus* sp., but not into stephacidin A nor notoamide B (nor for that matter, any metabolite possessing the bicyclo[2.2.2]diazaoctane ring system that we could detect).<sup>30d</sup> This result forced us to consider that the timing of the oxidative cyclization of the indolopyranyl ring system, might occur after the putative IMDA construction of the bicyclo[2.2.2]diazaoctane core.

At this point, we were fortunate to engage Professor David H. Sherman, at the University of Michigan, to take on the task of whole genome sequencing of *Aspergillus versicolor* and Tsukamoto's marine-derived *Aspergillus* sp. with the objective of using genome mining and proteomics technologies to characterize the biosynthetic gene clusters. From this work, which included some additional  $^{13}\text{C}$ -labeled metabolite synthesis and precursor incorporation experiments, the biosynthetic gene clusters for the production of the notoamides and stephacidin A have very recently been characterized.<sup>37</sup>

An open reading frame (*orf*) named *notE* (Figure 4) was identified from the genome sequence using the known fumitremorgin gene *ftmA* to probe for homologous genes. Eighteen genes *notA-R*, were identified and biochemical functions assigned to many of these based on bioinformatics analysis (Figure 4). Two aromatic prenyltransferases, *notC* and *notF* were functionally expressed in *E. coli* and were biochemically characterized as a normal prenyltransferase (*NotC*) and a reverse-prenyltransferase (*NotF*). Based on the finding that NotC catalyzes the conversion of 6-hydroxydeoxybrevianamide E into a substance we have identified as the 7-prenylation product, notoamide S, we very recently proposed a revised stephacidin-notoamide biogenetic pathway (Scheme 24).

NotE is a presumed bimodular NRPS (Scheme 24) with adenylation (A)- thiolation (T)- condensation (C)-A-T-C domain organization and was found to share 47% amino acid sequence identity with FtmA. We determined that brevianamide F is efficiently transformed to deoxybrevianamide E by NotF, a reverse-prenyl transferase that catalyzes the alkylation at the 2- position of the indole ring with DMAPP.

In a normal prenylation reaction, such as that mediated by NotC, DMAPP alkylates an aromatic substrate through its C1' atom via an  $\text{S}_{\text{N}}2$  displacement, while the C3' position is involved in the reverse prenyltransfer reaction *via* an  $\text{S}_{\text{N}}2'$  displacement. This reverse-prenylation was previously shown by our laboratory, to occur with lack of facial selectivity with respect to the C-C bond-forming step on the DMAPP in paraherquamide-, austamide-

and brevianamide-producing fungi.<sup>38,39</sup> Recent access to the recombinant and functionally expressed enzyme NotE, should facilitate future studies to elucidate the mechanism of the reverse-prenylation reaction.

Following the formation of notoamide S, we have hypothesized that oxidation of notoamide S occurs to give an alternative *achiral* azadiene species that suffers enantiospecific IMDA cyclization in each of the respective *Aspergillus* sp., providing notoamide T. We have recently prepared *D, L*-notoamide T by the same biomimetic IMDA strategy used to make stephacidin A (Scheme 16), and are currently preparing the isotopically labeled material for precursor incorporation experiments.

We have also very recently sequenced the genome of *Aspergillus versicolor* NRRL 35600 and have identified a biosynthetic gene cluster that is highly homologous to the one from Tsukamoto's marine-derived *Aspergillus* sp.<sup>37b</sup> Genome mining, bioinformatics analysis and functional expression of select genes are currently in progress. It is anticipated that the mystery to the key enantio-divergent step, currently suspected to be at the stage of the notoamide S to notoamide T construction, will soon be solved.

Another surprising discovery in this program, that also relied heavily on the development of a total synthesis platform, concerned the elucidation of the absolute stereochemistry of the minor metabolite, VM55599, isolated from the paraherquamide-producing organism *Penicillium* sp. IMI332995. Everett and co-workers at Pfizer, reported the isolation, structure determination and relative stereochemical assignment of VM55599, and further suggested that this substance might be a biosynthetic precursor to paraherquamide.<sup>14d</sup> We discovered that the  $\beta$ -methylproline ring of paraherquamide A was derived from the oxidative cyclization of isoleucine and was not derived from the methylation of proline *via* S-adenosylmethionine.<sup>40,41</sup>

We were able to determine that the mechanism for the oxidative cyclization of isoleucine to  $\beta$ -methylproline proceeded through a net four-electron oxidation of the d-methyl residue of isoleucine to an aldehyde or aldehyde equivalent. Cyclization to the imine **87** followed by a stereospecific reduction provided  $\beta$ -methylproline; which incorporates into both asperparaline A and paraherquamide A. This was made possible through the synthesis of l-[5-<sup>13</sup>C,5-<sup>2</sup>H<sub>3</sub>] isoleucine isotopomer. Precursor incorporation experiments with this amino acid in *Penicillium fellutanum*, followed by isolation and purification of the paraherquamide A produced, revealed 0.32% incorporation of the labeled amino acid. Detailed nmr spectroscopic analysis revealed that H-16a (3.21 ppm) is the deuteron, H-16b (2.22 ppm) is the proton and the *pro-S* hydrogen is retained in the oxidative cyclization. *This result mandates that reduction occurs on the same face of the proline ring as the methyl group, C-17.*

The take-away lessons from these experiments, revealed that: (1)  $\beta$ -methyl proline in the paraherquamide-producing *Penicillium* sp., is biosynthetically derived from *S*-isoleucine; (2) a net four-electron oxidation followed by a two-electron reductive amination fashions the pyrrolidine ring of  $\beta$ -methylproline; (3) hydroxylation of the C-14 position in paraherquamide biosynthesis occurs with net retention of stereochemistry; and, (4) most significantly, the absolute configuration of VM55599 should be *pseudo*-enantiomeric to that in paraherquamide A, precluding the possibility (suggested by Everett, et al.) that VM55599 was a biosynthetic precursor to paraherquamide A. VM55599 is therefore a shunt (dead-end) metabolite. If this substance was not a biosynthetic precursor to paraherquamide A, then what species was?

We were able to rigorously establish the absolute configuration of VM55599, through an asymmetric, biomimetic total synthesis as shown in Scheme 26.<sup>42a</sup> In this synthesis, *S*-

isoleucine served as the optically pure starting material that was subjected to a Hoffmann-Loeffler-Freytag conversion to optically pure  $\beta$ -methylproline. Dioxopiperazine formation, aldol condensation/dehydration afforded the unsaturated substrate **95** that was subjected to the IMDA cyclization conditions first reported by Liebscher, et al., to give three of the four possible diastereomeric Diels-Alder products. Significantly, none of the “pre-paraherquamide” diastereomer was formed, which reveals that the intrinsic facial bias of this IMDA cyclization favors the rare VM55599 relative stereochemistry, and not that of paraherquamide.

Based on these results, we speculated that compound **102**, (where X = H<sub>2</sub>) with the  $\beta$ -methyl residue in the proline ring on the  $\alpha$ -face, and having the correct absolute configuration, was a plausible hexacyclic precursor to paraherquamide. We endeavored to prepare a racemic, double <sup>13</sup>C-labeled isotopomer of **102**, which was accomplished using a biomimetic IMDA construction. This synthesis produced all four possible IMDA diastereomers, the major isomer corresponding to VM55599. We performed precursor incorporation experiments with both the dioxopiperazine and monooxopiperazine forms of VM55599 and **102** and found that only **102** incorporated into paraherquamide A. Soon thereafter, we were able to isolate trace amounts of this new metabolite (**102**), which we have named “pre-paraherquamide” from the paraherquamide-producing fungi *Penicillium fellutanum* as well as from the asperparaline-producing fungi *Aspergillus japonicus*.

An interesting and puzzling observation from these experiments, centered around the lack of incorporation of the dioxopiperazine congener to pre-paraherquamide, namely compound **101**. This suggests that the tryptophan-derived carboxyl residue is reduced at some point in the biosynthesis *prior to* the formation of the bicyclo[2.2.2]diazaoctane ring system or, suggests that the oxidation state of the putative azadiene in this family of metabolites proceeds through the reduced oxidation state directly providing pre-paraherquamide in the IMDA cyclization. Efforts to resolve this apparent anomaly, particularly when contrasted to the oxidation level apparent in the biosynthesis of the stephacidins, notoamides and brevianamides are an area of current focus.

On the basis of all of the available experimental data, we have proposed a “unified” biogenesis of the paraherquamides and asperparalines<sup>43</sup> as shown in Scheme 28. It appears as though pre-paraherquamide serves as the possible branch-point in the biogenesis of these two families where, in paraherquamide biosynthesis, the indole-derived benzenoid ring is further hydroxylated to a phenol and catechol, and prenylation steps fashion the dioxepin (such as in paraherquamide A) and pyranyl ring systems (such as in paraherquamide F) extant in within this family. In the asperparaline-producing fungi, such as *Aspergillus japonicus*, the indole-derived benzenoid ring is oxidatively cleaved, removing four carbon atoms followed by further oxidative remodeling to form the novel *spiro*-succinimide ring system that is unique among known natural products to the asperparalines.

Labeled precursor incorporation experiments in *A. japonicus*, revealed that the *spiro*-succinimide ring of asperparaline is derived from tryptophan; the  $\beta$ -methylproline residue is derived from S-isoleucine (as expected); and that serine only labels the two N-methyl residues (*via* conversion to SAM). The lack of incorporation of the labeled serine into the tryptophan-derived methylene residue was quite unexpected and suggests that tryptophan biosynthesis in these fungi, may proceed through an as yet, undetermined mechanism. Efforts to resolve this anomaly are also underway.

This program has benefited from a dynamic combination of total synthesis technologies that have advanced to a stage where we are confident that we can prepare, in isotopically labeled form, as either a racemate (which has become necessary to probe potential enantio-divergent

steps) or in optically pure form, the substrate and product of every single putative biosynthetic transformation. The whole genome sequencing, genome mining and proteomics technologies, have provided powerful new tools that are being deployed to clone and functionally express the biological catalysts that Nature has evolved to construct this structurally stunning family of indole alkaloids.<sup>44</sup> It remains to be established if the core bicyclo[2.2.2]diazaoctane ring system is indeed fashioned by a biosynthetic intramolecular hetero-Diels-Alder reaction, as the current evidence on this provocative key point is circumstantial and indirect.<sup>45</sup> We have extensively demonstrated the chemical feasibility of this construction, and we are very anxious to learn if Nature has stumbled onto this reaction inadvertently through the oxidative processing of these non-ribosomally generated dipeptides. The existence of the discreet enantiomers of stephacidin A, notoamide B and versicolamide B constitutes the most intriguing hint and puzzle surrounding this fascinating, and pedagogically controversial question.<sup>45</sup> This project is currently at the most exciting state and we are poised to delve more deeply into Nature's treasure chest of closely guarded biosynthetic secrets.

### III. Asymmetric Synthesis of $\alpha$ -Amino Acids

Returning to the bicyclomycin synthesis, we developed an electrophilic glycine equivalent (**1**, Scheme 1) to tackle the synthesis of the  $\beta,\beta$ -disubstituted isoleucine moiety. At the time, in the early 1980's, there were many laboratories engaged in developing asymmetric glycine enolate equivalents,<sup>46</sup> and we capitalized on this opportunity to design a chiral, non-racemic chiral auxiliary-based electrophilic glycine equivalent based on the successful C-C coupling reactivity of the *bis*-thiopyridyl dioxopiperazine species **1**. The molecular design of one such heterocyclic species was already present in the literature through a landmark paper by Kagan, who in 1968, published the asymmetric synthesis aspartic acid in very high enantiomeric ratio, through the catalytic hydrogenation of the diphenyloxazinone **107** as shown in Scheme 29.<sup>47</sup>

Based on the obvious extension of this heterocyclic system to a glycine template, we prepared the N-CBz and N-t-Boc diphenyloxazinones (**107** and **108**, Scheme 30)<sup>48,49</sup> from the same optically active diphenylamino alcohol (**106**) employed by Kagan. The preparation of the optically pure amino alcohols follows from a classical diasteromeric aspartate salt resolution published by Tishler in 1951.<sup>50–53</sup> The preparation of both enantiomers of the diphenyloxazinones, as either their N-CBz or N-t-Boc derivatives, is shown in Scheme 30 and has been published as an *Organic Syntheses* procedure.<sup>49</sup> In addition, these compounds have been commercially available from Aldrich Chemical since the late 1980's. This methodology therefore provides unambiguous and convenient access to either D-(*R*)- or L-(*S*)-configured  $\alpha$ -amino acids in a high degree of chemical and optical purity.

We have previously extensively reviewed the chemistry of these highly versatile amino acid templates, and only a few highlights of the application of this methodology to more complex natural products synthesis will be briefly touched on here.<sup>54</sup>

It must be stated clearly here, that these reagents are members of the "chiral auxiliary pool" for asymmetric synthesis; the 1,2-diphenylamino alcohol moiety is destroyed in the final deblocking step to access the new, optically active  $\alpha$ -amino acid and cannot be recycled. This might be considered to be a disadvantage of this methodology. These substances are therefore not readily applicable for large scale (>10 kg) industrial manufacturing of amino acids but are, rather, ideally suited to the preparation of research and pre-clinical quantities of amino acids where speed, flexibility and reliability are the major discerning criteria. On the other hand, the destruction of the chiral auxiliary in the setting for which this methodology is ideally suited, namely medicinal chemistry and other high throughput applications, turns out to be a *major advantage* of this system. As described in a number of

publications from our laboratory as well as many other laboratories, the diphenyl amino alcohol moiety is typically reduced to give a water-insoluble by-product: bibenzyl, which can be conveniently extracted away from the polar, water-soluble zwitterionic amino acid or *N-t*-BOC amino acid obviating, in most cases, chromatographic or ion-exchange purification of the final amino acid.

For the electrophilic reaction manifold, the oxazinone (eg., (−)-**107** or **108**) is treated with *N*-bromosuccinimide in a non-polar solvent delivering the *anti*-bromide **109** in essentially quantitative yield; reaction of **109** with a variety of carbon-based nucleophiles in the presence of mild Lewis acids furnishes the  $\alpha$ -substituted oxazinones (**111**) in good yield and with generally excellent diastereoselectivities. The key C-C bond-forming reaction is believed to proceed through the agency of a highly reactive *N*-acyl imminium ion species (**110**) that is attacked from the least-hindered face of the oxazinone, *anti*- to the two phenyl substituents. After purification of the derivatized oxazinone, the chiral auxiliary was cleaved in most cases *via* catalytic hydrogenation over a heterogeneous palladium catalyst, typically in excellent yields to give the free amino acids. Dissolving metal conditions were also successfully employed to produce the amino acid derivatives and, in the case of unsaturated side chains, obviated saturation of olefinic residues.

The scope of reactive intermediates that can be generated from these oxazinone heterocycles for participation in diastereoselective C-C bond-forming reactions, has been significantly expanded to include *N*-acyl imminium ions (glycine electrophile), enolate, radical, azomethine ylide,  $\alpha,\beta$ -dehydro functionalization and most recently, manipulation of the lactone carbonyl residue gaining access to peptide isosteres (Table 2 and Figure 5).

We have utilized the chiral glycine methodology to synthesize a variety of natural products including:  $\beta$ -carboxyaspartic acid,<sup>55</sup> (+)-6-hydroxymethyl-2,6-diaminopimelic acid,<sup>56</sup> (−)-cucurbitine,<sup>57</sup> norcoronamic acid,<sup>58</sup> coronamic acid,<sup>58</sup> 2,6-diaminopimelic acid,<sup>59</sup> statine,<sup>60</sup>  $\gamma$ -D(L)- glutamyl-L-*meso*-diaminopimelic acid dipeptide,<sup>61</sup> (−)- spirotryprostatin B,<sup>62</sup> (−)-spirotryprostatin A,<sup>63</sup> (−)-tetrazomine,<sup>64</sup> (2*S*,3*R*)-capreomycidine,<sup>65</sup> capreomycin IB,<sup>66</sup> (S)-(+)-carnitine,<sup>67</sup> (R)-(−)-carnitine,<sup>68</sup> hypusine,<sup>69</sup> negamycin,<sup>70</sup> renieramycin G,<sup>71</sup> jourumycin,<sup>71</sup> cylindrospermopsin,<sup>72</sup> 7-*epi*-cyclindrospermopsin,<sup>73</sup> and 7-deoxycylindrospermopsin.<sup>74</sup>

Cylindrospermopsin (CY) was isolated as the principal hepatotoxin from *Cylindrospermopsis raciborskii* in 1992 after suspicion of its involvement in an outbreak of hepatenteritis that hospitalized 150 people on Palm Island, Australia.<sup>75</sup> It has since been isolated in Japan from *Umezakia natans*<sup>76</sup> and in Israel from *Aphazinomenon ovalisporum*.<sup>77a</sup> Following the discovery of the parent compound, 7-*epi*-cylindrospermopsin was isolated from *A. ovalisporum* as a toxic minor metabolite.<sup>77b</sup> 7-deoxy-cylindrospermopsin was initially isolated from *C. raciborskii* and has recently been co-isolated with CY in China from *Raphidiopsis curvata*.<sup>78</sup> Cylindrospermopsin has been shown to be a potent hepatotoxin ( $LD_{50} = 0.2 \mu\text{g}/\text{kg}$  in mice),<sup>79</sup> 7-*epi*CY is equipotent with CY<sup>24</sup> while 2-deoxyCY was thought to be non-toxic.<sup>75c</sup> Unlike the peptidyl hepatotoxic microcystins and nodularins, the cylindrospermopsins do not inhibit PP1 or PP2A. Their toxicity appears to result at least in part from the inhibition of protein synthesis.<sup>75,80</sup> The translation step of protein synthesis is inhibited by the cylindrospermopsins, but the mechanism of this inhibition is not yet known. Cylindrospermopsin has also been shown, *in vitro*, to be a non-competitive inhibitor ( $K_I = 10 \mu\text{M}$ ) of the uridine monophosphate (UMP) synthase complex, although *in vivo* assays do not support a general inhibition of UMP synthesis.<sup>81</sup> Terau et al. were able to show that one of the first symptoms of poisoning with CY was the detachment of ribosomes from the membrane of the endoplasmic reticulum.<sup>80a</sup> It was also shown that in mammalian cell cultures, cell death was accompanied by a marked

decrease in glutathione (GSH), an essential endogenous reductant to the anti-oxidative capabilities of hepatocytes.<sup>82</sup>

At the onset of this project little was known about the mechanism of action of this family of hepatotoxins. This encouraged us to develop an efficient and flexible synthesis of these alkaloids. We were intrigued by the observations that CY and 7-*epi*CY are toxic and 7-deoxyCY reportedly was not (although our work later showed this to be incorrect). Cytochrome P450 oxidation had been purported to mediate their toxicity.<sup>80</sup> We thought that an oxidation event at C7 or C8 may produce the enol-guanidine **113** (Figure 6), alternatively C15 oxidation may generate the guanidinimine **114**. Both of these intermediates are potentially redundant through extensive tautomerization, and both are electrophilic intermediates, perhaps responsible for the observation that oxidized metabolites of CY may alkylate DNA.<sup>80,83</sup> These considerations helped guide our synthetic investigations.

In addition, Shaw, et al. proposed the unusual uracil tautomer (**115**, Figure 6) for 7-deoxyCY<sup>75c</sup> that we were suspicious was incorrect. We also sought to develop the first synthesis of 7- deoxyCY and interrogate both the structural proposal and the claim that this metabolite was non-toxic.<sup>75c</sup> Cylindrospermopsin has attracted considerable synthetic attention and has been synthesized in racemic form by Snider<sup>84</sup> and Weinreb<sup>85</sup> and in optically active form by White,<sup>86</sup> who was also the first to establish the absolute stereochemistry.

The glycine enolate reactivity was deployed for concise, asymmetric syntheses of all three natural cylindrospermopsin alkaloids *via* a key intramolecular nitrone [1,3]-dipolar cycloaddition reaction on the crotylglycine-derived species **119** (Scheme 32).<sup>72-74</sup> The desired regiochemistry of the dipolar cycloaddition (**119** to **120**) proceeded to the extent of 10:1 in hot toluene but Sc(OTf)<sub>3</sub> at 25 °C gave **120** in 78–84% yield (12:1 regioselectivity); X-ray analysis of **120** secured the assigned structure. Reductive processing of **120** provided the functionalized A-ring of the cylindrospermopsins which was then homologated to the nitroalkane (**122**) and coupled to the pyrimidine moiety. Reductive guanidinylation gave the tetracycle (**124**) that was sulfated to give 7-*epi*CY.

The same overall strategy was deployed to prepare cylindrospermopsin and 7-deoxyCY. Our synthesis of 7- deoxyCY corrected the structural mis-assignment made by Shaw, et al., and provided the first pure sample of this substance for biochemical and biological evaluation. Having completed the total syntheses of all the cylindrospermopsin alkaloids, we were able to examine the feasibility of our biomechanistic hypothesis for the intermediacy of **113** or **114** (Figure 6). This work was done through a collaboration with Prof. Maria Runnegar. While synthetic CY was a potent inhibitor of protein synthesis in hepatocytes (4% of control at 3.3 μM), the C8 diastereomer required a concentration of 320 μM to achieve the same level of inhibition. Two orders of magnitude less toxic, this suggests that they are not processed through a common metabolic intermediate. Most significantly, our synthetic (racemic) 2-deoxyCY also proved to be a potent inhibitor of protein synthesis, contrary to the initial report by Shaw, et al.<sup>75c</sup>

Protein synthesis was completely inhibited at 12 μM, *in vitro*, and at 10 μM in whole cells; displaying potency within an order of magnitude of CY. Resembling intoxication by CY, synthetic 2-deoxyCY also inhibits the synthesis of glutathione (GSH).<sup>82</sup> The deoxygenated C8 diastereomer, also required a 100-fold increase in concentration to elicit these effects. These results suggest that: (1) substitution at C7 is not requisite for the toxicity of these alkaloids; (2) a common oxidized metabolite at C8 is not involved; and (3) in agreement with previous studies, intermediates lacking the uracil showed greatly diminished toxicity. Our synthetic work on the cylindrospermopsins has thus served to reveal several

fundamentally new and important insights about the stereochemistry at C-7 and C-8, provided the correct structure of 7-deoxyCY and significantly revealed that C-7 oxygenation is not required for the expression of toxicity.

A more recent mode of reactivity that we and others have exploited *via* the diphenyloxazinones, is the generation of azomethine ylides for both intermolecular and intramolecular [1,3]-dipolar cycloaddition reactions. Three examples from our laboratory highlight this powerful pyrrolidine construction. As shown in Scheme 33, the asymmetric total synthesis of spirotryprostatin B, a structurally novel microtubule inhibitor isolated by Osada, et al., from *Aspergillus fumigatus*<sup>87</sup> was accomplished. This molecule and the closely related spirotryprostatin A, has attracted extensive synthetic attention.<sup>88,89</sup> The key three-component dipolar cycloaddition reaction was accomplished through the reaction of the oxazinone **125**, with the isatin-derived dipolarophile **126** and 3-methoxy-3-methylbutanal, which provided the desired cycloadduct **127** whose structure was confirmed by X-ray analysis.<sup>62</sup> Hydrogenation to the amino acid, coupling to D-proline benzyl ester and cyclization fashioned the pentacycle (**130**) that was subjected to a Barton-modified Hunsdiecker oxidative decarboxylation and final thermodynamic epimerization of the proline residue delivering spirotryprostatin B.

We deployed similar methodology to achieve a very concise five-step asymmetric synthesis of spirotryprostatin A.<sup>63,91</sup> This synthesis platform enabled us to prepare several derivatives of the spirotryprostatins and in particular, we prepared the enantiomer of the natural metabolite of spirotryprostatin B isolated from *Aspergillus fumigatus*; we also prepared C-12-*epi*-spirotryprostatin B and the corresponding dehydrospirotryprostatin B. These three substances represent incremental geometrical changes at the proline  $\alpha$ -methine residue, with the  $\alpha,\beta$ -dehydro(prolyl) analog possessing a geometry in-between that of natural spirotryprostatin B and the 12-*epi*-diastereomer (Figure 7). All three of these substances, along with several other synthetic analogs, were tested for cytotoxic activity and the capacity to disrupt microtubule formation by our collaborator and discoverer of the spirotryprostatins, Dr. Hiroyuke Osada at RIKEN, Japan. Surprisingly, C-12-*epi*-spirotryprostatin B proved cytotoxic to tsFT210 cells at about ten-fold higher concentrations than that for the natural product, but was not a microtubule inhibitor. Even more astonishing, was the observation that the dehydro analog, was devoid of cytotoxic activity. This reveals that the proline residue in the spirotryprostatin structural framework, must make very intimate contact with its receptor protein (as yet undetermined) as the subtle changes in geometry at the proline residue strongly impact biological activity.

In a second foray utilizing the dipolar cycloaddition methodology, we have recently constructed the cyclopentane core of palau'amine and congeners (Figure 8) as shown in Scheme 34.<sup>92</sup>

Palau'amine, a dauntingly complex hexacyclic *bis*-guanidine antibiotic isolated from the sponge *Stylorella agminata*,<sup>93</sup> is a biologically intriguing substance whose structure, stereochemistry, biosynthesis and total synthesis has attracted considerable attention.<sup>94</sup> Palau'amine displays potent cytotoxic and immunosuppressive activities<sup>93</sup> and a recent, brilliant total synthesis of racemic palau'amine by the Baran laboratory is particularly noteworthy.<sup>95</sup> The relative stereochemistry of palau'amine was recently revised independently by Quinn<sup>96a</sup> and Köck<sup>96b</sup> to the stereostructure depicted in Figure 8 and turned out to be a fortuitous stereochemical array for our approach based on an intramolecular [1,3]-dipolar cycloaddition reaction that sets up the fully substituted C-16 stereogenic center.

Our synthesis commences with the enolate acylation of commercially available oxazinone **108** to provide **131** (relative stereochemistry unassigned and inconsequential). Removal of the *t*-Boc group furnishes aminoketone **132** which was condensed with formaldehyde to generate the incipient azomethine ylid (*A*) that produced tricyclic intramolecular cycloaddition product **133** as a single diastereomer in 63% overall yield for the three steps. The intrinsic facial bias of this intramolecular cycloaddition remain unclear and constitutes the subject of ongoing studies.

Reductive processing of **133** led to **135** in 61% overall yield. Ruthenium-mediated oxidation to ketoamide **136** was next converted into the unsaturated ketone by IBX oxidation to enone **137** in 80% yield. Stereoselective installation of the two one-carbon arms to enone **137** was accomplished in two stages beginning with a Morita-Baylis-Hillman type of hydroxymethylation and a subsequent nitromethane addition to give exclusively the desired 1,2-*anti* product. The relative stereochemistry of the vicinal hydroxymethyl and nitromethyl substituents in **140** are set with the correct relative stereochemistry as per the newly reassigned stereochemistry of palau'amine. Studies to apply this asymmetric approach to construct palau'amine are currently under investigation.

A third, also unfinished foray into complex alkaloid synthesis, is an asymmetric approach to nakadomarin and the manzamine alkaloids.<sup>97</sup> As shown in Scheme 35, three-component condensation of the diphenoxazinone **125** with aldehyde **141** and the unstable *exo*-methylene piperidinone **142** gave the desired cycloadduct **143**. This substance has been transformed into the *spiro*-tricyclic species **144** that was subsequently reduced and converted into the alkynone substrate **146** that is currently being investigated for furan formation and final modeling to nakadomarin. The three-component azomethine ylid condensation reaction has proven particularly powerful as, three or more stereogenic centers can be generated in a single step and the tolerance of other functional groups has proven broad.

The azomethine ylid dipolar cycloaddition methodology has been recently utilized by the Schreiber laboratory to generate a focused, diversity-oriented synthesis library of *spiro*-oxindoles (Figure 9)<sup>98</sup>, some of which proved active with the diphenyloxazinone template still intact.

The asymmetric amino acid methodology continues to be refined and extended by our laboratory as well as many others, to access both simple as well as complex nitrogenous substances of biomedical significance. Our current focus has been to utilize this system where appropriate to other programs in alkaloid chemistry, some of which, will be briefly touched on here.

#### IV. Tetrahydroisoquinoline Alkaloids

We initially became interested in the family of tetrahydroisoquinoline alkaloids when the structure and preliminary mode of action of quinocarcin was disclosed by the Kyowa Hakko Kogyo Co. in Japan.<sup>99</sup> We were struck by the reported observation that quinocarcin damaged DNA in an oxygen-dependent manner independent of added metal salts such as iron or copper. We investigated the chemistry of this natural product and discovered that quinocarcin spontaneously disproportionates into the known, inactive co-metabolites quinocarcinol and the newly identified oxidation product quinocarcinamide.<sup>100a</sup> We subsequently demonstrated that this spontaneous redox disproportionation reaction is general for the fused oxazolidine-containing antitumor alkaloids, including quinocarcin, tetrazomine and bioxalomycin.<sup>100c</sup> In the presence of molecular oxygen, either the reduction radical species **150** or the oxidation radical **149** can react with dioxygen ultimately forming superoxide. In this scenario, these drugs serve as their own reductant. Given the presence of

an exogenous 1-electron reducing agent (such as DTT, GSH, ascorbate or other reducing agents), quinocarcin, tetrazomine and bioxalomycin, the natural members of this class that contain the fused oxazolidine, can *catalytically* mediate the reduction of molecular oxygen to superoxide, ultimately resulting in the production of reactive oxygen radical species that can damage DNA and other cellular macromolecules.

During the course of our studies on the mechanism of the redox disproportionation of the oxazolidine, we discovered an important stereoelectronic control element necessary for this process to occur.<sup>100</sup> As shown in Figure 10, we have ascertained through the chemical synthesis of configurationally defined analogs that, the fused oxazolidine ring must be capable of adopting a *trans*-antiperiplanar geometry of the oxazolidine nitrogen lone pair and the adjacent methine hydrogen that participates in the redox disproportionation; the corresponding *syn*-periplanar arrangement, renders such oxazolidines inert to redox cycling and are inactive with respect to mediating oxidative damage to DNA (Figure 10).<sup>100,101</sup>

The significant conclusion from these studies, which relied heavily on the synthesis of configurationally defined stereoisomers (**147** and **148**), can be summarized as follows: (1) An intact oxazolidine is required for the redox disproportionation culminating in superoxide production and subsequently, for inflicting oxidative damage to DNA; and (2) There is an obligatory stereoelectronic requirement for a *trans*-antiperiplanar arrangement of the nitrogen lone pair and adjacent methine of the oxazolidine for redox cycling and (unexpectedly) for DNA alkylation. The synthetic technology platforms we have developed during the course of this program, have enabled the total syntheses of quinocarcinamide, quinocarcin (a formal total synthesis),<sup>102</sup> tetrazomine (including assignment of the relative and absolute configuration),<sup>64</sup> jorumycin,<sup>71</sup> renieramycin G,<sup>71</sup> cribrostain 4<sup>103</sup> and Et-743 (a formal total synthesis).<sup>104</sup> Several synthetic strategies were examined over the course of this program to construct both the bicyclo[3.2.1]core of quinocarcin, tetrazomine and bioxalomycin as well as the bicyclic[3.3.1]core of Et-743, saframycin, jorumycin, crirostatin and congeners.

For the asymmetric syntheses of (−)-jorumycin and (−)-renieramycin G, we developed an asymmetric synthesis of the “left-half” tetrahydroisoquinoline (THIQ) deploying the oxazinone-based amino acid enolate chemistry discussed above. The initial Pictet-Spengler reaction with ethyl glyoxylate (Scheme 37, **156** to **157**), provided only the undesired *anti*-THIQ, which was readily epimerized to give the requisite *syn*- THIQ that was set up for connection to the second tyrosine-derived amino acid (Scheme 38).

Condensation of **158** with **159** was made possible through the acid chloride, followed by processing to the key carbinolamine **162**. It was found that acid-mediated removal of the *N*-t-Boc residue concomitant with the second Pictet- Spengler cyclization, delivered the desired pentacycle **163** that was used for both the synthesis of (−)-jorumycin and (−)-renieramycin G. During the course of these studies, it was found that, if the final Pictet- Spengler reaction were conducted on the corresponding *N*-methyl amine (as opposed to the N-t-Boc derivative), the initial *syn*-stereochemistry of THIQ **164**, suffered quantitative epimerization to the unnatural *anti*-stereochemistry shown for **165** (Scheme 39).

Undaunted by such unexpected, and undesired stereochemical behavior, we capitalized on this opportunity to evaluate the effect of this somewhat subtle change in geometry of the rather rigid pentacyclic framework of these alkaloids, which had heretofore, never been examined. We thus endeavored to convert the crystalline pentacycle **165**, into 3-*epi*jorumycin and 3-*epi*-renieramycin G, and these agents tested side-by-side, with synthetic samples of (−)-jorumycin and (−)- renieramycin G, for antiproliferative activity against two human cancer cell lines (human colon A549 and human lung HCT-116, Table 3). (−)-

Jorumycin displayed potent growth inhibition with  $GI_{50}$  values in the low nanomolar range (1.9–19.2 nM), while the other compounds were found to be substantially less cytotoxic. Comparing the results of (−)-reneiramycin G and its 3-*epi*-counterpart, it appears that these amide-containing substrates may be capable of exerting cytotoxic effects through alternative mechanisms, such as quinone-mediated redox cycling, which remain fully intact irrespective of the C3 stereochemical configuration.

A somewhat distinct conceptual approach was developed for the asymmetric synthesis of (−)-cribrostatin 4 (renieramycin H), that deployed a tricyclic  $\beta$ -lactam, as the synthetic precursor to the second Pictet-Spengler sequence (Scheme 40).<sup>103</sup> The tricyclic THIQ containing the fused  $\beta$ -lactam was prepared through the agency of an asymmetric Staudinger reaction. Despite the extensive chemistry of  $\beta$ -lactams in the literature spanning more than fifty years, very little has been published on methods to chemoselectively reduce  $\beta$ -lactams to  $\beta$ -amino aldehydes and  $\beta$ -amino alcohols. We found that L-selectride proved to be a useful reagent for the mild reduction of the  $\beta$ -lactam ring in **168**, to afford an incipient  $\beta$ -amino aldehyde, that spontaneously suffered  $\beta$ -elimination, followed by intramolecular iminium ion formation and Pictet-Spengler closure to pentacycle **169** in 62% yield. The final stages of the synthesis proved straightforward, and benefited from the known selenium dioxide oxidation of the benzylic position reported by Danishefsky and co-workers in their earlier and independent accomplishment of the cribrostatin 4 synthesis.<sup>105</sup>

Turning to the more complex problem of Et-743, we decided to solve a nagging stereochemical issue that came up in our total syntheses of quinocarcin, tetrazomine, jorumycin and renieramycin G; namely, the difficulty we encountered in setting the two arms of the left-half THIQ with the requisite *syn*-relative stereochemistry. Direct Pictet-Spengler cyclizations (such as **156** to **157**, Scheme 37) gave predominantly, or in some instances, exclusively, the undesired *anti*-THIQ that required thermodynamic epimerizations to set the correct relative stereochemistry.

We devised a radical-based cyclization to fashion the desired *syn*-THIQ core, as shown in Scheme 41, on a glyoxalimine-based substrate.<sup>104</sup> The use of Garner's aldehyde, in a Friedel-Crafts alkylation on aryl bromide **172**, provided the requisite amino alcohol substrate **173**, that was condensed with ethylglyoxylate to form the corresponding imine. Aryl radical generation, and cyclization, proceeded through the chair-chair transition state species (**176**), that disposed the carboethoxy residue equatorial, resulting in the desired *syn*-THIQ **177**.

With the correct relative and absolute stereochemistry now efficiently addressed, tricycle **177** was converted through to pentacycles **182** and **183**. This posed a regiochemistry problem we expected to encounter with the unsymmetrical tyrosine residue that we deliberately installed with the aim of economizing on the fashioning of the upper-right aryl residue that is unique to the ecteinascidins. While a solution to this regioselectivity issue has been recently devised, pentacycle **182** was transformed into a pentacyclic intermediate (**184**) prepared by Danishefsky and co-workers in their formal total synthesis of Et-743.<sup>106,107</sup>

We are also currently seeking to apply the methodologies we have developed for the total synthesis of several members of tetrahydroisoquinoline family of antitumor agents as described above, to the asymmetric synthesis of the bioxalomycins. While these ongoing studies will not be summarized here, we did discover another unique mechanism of action of bioxalomycin during the course of working with this agent in the oxazolidine redox disproportionation studies briefly described above. We discovered that bioxalomycin  $\alpha$ 2, is capable of covalent interstrand cross-linking duplex DNA in the minor groove, in a highly site-specific manner at 5'-CpG steps.<sup>108</sup> We further demonstrated that this reaction occurs

through alkylation of the exocyclic amine residues of the opposing deoxyguanosine residues. While the detailed structure of this lesion has not been completely elucidated, an accruing mass of indirect experimental evidence points to the mechanism and structure depicted in Figure 11. We have suggested, that the cross-link occurs between C7 and C13b, wherein an *ortho*-quinonemethide species (**186**, Figure 11) is the *bis*-electrophile.

Remers and co-workers, published a computational study<sup>109</sup> on this subject, wherein the presumed sites for cross-linking were C7 and C3a. Remers concluded that DNA cross-linking for this agent would not be possible. The optimal N2 to N2 distance in a 5' CpG<sup>3'</sup> step is between 3.1 and 3.6 Å for B-form DNA. We have carried out preliminary molecular mechanics calculations on bioxalomycin non-covalently bound to DNA in an effort to determine likely modes of DNA interstrand cross-linking. We have found that there is excellent presentation of the putative electrophilic sites at C7 and C13b for **186** if the aromatic portion of the drug partially intercalates into the DNA helix. The modeling exercise on the positioning of the C7/C13b presentation that would result in cross-linked species (**187**) places both C7 and C13b within ~4.5 Å of the proximal N2 of the opposing 2'-deoxyguanosine residues. Carrying out a similar modeling exercise on the presentation of the C7 and C3a sites (**185**, bottom Figure 12) also provides a feasible presentation of these electrophilic sites to the opposing 2'-deoxyguanosine residues although the distances are somewhat greater (~5–6 Å) than that for **186**. Modeling of two other possible electrophilic site combinations, C9/C13b and C3a/C9 gave a badly distorted DNA fragment that was not capable of maintaining Watson-Crick base-pairing; these sites are therefore thought to be highly unlikely.

We have also performed corroborating DNA cross-linking studies with cyanocycline (Scheme 43). In the absence of the reducing agent DTT, there is no cross-linked product formed. However, in the presence of 0.1 mM DTT, a cross-linked product with properties identical to that obtained with bioxalomycin  $\alpha_2$  was obtained, albeit in somewhat lower yield. We attribute the lower yield to the inefficient reduction of the quinone to the dihydroquinone under the reaction conditions. The fact that cyanocycline, in the absence of a reducing agent does not lead to cross-link, provides additional, indirect, yet provocative support for our contention that the *ortho*-quinone methide species **186** is a plausible species generated (via reduction of the quinone to the dihydroquinone) yielding the cross-linked adduct. These data are consistent with the molecular modeling picture we have of the most likely cross-linked species **187**.

This mode of reactivity, reveals the dense complexity of molecular reactivity that Nature has installed in this beautiful alkaloid and includes DNA mono-alkylation, interstrand cross-linking, redox disproportionation and redox cycling of reactive oxygen radical species. Our laboratory is continuing to apply our synthetic technology around this family of alkaloids to further explore and exploit the multiple modes of chemical and biochemical reactivity that these fascinating alkaloids display.

**Biosynthesis of Et-743**—Trabectedin® (Et-743 or Yondelis) has received authorization for commercialization from the European Commission for advanced soft tissue sarcoma, after failure of anthracyclines and ifosfamide, or for patients who are unsuited to receive these agents. Et-743 is also in phase III for ovarian cancer and phase II for prostate, breast and pediatric cancers.<sup>110</sup> Zalypsis® (PM00104/50) is a related analogue that has begun phase I clinical trials for the treatment of solid tumors. Clinical supplies of Et-743 has become a major challenge, as the sea whip that houses the producing organism is difficult to collect and has proven recalcitrant to culture. The current manufacturing process to make clinical supplies of Et-743, relies on the large-scale fermentation of cyanosafracin B, followed by a multi-step semi-synthesis.<sup>111</sup> As this drug becomes more widely adopted,

pressure on the price of this drug, which is very expensive to manufacture, will increase. A key challenge in natural product biosynthesis involves isolation, characterization and analysis of pathways from marine invertebrate (e.g. sponges, tunicates, ascidians, octacorals) symbionts. Although significant progress has been made toward identification and analysis of the biosynthetic gene clusters of several marine-derived natural products, such as bryostatin and onnamide,<sup>112</sup> the study of these systems have so far been limited to gene cluster sequencing and bioinformatic analysis. Et-743 on the other hand brings together a number of key elements to drive the search for an effective solution to this urgent source problem using a cross-disciplinary chemical biology approach. Although the natural product can be isolated directly from the marine tunicate *Ecteinascidia turbinata*, the yield is poor (1 mg of natural product/kg of marine tunicate). However, the high promise of this compound suggests that source restrictions will ultimately limit the scope of development and clinical use for treatment of a wider range of malignancies.

In collaboration with the Sherman laboratory, at the University of Michigan, we have endeavored to elucidate the biosynthesis of Et-743 using a combination of metagenomics, proteomics, metabolomics and chemical synthesis of probe substrates and putative biosynthetic intermediates. While this work is currently at a preliminary stage, we have used synthetic technologies developed in our laboratory to prepare probe substrates for the proteomics phase of this work, and modern whole-genome sequencing technologies for genome mining. Results of this exciting phase of our work on the tetrahydroisoquinoline natural products, will soon be made available and constitutes a major new thrust in direction for our work in this field.

## V. Taxol Biosynthesis

Chemists and biologists alike have been drawn to taxol (paclitaxel) due to its promising spectrum of antineoplastic activity, its unique mechanism of action, and the synthetic challenge that the complex, and densely functionalized ring system poses.<sup>113</sup> Taxol was first isolated from the bark of the Pacific Yew, *Taxus brevifolia*.<sup>114</sup> Unfortunately the Yew is slow-growing and is primarily found in environmentally sensitive areas of the Pacific Northwest and stripping the tree of its bark kills the Yew. It takes three trees to obtain ~10 Kg of bark from which 1 gm of taxol can be isolated.<sup>113c</sup> FDA approval of taxol for the treatment of advanced ovarian cancer<sup>113a</sup> has created a severe supply and demand problem. Collection of renewable *Taxus* sp. needles and clippings has attenuated this problem somewhat, but as the drug has become more widely adopted, particularly for use earlier in the course of cancer intervention and for new therapeutic applications, pressure on the Yew population has continued to increase worldwide. Alternative means of taxol production are therefore being vigorously pursued since cost and availability will continue to be significant issues.

To date, totally synthetic methods have fallen short as an alternative source for taxol production<sup>115</sup> due to the complex structure of taxol that mandates lengthy and expensive synthetic routes. A method that has proven viable is the semi-synthesis of taxol from 10-deacetylbaccatin III that can be isolated from the needles, a renewable source, of the European Yew, *Taxus baccata*.<sup>113b,113c</sup> The commercial supply of taxol and semisynthetic precursors will have to increasingly rely on biological methods of production. This can be reasonably achieved by: (1) extraction from intact *Taxus* plants, (2) *Taxus* cell culture,<sup>116</sup> or (3) microbial systems.<sup>117</sup> In order to produce large quantities of taxol or a pharmacophoric equivalent by semi-synthetic or perhaps, by genetically engineered biosynthetic methods, it is essential to gain a better understanding of the detailed biosynthetic pathways<sup>116–118</sup> in *Taxus* sp.

In 1966 Lythgoe and coworkers proposed a biosynthetic pathway in which the tricyclic carbon framework of the taxoids was envisioned to arise by the sequential intramolecular cyclizations of the double bonds of geranylgeranyl pyrophosphate (ggPP) to 1(S)-verticillene and then to taxa- 4(20),11(12)-diene (Scheme 44).<sup>119</sup>

Our group, in collaboration with the Croteau laboratory (Washington State University), have demonstrated that the “Lythgoe taxadiene” is not the first committed intermediate on the taxoid biosynthetic pathway but rather that, taxa- 4(5),11(12)-diene (**189**, Scheme 45) is the major metabolite.<sup>120–122</sup> This was demonstrated by a total synthesis<sup>122</sup> of both isomeric taxadienes and administration of synthetic <sup>13</sup>C-labeled taxa-4(20),11(12)-diene (**188**) to cell-free microsomes of *Taxus canadensis*.<sup>120c</sup> Cross-over experiments and the lack of biotransformation of the Lythgoe diene (**188**) in *Taxus* microsomes had initially cast considerable doubt on the intermediacy of this substance in taxoid biosynthesis.<sup>121</sup> On the other hand, using ggPP as a substrate, taxa-4(5), 11(12)-diene (**189**) has been shown to be the primary product of taxadiene synthase, an enzyme recently characterized, cloned and functionally expressed by the Croteau laboratory.<sup>120</sup> However, we have since demonstrated that recombinant taxadiene synthase indeed produces ~5% of the Lythgoe diene (**188**) plus <1% percent of the corresponding 3,4-diene isomer.<sup>121</sup>

Mechanistic work completed in our laboratories on taxadiene synthase revealed a very unique mode of terpenoid cyclization (Scheme 46). Croteau has reported that the taxadiene synthase step is slow and possibly limiting in the net metabolic carbon flux to taxol.<sup>120</sup> We have further established that the first hydroxylation product in the taxol pathway is taxa-4(20),11(12)-dien-5 $\alpha$ -ol (**190**) through total synthesis and biosynthetic incorporation into taxol, 10-deacetylbaaccatin III and cephalomannine *in vivo* in *Taxus brevifolia*.<sup>123</sup> Furthermore, a synthetic sample of taxa-4(20),11(12)-dien-5 $\alpha$ -acetate (**191**) has been used to establish that, following hydroxylation of **189** to **190**, the next step in the pathway appears to be acetylation of **190** to acetate **191**.<sup>124</sup> The Croteau lab has cloned and expressed taxa-4(20),11(12)-dien-5 $\alpha$ -ol-*O*-acetyl transferase from *Taxus canadensis* in *E. coli*.<sup>124</sup> Thus, the first three biosynthetic steps have now been established as shown in Scheme 45 and we have devoted considerable effort to elucidate the subsequent sequence of hydroxylations to the fully oxygenated taxol core.

Due to the very low yield of natural taxadiene obtainable from biological sources (an extract from 750 kg of *Taxus brevifolia* bark powder yielded<sup>120a</sup> ~1 mg of 85% pure **189**) and the remaining uncertainty as to the sequence of hydroxylation reactions to taxoids,<sup>120,123</sup> synthetic access to these isotopically labeled tricyclic diterpenes proved to be essential for several reasons: (1) synthesis provides access to stable- and/or radio-labeled substrates from which pathway metabolites can be made by microsomal and/or recombinant enzyme biotransformation and; (2) the synthetic metabolites facilitate the identification, isolation and structure elucidation of new pathway metabolites that are produced biosynthetically in very tiny amounts. The second point was amply demonstrated by our synthesis of taxa- 4(20), 11(12)-dien-5 $\alpha$ -ol (**190**) which preceded the identification and isolation of this substance from *Taxus brevifolia*.<sup>123</sup> Indeed, the identification of this substance as a biosynthetic intermediate would have proven far more difficult if the synthetic reference sample were not available. The first point has also been amply demonstrated as described below since, synthetic, tritium-labeled **190** and the corresponding acetate **191** have served as the *exclusive* substrates from which the intermediate hydroxylation products (diol, triol, tetraol and pentaol) have been produced biosynthetically. It should also be noted that taxol has now been identified in several strains of microorganisms<sup>117</sup> and our laboratory has provided samples of stable- and radio-isotopically labeled taxadienes to numerous other laboratories interested in identifying pathway intermediates to taxoids.

Since ggPP serves as a starting material for many other biosynthetic pathways,<sup>125</sup> any number of the steps may be rate-limiting in the secondary metabolic flux to taxol. Total synthesis as well as semi-synthesis technologies have enabled us to prepare many probe substrates as well as numerous putative biosynthetic intermediates that are produced in either cell culture or in *Taxus* sp. stems in amounts too small to isolate and determine the structure of such substances. Access to synthetic, authentic materials has proven absolutely key to penetrating the complex biosynthetic matrix of taxoid metabolism. We have used these synthetic probe substrates to elucidate several fundamentally novel enzymatic reactions such as, the taxadiene synthase-catalyzed cyclization of ggPP to taxadiene (**189**) and the cytochrome P450-mediated oxidation of taxadiene (**189**) to taxadienol (**190**).<sup>123</sup> While much remains unknown, detailed here, is a synopsis of the most exciting findings.

**Mechanism of Taxadiene Synthase**—In collaboration with the Croteau lab, the Coates lab (University of Illinois) and the Floss lab (University of Washington), we have determined the fascinating mechanism of the “one-step” cyclization of ggPP to taxa-4(5), 11(12)-diene (**189**) as shown in Scheme 46.<sup>120</sup>

Our group has focused on the stereochemistry and mechanistic implications of the unprecedented migration of the C11 hydrogen atom to C7.<sup>121</sup> The Floss lab synthesized the requisite deuterated ggPP substrate (shown, Scheme 46) and this substrate was converted into taxadiene *via* soluble recombinant synthase from *Taxus cuspidata*. We observed >90% retention of deuterium at C7. Our laboratory elucidated the stereochemistry of the deuteron migration by 2D NMR and 1D TOCSY and have unambiguously established that the deuterium atom migrates to the  $\alpha$ -face of C-7. The observation that the deuteron transfer from C11 to C7 occurs with such a high degree of isotopic retention, coupled with the exclusive transfer to the  $\alpha$ -face of C7, suggests that the mechanism for the transfer of the deuteron from C11 to C7 occurs *intramolecularly*. We are aware of no precedent for such an intramolecular proton transfer during an olefin-cation cyclization reaction and thus, the mechanism of taxadiene synthase is strikingly unique in this regard.<sup>121</sup>

Of further interest, is the facial bias of the final C8/C3 olefin-cation cyclization. Considering the known relative stereochemistry of the taxoid B/C ring juncture, the C3/C4  $\pi$ -system *must* attack the putative C8 cation formed immediately following the C11/C7 proton migration, from the *same face* to which the newly installed proton at C7 migrated. Molecular modeling of this process, which formally involves a criss-cross of bond formation across the C7/C8  $\pi$ -system, proved quite insightful. The molecular model of the C8 cation suggests that, upon pyramidalization at C7 and fashioning of the C11/C12 olefin, the conformation of the 12-membered ring twists, relative to that of the C12 cation, rocking the C3/C4  $\pi$ -system into the correct facial orientation for capture of the C8 cation establishing the *trans*-fused B/C ring juncture.

**Elucidation of the Mechanism of Taxadiene Hydroxylase**—This experiment was designed to discern if the cytochrome P450 hydroxylation of taxa-4(5), 11(12)-diene (**189**) to taxa-4(20), 11(12)-dien-5 $\alpha$ -ol (**190**) proceeds through an epoxide intermediate or an allylic radical species. We have examined the interesting mechanistic question regarding the cytochrome P450 conversion of taxa-4(5), 11(12)-diene into taxa-4(20), 11(12)-dien-5 $\alpha$ -ol with allylic transposition.<sup>126</sup> No isomerization of taxa-4(5), 11(12)-diene (**189**) to the 4(20), 11(12)-diene isomer (**188**) (or *vice versa*) was observed in *Taxus* sp. microsomes (or *Spodoptera* microsomes enriched in the recombinant 5 $\alpha$ -hydroxylase) under standard assay conditions. Similarly, no interconversion of either positional isomer was observed in the presence of Mg<sup>+2</sup>, NAD<sup>+</sup>, NADH, NADP<sup>+</sup>, or flavin cofactors, at pH values from 4~10. From these studies, we concluded that taxa-4(5), 11(12)-diene (**189**) is not appreciably isomerized to taxa-4(20), 11(12)-diene (**188**) under physiological conditions, and that the

migration of the double bond from the 4(5)- to the 4(20)-position in the process of taxadienol formation is an inherent feature of the cytochrome P450 oxygenase reaction with taxa-4(5),11(12)-diene (**189**) as substrate. It follows that taxa-4(20),11(12)-diene (**188**) is but a minor natural product of *Taxus* sp. formed by taxadiene synthase that is an adventitious, yet efficient, substrate for the 5 $\alpha$ -hydroxylase.

Previous efforts to evaluate the 5 $\alpha$ -hydroxylation reaction by the native enzyme, by search for an epoxide intermediate and through the use of [20- $^2$ H<sub>3</sub>]taxa-4(5),11(2)-diene to examine a kinetic isotope effect (KIE) on the deprotonation step, failed to distinguish between two reasonable mechanistic possibilities.<sup>123a</sup>

The two mechanistic manifolds that were considered involve: (1) preliminary conversion of the 4(5)-double bond of taxa-4(5),11(12)-diene (**189**) to the corresponding 4(5)-epoxide (**197**), followed by ring-opening to carbenium ion species **198** and elimination of a proton from the C20 methyl group to yield the allylic alcohol product (**190**) and, (2) an alternate route involving cytochrome P450-mediated abstraction of hydrogen from the C20 methyl of the substrate (**189**) to yield the allylic radical (**199**) to which oxygen is added at C5 yielding **190** (Scheme 47).

The utilization of the isomeric taxa- 4(20),11(12)-diene (**188**) by the hydroxylase, with efficiency comparable to that of the natural substrate, would appear to rule out an intermediate epoxide (**197**) in the reaction cycle. *These results instead suggest a mechanism involving abstraction of a hydrogen radical from C20 for **189** (or from C5 in the case of the 4(20)-isomer **188**), leading to the common intermediate, allylic radical **199**, followed by oxygen insertion selectively from the 5 $\alpha$ -face of this radical intermediate to accomplish the net oxidative rearrangement.* It also appears that the somewhat tighter binding of the 4(20)-isomer substrate (**188**) may be a reflection that this isomer more closely mimics the allylic radical intermediate.<sup>126</sup>

The synthesis of the lightly oxygenated taxoids, has proven much more difficult than initially anticipated and we have deployed both total synthesis technologies,<sup>122</sup> as well as semi-synthesis from two major taxoid shunt metabolites: taxusin, which is oxygenated at C5, C9, C10 and C13 and a related taxoid, obtained from the Japanese Yew, that is oxygenated at C5, C9, C10 and C14 (Figure 13).<sup>127</sup> A few highlights of our initial total synthesis of taxadiene are shown in Scheme 48.<sup>122</sup> Access to these lightly oxygenated substrates, has been extensively exploited in the selective removal and addition of oxygenation to the taxoid core. In several instances, the synthetic, authentic samples proved indispensable for the identification of these trace natural metabolites in Yew.

In collaboration with the Croteau laboratory, recent progress has included most notably, the construction of transgenic *Taxus* cell lines, which are enabling an understanding of late pathway steps (C13-side chain assembly) and early pathway steps leading to taxane tetraol intermediates. Current work has focused on the functional characterization of taxoid oxygenases (all appear to be P450's) and acyl transferases, and in the synthesis of labeled substrates for elucidating the remaining pathway steps. Of the nine presumptive taxane core oxygenases, the Croteau laboratory has cloned and characterized six of these P450's: the 2 $\alpha$ -,<sup>128</sup> 5 $\alpha$ -,<sup>126</sup> 7 $\beta$ -,<sup>129</sup> 9 $\alpha$ -,<sup>130</sup> 10 $\beta$ -<sup>131</sup> and 13 $\alpha$ -<sup>132</sup> hydroxylases, primarily by functional expression in yeast.<sup>133</sup> The remaining fourteen, functionally undefined, cytochrome P450 clones from an induced *Taxus* cell cDNA library have been transferred to the baculovirus/insect cell expression system because of the instability of these recombinant enzymes in yeast microsomes, and eight of these were satisfactorily co-expressed with the *Taxus* P450 reductase for subsequent evaluation which is ongoing work.

What has become clear from these studies, is that the mid-section of the taxol biosynthesis pathway, is in fact not a “path” way at all.<sup>134</sup> Rather, there is a softening of substrate specificity among the P450 enzymes that are each designed to oxygenate the taxoid core at a specific position. The net result, is that each oxygenated product, can function as a substrate of altering efficiency, for each P450 resulting in a complex matrix of oxygenated polyols, many of which finding their way all the way to baccatin III and taxol. We believe that this may prove to be a general phenomenon among secondary metabolite biogenetic oxygenations, particularly where there are multiple oxygenases, such as exists in the taxol system. We have further observed that metabolites which accumulate, such as taxusin, often turn out to be shunt metabolites as they are not processed further by down-stream modeling enzymes. It is easy to be fooled into looking at metabolite co-occurrence, as a potential blueprint for a putative biosynthetic pathway. The real intermediate biosynthetic substrates, are often produced in trace or undetectable amounts (and thus don’t accumulate), requiring the engagement of synthetic chemistry to prepare and then test these substances for bioconversion. This project, as well as the prenylated indole alkaloid project discussed above, have firmly underscored the importance of total synthesis to access biosynthetic substrates which are after all, natural products in their own right.

## VI. FR900482 and Mitomycin C

Another natural product family in which we have become deeply interested, is the FR900482-mitomycin family of antitumor drugs. FR900482, and FR66979 are natural products obtained from the fermentation harvest of *Streptomyces sandaensis* No. 6897 at the Fujisawa Pharmaceutical Co. in Japan.<sup>135–137</sup> FR900482 along with its derived triacetate FK973 and the O-methylated analog FK317 have been advanced into human clinical trials as potential chemotherapeutic agents for the treatment of a variety of solid malignancies. In preliminary mode of action studies carried out at Fujisawa Co., FK973 was demonstrated to effect the formation of DNA interstrand crosslinks and DNA-protein cross-links in L1210 cells.<sup>136</sup> In contrast to MMC,<sup>138</sup> FK973 does not cause oxidative single strand scission of DNA. Furthermore, FK973 was found to be significantly less toxic than mitomycin C and is approximately three-fold more potent.<sup>139</sup> Of significant interest, is the finding that both FK973 and FR900482 are active against multidrug-resistant P388 cells.<sup>136a,c</sup> In initial phase I clinical trials, patients treated with FK-973 exhibited vascular leak syndrome (VLS) and this substance was subsequently withdrawn from clinical development.<sup>137</sup> VLS is characterized by an increase in vascular permeability that leads to increased leakage of fluids into interstitial spaces resulting in peripheral edema and ultimately organ failure.<sup>140</sup> Additional VLS symptoms include weight gain, hypoalbuminemia, pleural, and pericardial infusion and pulmonary and cardiovascular failure. VLS has been linked to exposure to immunotoxins such as ricin A, and to treatment with high concentrations of cytokines such as interleukin-2 (IL-2), as well as to various pathological conditions such as T-cell lymphoma, sepsis, trauma, and burns.<sup>140</sup>

On the other hand, FK-317 has shown considerable promise to become a clinically important therapeutic alongside the structurally related and widely used anti-tumor drug mitomycin C (MMC).<sup>138</sup> Significantly, FK-317 was found not to induce vascular leak syndrome in patients and recently advanced from a very successful phase I trial to phase II human clinical trials.

The structurally and mechanistically related antitumor drug MMC, has been in clinical use for over thirty years and as will be discussed, considerable overlap between the two families of drugs exists with some critical differences. It is well-established<sup>138,139</sup> that MMC is reductively activated by either a one-electron or two-electron pathway to provide the electrophilic mitosene (**204**) via the semi-quinone radical anion (**203**, Scheme 49). MMC cross-links DNA (structure **206**) preferentially at 5' CpG<sup>3'</sup> sites<sup>4</sup> and also mediates oxidative

cleavage of DNA. The oxidative cleavage reaction is a manifestation of superoxide production by MMC resulting from the adventitious reduction of molecular oxygen by the semi-quinone radical anion intermediates (**203**, **204** or **205**); subsequent Haber-Weiss/Fenton cycling produces hydroxyl radical and related reactive oxidants capable of causing non-selective tissue damage. The relatively low host toxicity of FR900482, FK973 and FK317 in human clinical trials relative to MMC may be correlated to the incapacity of these [formerly Fujisawa or “FR”] drugs to cause indiscriminate oxidative damage to DNA and other healthy cellular constituents.

Like MMC, the FR drugs also require reductive activation both *in vivo* and *in vitro*. The FR drugs do not produce random single strand breaks in DNA which is typically associated with redox cycling of reactive oxygen radical species. The low toxicity of the Fujisawa drugs relative to MMC may thus be a manifestation of differences in the chemical means by which the drugs are activated. The Fujisawa drugs and MMC both share the ability to cross-link DNA (with the *same* 5'CpG<sup>3'</sup> sequence selectivity)<sup>138</sup> through the agency of a bioreductively generated mitosene. The major structural difference between MMC and FR900482 and congeners, is the presence of the quinone moiety in MMC and the hydroxylamine hemi-ketal of the Fujisawa drugs.

In MMC, the quinone functionality, is an obligate functional array for the reductive unmasking of the potent, *bis*-electrophilic mitosene (**204**). In the Fujisawa drugs, it has been unambiguously established that the reductively labile functionality, is the N-O bond of the unique hydroxylamine hemi-ketal.<sup>141</sup> Given the potential clinical promise of the Fujisawa drugs coupled with both their unusual structures and relationship to MMC, a great deal of effort has been directed towards the synthesis of these natural products.<sup>142</sup>

It has been demonstrated that FR900482 (and by analogy, FR66979, FK317, and FK973) undergo reductive activation *in vitro* to form the reactive mitosene derivative **209** (Scheme 50) which preferentially cross-links duplex DNA at 5'CpG<sup>3'</sup> steps.<sup>141</sup>

The mechanism of reductive activation, that has been examined by both our laboratory and the Hopkins laboratory, has been established to involve the thiol-mediated *two-electron* reduction of the N-O bond<sup>141</sup> in the presence of trace Fe(II) salts<sup>141</sup> generating the transient ketone **207** which rapidly cyclizes to the carbinolamines **208**. Expulsion of water has been inferred as the rate-determining step enroute to the electrophilic mitosene **209**.<sup>141</sup>

It can thus be seen that FR900482 and MMC are actually naturally occurring clever “pro-drugs” that must be reductively activated *in vivo* to expose the highly reactive *bis*-electrophilic mitosene derivatives that are responsible for the biological activity displayed by these substances. We have sought to exploit the concept of latent triggering of mitosenes through the design and synthesis of new antitumor agents with improved selectivity and therapeutic potential based on the FR900482 structural array.

We have completed the asymmetric total synthesis of (+)-FR900482 and (+)-FR66979 as shown in Scheme 51.<sup>143</sup> This highly convergent synthesis has been accomplished in thirtythree steps from commercially available materials and constitutes one of the shortest synthesis of these drugs on record. We developed a novel, one-step method to construct the unique hydroxylamine hemi-ketal of these agents involving a dimethyldioxirane (DMDO) mediated removal of the *N*-*para*-methoxybenzyl protecting group concomitant with hydroxylation of the aniline nitrogen atom as shown in the conversion of **216** → **218**.

The aldol condensation of **215**, which yields a 1:1 mixture of diastereomers, fortuitously allowed epimerization of the undesired epimer to **216** without attendant dehydration. Synthetic (+)-FR66979 was obtained from **218** after protecting group removals and

installation of the carbamoyl residues and LiBH<sub>4</sub> reduction; a final Swern oxidation reaction converts FR66979 into FR900482.

We have exploited the synthetic technology developed for FR900482 to construct the first biochemically functional mitosene progenitor that can be activated photochemically.<sup>64,65</sup> As shown in Scheme 52 acetylation of **214** (from Scheme 51) with the photo-labile 6-nitroveratryl chloroformate (NVOC-Cl) (75%) followed by a similar series of steps to that used in the total synthesis of FR900482, gave the crystalline mitosene progenitor **219** (X-ray).

The capacity of **219** to cross-link DNA was initially evaluated using linearized pBR322 plasmid DNA by denaturing alkaline agarose gel electrophoresis and then, at high resolution, using a 5'-<sup>32</sup>P-labeled 33 bp oligonucleotide substrate. Footprint analysis of the cross-linked product, revealed that **219** cross-links a synthetic DNA duplex at the identical 5'CpG<sup>3'</sup> step as that observed for FR900482. Corroboration of the footprinting data was secured by substitution of the 2'-deoxyguanosine base with 2'-deoxyinosine at the 5'CpG<sup>3'</sup> steps. Reactions with the 2'-deoxyinosine modified duplex resulted in no observable crosslink, while the use of the 2'-deoxy-7-deazaguanosine showed cross-links in the same manner as the unmodified 2'-deoxyguanosine-containing duplex. These results strongly implicate the N-2 exocyclic amine of 2'-deoxyguanosine as the site of alkylation in the same manner as the natural products.

Another manner in which we have exploited the creative invention that Nature has designed into FR900482, was through the semi-synthetic installation of the hydroxylamine hemi-ketal functionality, which is unique to FR900482 and congeners, into a pyrrolizidine alkaloid framework. The pyrrolizidine alkaloids are a large family of primarily plant alkaloids, that are typically rendered toxic by oxidation *via* liver cytochrome P450 enzymes. We wondered if we could “borrow” the reductively-activated hydroxylamine hemi-ketal from FR900482, and “insert” this into the pyrrolizidine alkaloid structural framework to create a hitherto unknown reductively activated pyrrolizidine alkaloid (Scheme 53).<sup>145</sup>

This was accomplished by the vonBraun-type ring-opening of commercially available monocrotaline, oxidation to the aldehyde, acetal protection and oxidation of the secondary amine to the hydroxylamine with *m*-CPBA (Scheme 54).<sup>145</sup>

Removal of the acetal gave the tricyclic hydroxylamine hemi-ketal **228**, which constitutes the first reductively activated pyrrolizidine alkaloid. Treatment of this species with Fe(II)-EDTA, resulted in the generation of the highly reactive and toxic species dehydromonocrotaline, that mediated covalent cross-linking of DNA.

This same strategy was also deployed to make the first photo-triggered dehydromonocrotaline progenitor (**230**, Scheme 55), by simply installing an N-VOC residue on the same ring-opened intermediate **227** used in Scheme 54. Photolytic removal of the N-VOC residue in the presence of duplex DNA, resulted in multiple covalent cross-links.<sup>146</sup>

The synthetic chemistry developed for the total synthesis of FR900482, has borne multiple fruit and still holds vast untapped potential for further exploiting the fascinating chemical and biochemical reactivities packed into this small, heterocyclic natural product. We are continuing to refine and develop this chemistry for the preparation of biochemical and biological tools to study the interactions of these drugs in the context of chromatin.

In collaboration with Karolin Luger’s laboratory, we used the synthetic photochemically activated derivative of FR400482 (compound **219**) to investigate the molecular mechanism of this class of drugs in a biologically relevant context.<sup>147</sup> We found that the organization of

DNA into nucleosomes effectively protects the DNA against drug-mediated interstrand cross-linking, while permitting mono-alkylation. This mono-alkylated, nucleosomal DNA, has the potential to form covalent cross-links between chromatin and nuclear proteins. Using *in vitro* techniques, we observed that interstrand cross-linking of free DNA results in a significant decrease in basal and activated transcription. In addition, we found that covalently cross-linked plasmid DNA by the photo-activated FR900482 analog, is inefficiently assembled into chromatin.

**Cross-linking of FR900482 to HMG-A1**—In collaboration with Prof. Raymond Reeves' laboratory at Washington State University, we have discovered that FR900482 covalently cross-links the high-mobility group-A1 (HMG-A1) oncoproteins to chromosomal DNA in Jurkat cells.<sup>148</sup> The basic strategy we have deployed is shown in Figure 14 and involved treatment of Jurkat cells that over-express the HMG-A1 oncoproteins, with sub-lethal concentrations of FR900482 (typically < 1 μM). Using a modified chromatin immunoprecipitation (ChIP) procedure, fragments of DNA that have been covalently cross-linked by FR900482 to HMG-A1 proteins *in vivo* were PCR-amplified, isolated and characterized. The nuclear samples from control cells were devoid of DNA fragments whereas the nuclear samples from cells treated with FR900482 contained DNA fragments which were cross-linked by the drug to the minor groove-binding HMG-A1 proteins *in vivo*.

Additional control experiments established that the drug also cross-linked other non-oncogenic minor groove-binding proteins (HMG-B1 and HMG-B2) but does not cross-link major groove-binding proteins (ie., Elf-1 and NFkB) *in vivo*. These results constituted the first demonstration that FR900482 cross-links a number of minor groove-binding proteins *in vivo* and suggests that the cross-linking of the HMG-A1 oncoproteins to chromosomal DNA may significantly participate in the mode of efficacy of FR900482 as a chemotherapeutic agent. *The ability of this class of compounds to cross-link the HMG-A1 proteins in the minor groove of DNA represents the first demonstration of drug-induced cross-linking of a specific cancer-related protein to DNA in living cells.* The capacity of FR900482 to cross-link the HMG-A1 oncoprotein with nuclear DNA *in vivo* potentially represents a significant elucidation of the antitumor efficacy of this family of anticancer agents.

**Elucidation of the Mechanistic Basis for the Induction of Vascular Leak Syndrome by FR900482**—In a second study, we have obtained chromatin immunoprecipitation (ChIP) data showing that the two drugs FK317 and FR900482, differ markedly in the manner in which they induce cell death.<sup>148</sup> Four different diagnostic procedures, including flow cytometric analyses employing Annexin-V staining and caspase activation assays, demonstrated that *whereas FR900482 induces necrosis, FK317 induces an unusual necrosis-to-apoptosis switch that is drug concentration dependent:* at low doses FK317 induces necrosis and at higher concentrations it induces apoptosis (Figure 15). Northern blot analyses of drug-treated cells suggest that this 'switch' is mediated, at least in part, by modulation of the expression levels of the gene coding for the anti-apoptosis protein Bcl-2. Additional support for this idea comes from the observation that FR900482, in contrast to FK317, induces the expression of proteins such as IL-2 and IL-2R $\alpha$  which are known elicitors of both *Bcl-2* gene expression and VLS.

**FK317 versus FR900482: Mode of Cell Death**—We have thus discovered very significant differences in the mode of cell death induced by the two closely related antitumor agents FR900482 and FK317. There seemed to be a mysterious paradox with respect to why FR900482 led to the expression of vascular leak syndrome (VLS) in patients whereas FK317 treatments are devoid of this seriously deleterious side-effect. Indeed, the termination of human clinical trials for FR900482 was a direct consequence of VLS. *Very surprisingly, FK317 does not induce VLS* and as a consequence, FK317 advanced from Phase I to Phase

II human clinical trials. In an effort to elucidate the underlying cellular mechanisms of FR900482 and FK317 with respect to VLS, we have examined the differential expression of IL-2, a cytokine well-known to be a causative agent in VLS, in cells treated with FK317 and FR900482. Our findings are summarized below:

1. Both IL-2 and IL-2Ra are over-expressed in cells as evidenced by Northern blot and Western blot analysis. Over-expression of IL-2 is known to be the causative agent in the induction of VLS.
2. The anti-apoptosis gene *Bcl-2*, is over-expressed in cells treated with FR900482 at all concentrations tested (Northern Blot analysis). This succinctly explains why FR900482-treated cells die by necrosis instead of apoptosis.
3. Cells treated with FR900482 display cellular characteristics of necrotic cell death at all concentrations tested.
4. Cells treated with FK317 display *IL-2* and *IL-2Ra* expression at levels of healthy, untreated cells (Northern and Western blot analysis). This clearly explains why patients treated with FK317 do not display VLS. We believe that this is a very significant finding that should be of *general* use in the pre-clinical evaluation of all anti-tumor drugs and should provide a simple pre-clinical expression profile of antitumor drugs headed for clinical trials that could potentially save enormous amounts of money on drugs doomed for failure through induction of VLS.
5. Cells treated with FK317 display *Bcl-2* expression levels that are slightly upregulated at ~1mM but, *Bcl-2* expression is significantly down-regulated at concentrations greater than 1 mM (Northern blot analysis). *This exciting finding reveals that FK317 is capable of inducing a rare concentration-dependent necrosis to apoptotic switch.*

The molecular and mechanistic bases of these striking differences between FR900482 and FK317 are at present unknown and rendered all the more puzzling by the fact that both drugs mediate covalent adduction of the HMG-A1 protein on the *same* IL-2 and IL-2Ra genes. It has been established that FK317 is metabolized *in vivo*, to give the active agent, FR157471 and thus, the only structural difference between FR900482 and FK317, is the phenolic O-methyl residue in FK317 versus the hydroxyl residue in FR900482. The fact that such a small difference in structure can have such profound effects on the cell biology of these agents, remains striking and demands an explanation. Elucidation of the structural and mechanistic reasons for these highly unexpected observations will be fascinating to unravel.

**Biosynthesis of FR900482 and MMC**—In a new direction for this program, we have established a collaboration with Prof. David Sherman's laboratory at the University of Michigan to elucidate the biosynthesis of FR900482 and MMC which are close biogenetic cousins. We have also harnessed the synthetic chemistry we have developed for the total synthesis of FR900482 and MMC to prepare isotopomers of certain putative biosynthetic intermediates, thereby obtaining structural and mechanistic information on the biosynthesis of these closely structurally related antibiotics. The biosynthesis of these agents is poorly understood and we have embarked on a multi-disciplinary approach to elucidating a number of fascinating details of the respective biosynthetic pathways.

Through precursor labeling and feeding experiments done primarily in the 1970's, the basic biosynthetic constituents of MMC were elucidated and are summarized in Figure 16. The primary building blocks are erythrose, AHBA, D-glucosamine, pyruvate, carbamoyl phosphate and methionine.

Recently, the biosynthesis of MMC and FR900482, has been more deeply investigated by the Sherman laboratory.<sup>149</sup> These studies have led to the identification, cloning and sequencing of the biosynthetic gene cluster in *Streptomyces sandaensis* (FR900482) and *Streptomyces lavendulae* (MMC) by the Sherman laboratory.<sup>149</sup> The FR900482 biosynthetic gene cluster (the *frb/fbc* gene cluster) consists of forty-nine FR900482 biosynthetic genes spanning 56-kb of contiguous DNA.<sup>25</sup> The functions of the gene-encoded protein products involved in the biosynthesis of MMC (and, by homology, FR900482) includes the assembly of the primary biosynthetic precursors, dihydrobenzoxazine structure formation, tailoring functionality (i.e. hydroxylation, carbamoylation, and carbonyl reduction), plus resistance and export of the drugs. A unified biogenesis for the elaboration of FR900482 and MMC is shown below in Scheme 56.

Based primarily on precursor structure and metabolite co-occurrence, the biosynthetic proposal shown in Scheme 56 has been formulated by Sherman and recently modified by our group.<sup>150</sup> First, AHBA is loaded onto an acyl carrier protein *via* a CoA ligase (*Frbd* or *MitE*). A glycosyl transferase connects the amino group of AHBA to the anomeric center of D-glucosamine (*mitB*).

Several steps are particularly interesting to us and have implications regarding the genetic overlap between the two families of natural products. For instance, the relative stereochemistry of the aziridine ring (C1/C2) and the carbamoyl-containing hydroxymethyl residue (C9, MMC numbering) is *anti*- in FR900482 and *syn*- in MMC. Of additional note, is that within the mitomycin family, MMC, MMA, MMF and porfiromycin posses the *anti*-relative stereochemistry whereas MMB and MMD have the *syn*- relative stereochemistry. Thus, the formation of the aryl C8a-C9 bond either occurs *via* distinct genetically-encoded pathways and intermediates or, the C9 stereogenic center is subject to epimerization resulting in both diastereomeric relationships. Sherman initially suggested that this bond-formation might occur through an intramolecular Friedel-Crafts type of alkylation from a phosphorylated intermediate such as **235** and we have subsequently suggested that the corresponding epoxide species **236** that may also be subject to Payne rearrangement prior to cyclization to an eight-membered ring core. The potential Payne rearrangement would thus provide a third mechanistic possibility for the divergence to the C1/C9 *syn*- and *anti*-stereochemistries.

A second issue of intrigue, concerns the modeling of the hydroxylamine hemi-ketal in FR9004882 *versus* the quinone-containing 5/5-carbinolamine system of the mitomycins. Is there a common, late-stage intermediate that is diverted by distinct oxidases in each biosynthetic system? Or, do the two biosynthetic pathways diverge at a much earlier stage?

Finally, due to the intrinsic lability of the eight-membered ketone-containing substrates to form mitosene intermediates, this strongly suggests that oxidation of the C9a secondary alcohol to the corresponding ketone, must occur *after* the formation of the quinone (for MMC, see **239 → 242 → 243**) and hydroxylamine (for FR900482, see **239 → 240 → 241**). While many other possible pathways and intermediates might be envisioned including alternative sequencing of the transformations postulated in Scheme 56, our approach to unravel these pathways will begin with the synthesis, labeling and incorporation studies of some reasonable early- and late-stage intermediates from which we hope to narrow and ultimately completely define the two pathways.

## VII. HDAC Inhibitors

The most recent area that has attracted our attention, concerns the relatively recent discovery of several macrocyclic natural products that potently inhibit histone deacetylase enzymes. Histone deacetylases (HDACs) are enzymes involved in the epigenetic regulation of gene

expression. The discovery of the first human histone deacetylase protein derived from studies of a natural product, trapoxin, which conferred a differentiation phenotype upon cultured cancer cells. Using ligand affinity chromatography and protein biochemistry, the laboratory of Stuart Schreiber at Harvard University discovered HDAC1 and HDAC2.<sup>151</sup> Subsequent efforts in the Schreiber laboratory discovered additional related deacetylases, HDAC4, HDAC5 and HDAC6.<sup>152</sup> To date eighteen HDACs have been identified, which are generally divided into four classes, based on sequence homology to yeast counterparts. It has been widely recognized that HDACs are promising targets for therapeutic interventions intended to reverse aberrant epigenetic states associated with cancer.<sup>153,154</sup> In addition, experimental evidence identifies a plausible therapeutic benefit for patients with non-malignant diseases, such as inflammatory/autoimmune illness (e.g. psoriasis,<sup>155</sup> rheumatoid arthritis<sup>156</sup>), genetic conditions (e.g. sickle cell anemia,<sup>157</sup> spinal muscle atrophy<sup>158</sup>) and neurodegenerative diseases (e.g. Huntington's Disease<sup>159</sup>). However, the genotoxicity of HDAC inhibitors observed in preclinical studies has limited their promise beyond cancer, highlighting the pressing need for highly selective, pharmaceutically tractable agents. Within cancer research, a number of HDAC inhibitors have progressed rapidly through clinical trials.<sup>160,161</sup> For example, suberoylanilide hydroxamic acid (SAHA, also known as Vorinostat and marketed as Zolinza; Merck & Co., Inc., NJ, USA) was approved last year for the treatment of advanced cutaneous T-cell lymphoma. Approval was granted as part of the FDA orphan drug program, following a priority review. Depsipeptide (also known as FK228 or FR901228 and given the general name Romidepsin; Gloucester Pharmaceuticals Inc., MA, USA) has also demonstrated potent antiproliferative effects at well-tolerated doses and has progressed well through clinical trials. However, during a phase II study serious cardiac adverse events were observed, limiting enthusiasm for the agent and requiring a careful reconsideration of the structure-activity relationships and pharmacotoxicology.<sup>162,163</sup> Consequently, FK228 is in limited development in advanced cancers, such as relapsed, refractory multiple myeloma. A number of other cyclic peptides with structures analogous to that of FK228, have exhibited potent HDAC inhibitory activity and some of these are also candidates in varying stages of clinical trials (Figure 17).<sup>164,165</sup>

We first became interested in the depsipeptide natural product FK228 and developed an improved synthesis of this drug, based off of the pioneering work of Simon.<sup>166,167</sup> We were particularly interested if the depsipeptide played a functional role in the mode of binding to the Class I HDACs, of which FK228 is a very potent and selective inhibitor.

During our work on the synthesis of a variety of FK228 analogs, Leusch, et al., published the isolation and structure determination of the marine natural product largazole.<sup>168</sup> It became immediately apparent from an examination of the structure, that largazole should also be an HDAC inhibitor, as it shares the same thiol-containing side chain that the known HDACi's FK228, FR901375 and spiruchostatin possess (Figure 17).

FK228 is a pro-drug, that must be activated by reductive-opening of the disulfide linkage to expose the (S)-3-hydroxy-7- mercaptohept-4-enoate moiety, which coordinates tightly to the active site  $Zn^{+2}$  atom of the Class I HDACs (Figure 18). As this sulfhydryl residue is acylated in largazole, it seemed plausible to us, that esterase or lipase-based removal of the octanoyl residue from largazole (a pro-drug) would give the active form of this species, the largazole thiol. This has been firmly validated by our laboratory and others.<sup>169,170</sup>

Most known HDACi's, are composed of a cap group, responsible for surface recognition of the opening to the active site of the enzymes, a linker region and a metal-binding functionality (see Figure 18 for SAHA). This three-component model, renders the design and synthesis of new HDACi's an intellectually challenging and potentially highly rewarding endeavor.

Based on the rather difficult total synthesis of FK228 itself, as well as the commensurate challenges of synthesizing analogs of FK228, we turned our attention to largazole as a scaffold from which changes to the cap group, linker and thiol-binding domain seemed more amenable. Largazole is conformationally more rigid than FK228 while also possessing a 16-membered depsipeptide macrocycle. While we recognize that the sum-total of these structural features should not be over-simplified in terms of manifestation of biochemical HDAC inhibitory activity and whole-cell biological activity, we suggest that the structural features of these natural products might be conceptualized (and chemically manipulated) as having major (but not exclusive) impacts on the following properties of these drugs:

1. The length (from the peptide backbone) and functionality in the zinc-binding arms are largely responsible for potency with respect to HDAC inhibition and contribute to HDAC isoform selectivity.
2. The specific amino acid sequences and side-chain residues in the cap region impart further HDAC isoform selectivity.
3. The macrocycle size and conformational display of the scaffold are intimately associated with binding affinity (biochemical potency) and should be candidates for manipulation to achieve altered potency as well as isoform selectivity.

We quickly moved to develop a total synthesis of largazole, that would be amenable to making deep-seated structural changes. Our synthesis, shown in Scheme 57, proved to be rapid and scaleable and also provided an authentic specimen of largazole thiol, the presumptive active form of the drug.<sup>169</sup>

It was exciting to observe the amount of synthetic attention that largazole received, as eight independent total syntheses of this natural product were reported in the literature within just a few months of the disclosure of the structure.<sup>169,170</sup> We next decided to prepare the peptide isostere of largazole, as it is well-known that depsipeptides are rapidly cleaved by serum esterases and might severely limit the bioavailability of the natural product as a potential drug candidate. In conjunction with this study, we also endeavored to prepare the peptide isostere of FK228, by modifying our total synthesis of the depsipeptide natural product.<sup>171</sup> We were fortunate to establish a dynamic collaboration with Prof. James E. Bradner, of the Dana-Farber Cancer Research Institute, and Prof. Stuart L. Schreiber, of the Broad Institute of Harvard and MIT, to biochemically and biologically evaluate our synthetic compounds. As shown in Table 4, the HDAC inhibitory activities of synthetic FK228, the FK228 peptide isostere, largazole thiol, the largazole peptide isostere thiol and the largazole peptide isostere were compared to SAHA.

A striking observation emerged from these experiments. Comparable potencies are observed between FK228 and largazole thiol, as expected. However, disparate potencies are observed between their respective peptide isosteres. As demonstrated in Table 4, the amide isostere of FK228 is 50-fold less potent an inhibitor of HDAC1 than is the natural product.

The peptide isostere of largazole thiol (**257**) is, indeed, modestly reduced in potency against HDAC1 compared to the natural product, but only by 9-fold. The trend of increased potency for the largazole peptide isostere thiol *versus* the FK228 peptide isostere was preserved across all human class I HDACs tested (Table 4). We decided to deploy computational methods to study the effects of isostere replacement and model the disparate observed target potencies. We were fortunate to engage Prof. Olaf Wiest, of the University of Notre Dame, to analyze the lowest energy unbound and protein-bound conformations of the four thiol derivatives by employing Monte carlo methods.

The preferred coordination modes of the four analyzed structures are shown in Figure 19. The thiol extends towards the zinc ion at the bottom of the entrance channel with a Zn-S distance of ~2.5 Å while the macrocycle sits on the mouth of the pocket. The hydrocarbon chain fills the hydrophobic channel lined by Phe150 and Phe205. The orientation of the macrocycle is similar in the ester and the amide isostere, maximizing lipophilic interactions with cap residues.

Analysis of the structures and energetic of the conformational space of the four compounds revealed an interesting conformation-activity relationship. Superimposed in Figure 20 are the binding conformations (orange for FK228 and largazole, yellow for amide isosteres) and the global minimum conformation (blue for depsipeptides and green for amide isosteres) as well as the relative energies (in kJ/mol) and rms values for higher energy conformations of the four compounds under study. For FK228, the optimum binding geometry is only 5 kJ/mol above the global minimum conformation, which is within an RMS of 1.8 Å and therefore structurally similar. In contrast, the amide isostere is much more rigid and the preferred geometry for binding is not only much higher in energy (40 kJ/mol) than lowest energy conformation, but with an RMS of 3.11 Å also structurally very different. There are no conformations that are energetically accessible and that resemble the bound conformation. Binding of the amide isostere of FK228 will therefore involve a significant distortion of the protein surface and/or loss of binding interactions, leading to the experimentally observed loss of activity.

For largazole thiol, the lowest energy conformation is also the preferred binding conformation. Although the optimum binding geometry for the largazole isostere is 48 kJ/mol higher in energy than the most stable conformation, the geometries are within an RMS of 1.41 Å and thus very similar, as seen on the top right of Figure 20. As a result, the conformational change of the protein required to bind the low energy conformation of the macrocycle cap is relatively small, and much of the binding interaction will be maintained even if the low-energy conformation is bound. The effect of the isostere substitution in the largazole macrocycle is predicted to be smaller than in FK228, and in agreement with the experimental results. This was exploited for the design of improved binders with predicted, and subsequently confirmed, picomolar activity.<sup>172</sup>

With Prof. Wiest's molecular modeling as our design guide, we have endeavored to begin what might prove to be a long and interesting journey of harnessing the synthetic chemistry platform originally deployed to make the natural product, for the preparation of isoform-selective HDACi's. We are particularly interested in achieving isoform selectivity within the Class I HDACs, as there are no known agents that currently discriminate between these enzymes. To date, we have made numerous deep-seated structural changes to the largazole framework, and a few of the many synthetic analogs we have prepared are displayed in Figure 21. We are tackling alterations to the cap group, with the objective of exploiting differences of surface amino acid residues among HDACs 1–3, that might impart isoform selectivity. We are also examining alternative zinc-binding functionality, as well as making changes to the linking chain of atoms between the macrocycle and the zinc-binding residue. Finally, disulfide (activated by reduction) and other masked forms of the zinc-binding sulphydryl residue are on our drawing board of synthetic targets.

## Conclusion

In this Perspective, the objective was to illustrate how the concepts, strategies and development of practical tools for total syntheses have been extensively applied in our laboratory to interrogate interesting biomechanistic and/or biosynthetic aspects of complex, biologically relevant natural products. Our laboratory has been fortunate to have been able

to accomplish the synthesis of many of the natural products described herein that attracted our interest. The synthetic strategies and ultimate solutions we have developed in many cases, were driven by the quest for obtaining powerful, and often indispensable tools for interrogating some of these very tantalizing puzzles. As a ubiquitous trait of scientific research, the more questions we asked and attempted to address with the synthetic probe molecules in hand, the more new unanswered questions emerged, irresistibly drawing us deeper and deeper into each family of metabolites. We have come to realize that total synthesis projects can very much be viewed as a true beginning of a larger program and not an abrupt conclusion once the natural target molecule has been assembled. When chemistry begins at the advanced vantage point of an established synthesis, new and often unanticipated opportunities for enquiry can be contemplated. As synthetic organic chemists continue to grapple with an ever-changing landscape of funding opportunities and justifications for our art, we do not hesitate to strongly advocate the case for exploiting natural products synthesis for connecting organic chemistry as a discipline, to a broader swath of science. We have been additionally fortunate, to have been able to interest and engage a wide range of collaborators in some of these projects and their skills and expertise have made our journeys both fruitful and intellectually satisfying.

## Acknowledgments

I am deeply indebted to all of my former and current co-workers whose names appear in the publications cited, for their hard work, dedication, creativity and scientific passion. I am especially grateful to a large number of collaborators all over the world, who have enriched our research program immeasurably. I also need to acknowledge my wife Jill and two sons Ridge and Rainier for their love and support. Our research program over the years, has been generously funded by the National Institutes of Health, the National Science Foundation, The Herman Frasch Foundation, The Infectious Diseases Research Institute, the Multiple Myeloma Research Foundation, The Colorado State University Cancer Super Cluster, The Petroleum Research Fund of the American Chemical Society and several corporations including, Eli Lilly, Merck & Co., G.D. Searle, Ajinomoto Co., Japan, Fujisawa Pharmaceutical Co., Japan, Kyowa Hakko Kogyo Co., Japan, Sankyo Co., Japan, Fujisawa, The Japanese Society for the Promotion of Science, Microcide Pharmaceutical Co., HemaQuest, Xcyte Therapies, Phoenicia, and the American Chemical Society. The images in the TOC Graphic and Scheme 22 of *Aspergillus versicolor* were provided by doctorfungus.org.

## References

1. (a) Miyoshi T, Miyairi N, Aoki H, Kohsaka M, Sakai H, Imanaka H. *J Antibiot*. 1972; 25:569–575. [PubMed: 4648311] (b) Kamiya T, Maeno S, Hashimoto M, Mine Y. *J Antibiot*. 1972; 25:576–581. [PubMed: 4648312] (c) Nishida M, Mine Y, Matsubara T. *J Antibiot*. 1972; 25:582–593. [PubMed: 4567453] (d) Nishida M, Mine Y, Matsubara T, Goto S, Kuwahara S. *J Antibiot*. 1972; 25:594–601. [PubMed: 4648313] Bicyclomycin (Aizumycin) was simultaneously isolated from *Streptomyces aizunensis*; (e) Miyamura S, Ogasawara N, Otsuka H, Niwayama S, Tanaka H, Take T, Uchiyama T, Ochiai H, Abe K, Koizumi K, Asao, Matsuki K, Hoshino T. *J Antibiot*. 1972; 25:610–612. [PubMed: 4648315] (f) Miyamura S, Ogasawara N, Otsuka H, Niwayama S, Tanaka H, Take T, Uchiyama T, Ochiai H. *J Antibiot*. 1973; 26:479–484. [PubMed: 4792062] (g) Miyoshi T, Iseki M, Konomi T, Imanaka H. *J Antibiot*. 1980; 33:480–487. [PubMed: 7000736] (h) Iseki M, Miyoshi T, Konomi T, Imanaka H. *J Antibiot*. 1980; 33:488–493. [PubMed: 6448830] (i) Ochi K, Tsurumi Y, Shigematsu N, Iwami M, Umehara K, Okuhara M. *J Antibiot*. 1988; 41:1106–1115. [PubMed: 3170345]
2. (a) Williams RM, Armstrong RW, Dung JS. *J Am Chem Soc*. 1984; 106:5748–5750.(b) Williams RM, Armstrong RW, Dung JS. *J Am Chem Soc*. 1985; 107:3253–3266.(c) Williams RM. *Tetrahedron Lett*. 1981; 22:2341–2344.(d) Williams RM, Dung JS, Josey J, Armstrong RW, Meyers H. *J Am Chem Soc*. 1983; 105:3214–3220.
3. (a) Zwiefka A, Kohn H, Widger WR. *Biochemistry*. 1993; 32:3564–3570. [PubMed: 8466900] (b) Magyar A, Zhang X, Kohn H, Widger WR. *J Biol Chem*. 1996; 271:25369–25374. [PubMed: 8810302] (c) Riba I, Gaskell SJ, Cho H, Widger WR, aKohn H. *J Biol Chem*. 1998; 273:34033–34041. [PubMed: 9852059] (d) Magyar A, Zhang X, Abdi F, Kohn H, Widger WR. *J Biol Chem*. 1999; 274:7316–7324. [PubMed: 10066795] (e) Weber TP, Widger WR, Kohn H. *Biochemistry*.

- 2002; 41:12377–12383. [PubMed: 12369827] (f) Skordalakes E, Brogan AP, Boon Park S, Kohn H, Berger JM. *Structure*. 2005; 13:99–109. [PubMed: 15642265]
4. (a) Kohn H, Abuzar S. *J Am Chem Soc*. 1988; 110:3661–3663.(b) Syed Abuzar S, Kohn H. *J Am Chem Soc*. 1990; 112:3114–3121.
5. Someya A, Iseki M, Tanaka N. *J Antibiot*. 1979; 32:402–407. [PubMed: 38239]
6. (a) Williams RM, Tomizawa K, Armstrong RW, Dung JS. *J Am Chem Soc*. 1985; 107:6419–6421. (b) Williams RM, Tomizawa K, Armstrong RW, Dung JS. *J Am Chem Soc*. 1987; 109:4028–4035.
7. Williams RM, Sabol MR, Kim H, Kwast A. *J Am Chem Soc*. 1991; 113:6621–6633.
8. For reviews on the chemistry of bicyclomycin, see: (a) Williams RM, Durham CA. *Chem Rev*. 1988; 88:511–540. *Stereoselective Synthetic and Mechanistic Chemistry of Bicyclomycin* (b) Williams RM. *Atta-ur-Rahman. Studies in Natural Products Chemistry*. Elsevier Pub1993; Amsterdam12
9. Williams RM, Armstrong RW, Maruyama LK, Dung JS, Anderson OP. *J Am Chem Soc*. 1985; 107:3246–3253.
10. (a) Birch AJ, Wright JJ. *J Chem Soc, Chem Commun*. 1969:644–645.(b) Birch AJ, Wright JJ. *Tetrahedron*. 1970; 26:2329–2344. [PubMed: 5419195] (c) Birch AJ, Russell RA. *Tetrahedron*. 1972; 28:2999–3008.(d) Bird BA, Remaley AT, Campbell IM. *Appl Environ Microbiol*. 1981; 42:521–525. [PubMed: 16345847] (e) Bird BA, Campbell IM. *Appl Environ Microbiol*. 1982; 43:345. [PubMed: 16345939] (f) Robbers JE, Straus JW. *Lloydia*. 1975; 38:355–356. [PubMed: 1186436] (g) Paterson RRM, Hawksworth DL. *Trans Br Mycol Soc*. 1985; 85:95–100.(h) Wilson BJ, Yang DTC, Harris TM. *Appl Microbiol*. 1973; 26:633–635. [PubMed: 4751807] (i) Coetzer J. *Acta Cryst*. 1974; B30:2254–2256.
11. Williams RM, Glinka T. *Tetrahedron Lett*. 1986; 27:3581–3584.
12. (a) Williams RM, Glinka T, Kwast E. *J Am Chem Soc*. 1988; 110:5927–5929.(b) Williams RM, Glinka T, Kwast E, Coffman H, Stille JK. *J Am Chem Soc*. 1990; 112:808–821.
13. (a) Polonsky J, Merrien MA, Prange T, Pascard C. *J Chem Soc, Chem Comm*. 1980:601–602.(b) Prange T, Buillion MA, Vuilhorgne M, Pascard C, Polonsky J. *Tetrahedron Lett*. 1981; 22:1977–1980.
14. (a) Yamazaki M, Fujimoto H, Okuyama E, Ohta Y. *Proc Jpn Assoc Mycotoxicol*. 1980; 10:27.(b) Yamazaki M, Okuyama E. *Tetrahedron Lett*. 1981; 22:135–136.(c) Blanchflower SE, Banks RM, Everett JR, Manger BR, Reading C. *J Antibiot*. 1991; 44:492–497. [PubMed: 2061192] (d) Blanchflower SE, Banks RM, Everett JR, Reading C. *J Antibiot*. 1993; 46:1355–1363. [PubMed: 8226314] (e) Whyte AC, Gloer JB. *J Nat Prod*. 1996; 59:1093–1095. [PubMed: 8946752]
15. Porter AEA, Sammes PG. *J Chem Soc Chem Comm*. 1970:1103.
16. Birch AJ. *J Agr Food Chem*. 1971; 19:1088–1092.
17. Baldas J, Birch AJ, Russell RA. *J Chem Soc Perkin Trans I*. 1974:50–52.
18. (a) Sanz-Cervera JF, Glinka T, Williams RM. *J Am Chem Soc*. 1993; 115:347–348.(b) Sanz-Cervera JF, Glinka T, Williams RM. *Tetrahedron*. 1993; 49:8471–8482.
19. (a) Domingo LR, Sanz-Cervera JF, Williams RM, Picher MT, Marco JA. *J Org Chem*. 1997; 62:1662–1667.(b) Domingo LR, Zaragozá RJ, Williams RM. *J Org Chem*. 2003; 68:2895–2902. [PubMed: 12662067]
20. (a) Williams RM, Sanz-Cervera JF, Sancenón F, Marco JA, Halligan K. *J Am Chem Soc*. 1998; 120:1090–1091.(b) Williams RM, Sanz-Cervera JF, Sancenón F, Marco JA, Halligan K. *Bioorg Med Chem*. 1998; 6:1233–1241. [PubMed: 9784865] (c) Sanz-Cervera JF, Williams RM, Marco JA, López-Sánchez JM, González F, Martínez ME, Sancenón F. *Tetrahedron*. 2000; 56:6345–6358.(d) Adams LA, Valente MWN, Williams RM. *Tetrahedron*. 2006; 62:5195–5200.
21. Cushing TD, Sanz-Cervera JF, Williams RM. *J Am Chem Soc*. 1993; 115:9323–9324.(b) Cushing TD, Sanz-Cervera JF, Williams RM. *J Am Chem Soc*. 1996; 118:557–579.
22. (a) Williams RM, Cao J, Tsujishima H. *Angew Chem Int Ed*. 2000; 39:2540–2544.(b) Williams RM, Cao J, Tsujishima H. *J Am Chem Soc*. 2003; 125:12172–12178. [PubMed: 14519003]
23. Artman GD, Grubbs AW, Williams RM. *J Am Chem Soc*. 2007; 129:6336–6342. [PubMed: 17455936]
24. Artman GD, Williams RM. *Org Synth*. 2009; 86:262–273. [PubMed: 21331348]

25. (a) Seebach D, Boes M, Naef R, Schweizer WB. *J Am Chem Soc.* 1983; 105:5390–5398.(b) Beck AK, Blank S, Job K, Seebach D, Sommerfield T. *Org Syn.* 1995; 72:62–73.
26. Chatterjee AK, Choi TL, Sanders DP, Grubbs RH. *J Am Chem Soc.* 2003; 125:11360–11370. [PubMed: 16220959]
27. (a) Baran PS, Guerrero CA, Ambhaikar NB, Hafensteinner BJ. *Angew Chem Int Ed.* 2005; 44:606–609.(b) Baran PS, Guerrero CA, Ambhaikar NB, Hafensteinner BJ. *Angew Chem Int Ed.* 2005; 44:3892–3895.(c) Baran PS, Hafensteinner BD, Ambhaikar NB, Guerrero CA, Gallagher JD. *J Am Chem Soc.* 2006; 128:8678–8693. [PubMed: 16802835]
28. (a) Qian-Cutrone J, Haung S, Shu YZ, Vyas D, Fairchild C, Menendez A, Krampitz K, Dalterio R, Klohr SE, Gao Q. *J Am Chem Soc.* 2002; 124:14556–14557. [PubMed: 12465964] (b) Qian-Cutrone, J.; Krampitz, KD.; Shu, Y-Z.; Chang, LP. US Patent. 6,291,461. 2001. (c) Nussbaum F. *Angew Chem Int Ed.* 2003; 42:2068–3071.(d) Fenical, W.; Jensen, PR.; Cheng, XC. US Patent. 6,066,635. 2000. (e) Sugie Y, Hirai H, Inagaki T, Ishiguro M, Kim YJ, Kojima Y, Sakakibara T, Sakemi S, Sugiura A, Suzuki Y, Brennan L, Duignan J, Huang LH, Sutcliffe J, Kojima N. *J Antibiot.* 2001; 54:911–916. [PubMed: 11827033]
29. (a) Herzon SB, Myers AG. *J Am Chem Soc.* 2005; 127:5342–5344. [PubMed: 15826171] (b) Myers AG, Herzon SB. *J Am Chem Soc.* 2003; 125:12080–12081. [PubMed: 14518979]
30. (a) Kato H, Yoshida T, Tokue T, Nojiri Y, Hirota H, Ohta T, Williams RM, Tsukamoto S. *Angew Chem Int Ed.* 2007; 46:2254–2256.(b) Tsukamoto S, Kato H, Samizo M, Nojiri Y, Onuki H, Hirota H, Ohta T. *J Nat Prod.* 2008; 71:2064–2067. [PubMed: 19053517] (c) Greshock TJ, Grubbs AW, Jiao P, Wicklow DT, Gloer JB, Williams RM. *Angew Chem Int Ed.* 2008; 47:3573–3577.(d) Tsukamoto S, Kato H, Greshock TJ, Hirota H, Ohta T, Williams RM. *J Am Chem Soc.* 2009; 131:3834–3835. [PubMed: 19292484] (e) Tsukamoto S, Kawabata T, Kato H, Greshock TJ, Hirota H, Ohta T, Williams RM. *Org Lett.* 2009; 11:1297–1300. [PubMed: 19281134]
31. (a) Greshock TJ, Grubbs AW, Tsukamoto S, Williams RM. *Angew Chem Int Ed.* 2007; 46:2262–2265.(b) Greshock TJ, Williams RM. *Org Lett.* 2007; 9:4255–4258. [PubMed: 17854197]
32. Finefield JM, Greshock TJ, Sherman DH, Tsukamoto S, Williams RM. unpublished results.
33. (a) Miller KA, Welch TR, Greshock TJ, Ding Y, Sherman DH, Williams RM. *J Org Chem.* 2008; 73:3116–3119. [PubMed: 18345688] (b) Ding Y, Greshock TJ, Miller K, Sherman DH, Williams RM. *Org Lett.* 2008; 10:4863–4866. [PubMed: 18844365]
34. Greshock TJ, Grubbs AW, Williams RM. *Tetrahedron.* 2007; 63:6124–6130. [PubMed: 18596842]
35. Miller KA, Tsukamoto S, Williams RM. *Nature Chem.* 2009; 1:63–68. [PubMed: 20300443]
36. Phil Baran and co-workers, were the first to corroborate the absolute configuration of the (+)-stephacidin A produced by *Aspergillus ochraceus* through their elegant total synthesis of both antipodes; see ref. 27.
37. The Tsukamoto marine-derived Aspergillus sp.: (a) Ding Y, de Wet JR, Cavalcoli J, Li S, Greshock TJ, Miller KA, Finefield JM, Sunderhaus JD, McAfoos T, Tsukamoto S, Williams RM, Sherman DH. *J Am Chem Soc.* 2010; 132:12733–12740. [PubMed: 20722388] Aspergillus versicolor NRRL 35600: (b) Li S, Finefield JM, Tsukamoto S, Williams RM, Sherman DH. unpublished results.
38. (a) Stocking EM, Sanz-Cervera JF, Williams RM. *Angew Chem Int Ed.* 1999; 38:786–789.(b) Stocking EM, Sanz-Cervera JF, Williams RM. *J Am Chem Soc.* 2000; 122:9089–9098.
39. For related work on reverse prenylation, see: Balibar CJ, Howard-Jones AR, Walsh CT. *Nature Chem Biol.* 2007; 3:584–592. [PubMed: 17704773]
40. (a) Stocking E, Sanz-Cervera JF, Williams RM, Unkefer CJ. *J Am Chem Soc.* 1996; 118:7008–7009. ERRATA: *J. Am. Chem. Soc.*, 1997, 119, 9588. (b) Stocking EM, Sanz-Cervera JF, Williams RM. *Angew Chem Int Ed.* 2001; 40:1296–1298.(c) Stocking EM, Sanz-Cervera JF, Unkefer CJ, Williams RM. *Tetrahedron.* 2001; 57:5303–5320.(d) Gray C, Sanz-Cervera JF, Williams RM. *J Am Chem Soc.* 2003; 125:14692–14693. [PubMed: 14640629]
41. Arigoni and Kellenberger studied the biosynthesis of  $\beta$ -methylproline in bottromycin and found this to be derived from *S*-proline and *S*-adenosyl methionine, see: Kellenberger JL. PhD thesis. ETH1997
42. (a) Sanz-Cervera JF, Williams RM. *J Am Chem Soc.* 2002; 124:2556–2559. [PubMed: 11890806] (b) Stocking EM, Sanz-Cervera JF, Williams RM. *J Am Chem Soc.* 2000; 122:1675–1683.

43. Isolation of the asperparalines: (a) Hayashi H, Nishimoto Y, Nozaki H. *Tetrahedron Lett.* 1997; 38:5655–5658.(b) Hayashi H, Nishimoto Y, Akiyama K, Nozaki H. *Biosci Biotechnol Biochem.* 2000; 64(1):111–115. [PubMed: 10705455] (c) Banks RM, Blanchflower SE, Everett JR, Manger BR, Reading C. *J Antibiot.* 1997; 50:840–846. [PubMed: 9402989]
44. For some reviews on the synthesis and biosynthesis of the prenylated indole alkaloids, see: (a) Biosynthesis of Prenylated Alkaloids Derived from Tryptophan. Williams RM, Sanz-Cervera JF, Stocking E, Leeper F, Vederas JC. *Topics in Current Chemistry, Volume on Biosynthesis-Terpenes and Alkaloids.* Springer-Verlag Berlin 2000; 209:97–173.(b) Williams RM. *Chem Pharm Bull.* 2002; 50:711–740. [PubMed: 12045324] (c) Cox RJ, Williams RM. *Acc Chem Res.* 2003; 36:127–139. [PubMed: 12589698] (d) Miller KA, Williams RM. *Chem Soc Rev.* 2009; 38:3160–3174. [PubMed: 19847349] Biomimetic Synthesis of Alkaloids Derived from Tryptophan: Dioxopiperazine Alkaloids (e) Welch T, Williams RM. Poupon E, Nay B. chapter in *Biomimetic Organic Synthesis.* Wiley-VCH 2011:0000.in press(f) Sunderhaus JD, Williams RM. *Israel J Chem.* 2011:0000. (in press).
45. Stocking E, Williams RM. *Angew Chem Int Ed.* 2003; 42:3078–3115.
46. For a review on the asymmetric synthesis of  $\alpha$ -amino acids, see: Williams RM. *Synthesis of Optically Active  $\alpha$ -Amino Acids.* Pergamon Press Oxford 1989; 7
47. Vigneron JP, Kagan H, Horeau A. *Tetrahedron Lett.* 1968;5681–5683.
48. (a) Sinclair PJ, Zhai D, Reibenspies J, Williams RM. *J Am Chem Soc.* 1986; 108:1103–1104.(b) Williams RM, Sinclair PJ, Zhai D, Chen D. *J Am Chem Soc.* 1988; 110:1547–1557.(c) Williams RM, Zhai D, Sinclair PJ. *J Org Chem.* 1986; 51:5021–5022.
49. (a) Williams RM, Sinclair PJ, DeMong D, Chen D, Zhai D. *Org Synth.* 2003; 80:18–30.(b) Williams RM, Sinclair PJ, DeMong DE. *Org Synth.* 2003; 80:31–37.
50. (a) Weijlard J, Pfister K, Swanezy EF, Robinson CA, Tishler M. *J Am Chem Soc.* 1951; 73:1216–1218.for an improved, alternative resolution, see: (b) Dastlik KA, Sundermeier U, Johns DM, Chen Y, Williams RM. *Syn Lett.* 2005:693–696.
51. Sharpless-based methodology has been applied to the synthesis of these amino alcohols, see: Chang HT, Sharpless KB. *Tetrahedron Lett.* 1996; 37:3219–3222.
52. A lipase-based resolution of benzoin has also been reported as a method to prepare (1R, 2S)-erythro-2-Amino-1,2-diphenylethanol: Aoyagi Y, Agata N, Shibata N, Horiguchi M, Williams RM. *Tetrahedron Lett.* 2000; 41:10159–10162.
53. van den Nieuwendijk AMCH, Warmerdam EGJC, Brussee J, van der Gen A. *Tetrahedron: Asymm.* 1995; 6:801–806.
54. (a) Williams RM. *Aldrichimica Acta.* 1992; 25:11–25.(b) Williams RM, Hendrix JA. *Chem Rev.* 1992; 92:889–917.(c) Williams RM. Hassner A. *Advances in Asymmetric Synthesis.* JAI Press 1995; 1:45–94.(d) Burnett C, Williams RM. *Strategies and Tactics in Organic Synthesis.* 2008; 7(8):268–327.New Tricks in Amino Acid Synthesis: Applications to Complex Natural Products. ACS Symposium Book Series (e) Soloshonok VA, Izawa K. American Chemical Society Washington, D.C.Burnett C, Williams RM. 2009; 26:420–442.
55. Williams RM, Sinclair PJ, Zhai W. *J Am Chem Soc.* 1988; 110:482–483.
56. Williams RM, Im MN, Cao J. *J Am Chem Soc.* 1991; 113:6976–6981.
57. Williams RM, Fegley GJ. *Tetrahedron Lett.* 1992; 33:6755–6758.
58. Williams RM, Fegley GJ. *J Am Chem Soc.* 1991; 113:8796–8806.
59. Williams RM, Yuan C. *J Org Chem.* 1992; 57:6519–6527.
60. Williams RM, Colson PJ, Zhai W. *Tetrahedron Lett.* 1994; 35:9371–9374.
61. Williams RM, Yuan C. *J Org Chem.* 1994; 59:6190–6193.
62. (a) Sebahar P, Williams RM. *J Am Chem Soc.* 2000; 122:5666–5667.(b) Sebahar PR, Osada H, Williams RM. *Tetrahedron.* 2002; 58:6311–6322.
63. Onishi T, Sebahar PR, Williams RM. *Org Lett.* 2003; 5:3135–3137. [PubMed: 12917000]
64. (a) Scott JD, Williams RM. *Angew Chem Int Ed.* 2001; 40:1463–1465.(b) Williams RM, Scott JD. *J Am Chem Soc.* 2002; 124:2951–2956. [PubMed: 11902886] (c) Scott JD, Tippie TN, Williams RM. *Tetrahedron Lett.* 1998; 39:3659–3662.
65. DeMong DE, Williams RM. *Tetrahedron Lett.* 2001; 42:3529–3532.

66. DeMong DE, Williams RM. *J Am Chem Soc.* 2003; 125:8561–8565. [PubMed: 12848564]
67. Jain RP, Williams RM. *Tetrahedron.* 2001; 57:6505–6509.
68. Jain RP, Williams RM. *Tetrahedron Lett.* 2001; 42:4437–4440.
69. Jain RP, Albrecht BK, DeMong DE, Williams RM. *Org Lett.* 2001; 24:4287–4289. [PubMed: 11784199]
70. Jain RP, Williams RM. *J Org Chem.* 2002; 67:6361–6365. [PubMed: 12201754]
71. Lane JW, Chen Y, Williams RM. *J Am Chem Soc.* 2005; 127:12684–12690. [PubMed: 16144418]
72. (a) Looper R, Williams RM. *Tetrahedron Lett.* 2001; 42:769–771.(b) Looper RE, Runnegar MTC, Williams RM. *Tetrahedron.* 2006; 62:4549–4562.
73. Looper RE, Williams RM. *Angew Chem Int Ed.* 2004; 43:2930–2933.
74. Looper RE, Runnegar MTC, Williams RM. *Angew Chem Int Ed.* 2005; 44:3879–3881.
75. (a) Ohtani I, Moore RE, Runnegar MTC. *J Am Chem Soc.* 1992; 114:7941–7942.(b) Moore RE, Ohtani I, Moore BS, deKoning CB, Yoshida WY, Runnegar MTC, Carmichael WW. *Gazz Chim Ital.* 1993; 123:329–336.(c) Norris RL, Eaglesham GK, Pierens G, Shaw GR, Smith MJ, Chiswell RK, Seawright AA, Moore MR. *Environ Toxicol.* 1999; 14:163–165.(d) Li R, Carmichael WW, Brittain S, Eaglesham GK, Shaw GR, Mahakant A, Noparatnaraporn N, Yongmanitchai W, Kaya K, Watanabe MM. *Toxicol.* 2001; 39:973–980. [PubMed: 11223086] (e) Norris RLG, Eaglesham GK, Shaw GR, Senogles P, Chiswell RK, Smith MJ, Davis BC, Seawright AA, Moore MR. *Environ Toxicol.* 2001; 16:391–396. [PubMed: 11594025] (f) Griffiths DJ, Saker ML. *Environ Toxicol.* 2003; 18:78–93. [PubMed: 12635096]
76. Harada K, Ohtani I, Iwamoto K, Suzuki M, Watanabe MF, Watanabe M, Terao K. *Toxicol.* 1994; 32:73–84. [PubMed: 9237339]
77. (a) Banker R, Carmeli S, Hadas O, Teltsch B, Porat R, Sukenik A. *J Phycol.* 1997; 33:613–616.(b) Banker R, Teltsch B, Sukenik A, Carmeli S. *J Nat Prod.* 2000; 63:387–389. [PubMed: 10757726]
78. Li RH, Carmichael WW, Brittain S, Eaglesham GK, Shaw GR, Liu YD, Watanabe MM. *J Phycol.* 2001; 37:1121–1126.
79. (a) Shaw GR, Seawright AA, Moore MR, Lam PKS. *Therapeutic Drug Monitoring.* 2000; 22:89–92. [PubMed: 10688267] (b) Fessard V, Bernard C. *Environ Toxicol.* 2003; 18:353–359. [PubMed: 14502589]
80. (a) Shaw GR, Seawright AA, Moore MR, Lam PKS. *Therapeutic Drug Monitoring.* 2000; 22:89–92. [PubMed: 10688267] (b) Fessard V, Bernard C. *Environ Toxicol.* 2003; 18:353–359. [PubMed: 14502589]
81. Banker R, Carmeli S, Werman M, Teltsch B, Porat R, Sukenik A. *J Toxicol Environ Health Part A.* 2001; 62:281–288. [PubMed: 11245397]
82. (a) Runnegar MJT, Kong SM, Zhong YZ, Ge JL, Lu SC. *Biochem Biophys Res Comm.* 1994; 201:235–241. [PubMed: 8198579] (b) Runnegar MT, Kong SM, Zhong YZ, Lu SC. *Biochem Pharmacol.* 1995; 49:219–225. [PubMed: 7840799]
83. (a) Shen XY, Lam PKS, Shaw GR, Wickramasinghe W. *Toxicol.* 2002; 40:1499–1501. [PubMed: 12368121] (b) Falconer IR, Humpage AR. *Environ Toxicol.* 2006; 21:299–304. [PubMed: 16841306]
84. Xie C, Runnegar MTC, Snider BB. *J Am Chem Soc.* 2000; 122:5017–5024.
85. Heintzelman GR, Fang WK, Keen SP, Wallace GA, Weinreb SM. *J Am Chem Soc.* 2001; 123:8851–8853. [PubMed: 11535093]
86. White JD, Hansen JD. *J Am Chem Soc.* 2002; 124:4950–4951. [PubMed: 11982346]
87. (a) Cui CB, Kakeya H, Osada H. *J Antibiot.* 1996; 49:832–835. [PubMed: 8823522] (b) Cui CB, Kakeya H, Osada H. *Tetrahedron.* 1996; 51:12651–12666.
88. For total syntheses of spirotryprostatin A, see: (a) Edmonson SD, Danishefsky SJ. *Angew Chem Int Ed.* 1998; 37:1138–1140.(b) Edmonson S, Danishefsky SJ, Sepp-Lorenzino L, Rosen N. *J Am Chem Soc.* 1999; 121:2147–2155.(c) Onishi T, Sebahar PR, Williams RM. *Org Lett.* 2003; 5:3135–3137. [PubMed: 12917000] (d) Onishi T, Sebahar PR, Williams RM. *Tetrahedron.* 2004; 60:9503–9515.(e) Miyake FY, Yakushijin K, Horne DA. *Org Lett.* 2004; 6:4249–4251. [PubMed: 15524455]

89. For total syntheses of spirotryprostatin B, see: (a) von Nussbaum F, Danishefsky SJ. *Angew Chem Int Ed*. 2000; 39:2175–2178.(b) Overman LE, Rosen MD. *Angew Chem Int Ed*. 2000; 39:4596–4599.(c) Wang H, Ganesan H. *J Org Chem*. 2000; 65:4685–4693. [PubMed: 10959875] (d) Bagul TD, Lakshmaiah G, Kawataba T, Fuji K. *Org Lett*. 2002; 4:249–251. [PubMed: 11796062] (e) Meyers C, Carreira EM. *Angew Chem Int Ed*. 2003; 42:694–696.(f) Marti C, Carreira EM. *Eur J Org Chem*. 2003;2209–2219.(g) Miyake FY, Yakushijin K, Horne DA. *Angew Chem Int Ed*. 2004; 43:5357–5360.(h) Marti C, Carreira EM. *J Am Chem Soc*. 2005; 127:11505–11515. [PubMed: 16089481] (i) Trost BM, Stiles DT. *Org Lett*. 2007; 9:2763–2766. [PubMed: 17592853] For a review, see: (j) Lindel T. *Nachrichten aus der Chemie*. 2000; 48:1498–1501.
90. See ref. #62; see also: Sebahar P. PhD dissertation. Colorado State University2003
91. See ref. #63 and Onishi T, Sebahar PR, Williams RM. *Tetrahedron*. 2004; 60:9503–9515.
92. (a) Namba K, Greshock TJ, Sundermeier U, Li H, Williams RM. *Tetrahedron Lett*. 2010; 51:6557–6559. [PubMed: 21286237] see also: (b) Namba K, Kaihara Y, Yamamoto H, Imagawa H, Tanino K, Williams RM, Nishizawa M. *Chem Eur J*. 2009;6560–6563.
93. (a) Kinnel RB, Gehrken HP, Scheuer PJ. *J Am Chem Soc*. 1993; 115:3376–3377.(b) Kinnel RB, Gehrken HP, Swali R, Skoropowski G, Scheuer PJ. *J Org Chem*. 1998; 63:3281–3286.
94. For synthetic approaches to palau'amine and congeners, see references cited in 92a.
95. Seiple IB, Su S, Young IS, Lewis CA, Yamaguchi J, Baran PS. *Angew Chem Int Ed*. 2010; 49:1095–1098.
96. (a) Buchanan MS, Carroll AR, Addepalli R, Avery VM, Hooper JNA, Quinn RJ. *J Org Chem*. 2007; 72:2309–2317. [PubMed: 17315930] (b) Grube A, Köck M. *Angew Chem Int Ed*. 2007; 46:2320–2324.
97. Ahrendt KA, Williams RM. *Org Lett*. 2004; 6:4539–4541. [PubMed: 15548070]
98. Lo MMC, Neumann CS, Nagayama S, Perlstein EO, Schreiber SL. *J Am Chem Soc*. 2004; 126:16077–16086. [PubMed: 15584743]
99. Tomita F, Takahashi K, Tamaoki T. *J Antibiot*. 1984; 37:1268–1272. [PubMed: 6094411]
100. (a) Williams RM, Glinka T, Flanagan ME, Gallegos R, Coffman H, Pei D. *J Am Chem Soc*. 1992; 114:733–740.(b) Williams RM, Glinka T, Gallegos R, Ehrlich P, Flanagan ME, Coffman H, Park G. *Tetrahedron*. 1991; 47:2629–2642.(c) Williams RM, Flanagan ME, Tippie T. *Biochemistry*. 1994; 33:4086–4092. [PubMed: 8142411]
101. Flanagan ME, Rollins SB, Williams RM. *Chem Biol*. 1995; 2:147–156. [PubMed: 9383416]
102. Flanagan ME, Williams RM. *J Org Chem*. 1995; 60:6791–6797.
103. (a) Vincent G, Williams RM. *Angew Chem Int Ed*. 2007; 46:1517–1520.(b) Vincent G, Chen Y, Lane JW, Williams RM. *Heterocycles*. 2007; 72:385–398.
104. Fishlock D, Williams RM. *J Org Chem*. 2008; 73:9594–9600. [PubMed: 18687003]
105. Chan C, Heid R, Zheng SP, Guo JS, Zhou BS, Furuuchi T, Danishefsky SJ. *J Am Chem Soc*. 2005; 127:4596–4598. [PubMed: 15796524]
106. Zheng S, Chan C, Furuuchi T, Wright BJD, Zhou B, Guo J, Danishefsky SJ. *Angew Chem Int Ed*. 2006; 45:1754–1759.
107. Endo A, Yanagisawa A, Abe M, Tohma S, Kan T, Fukuyama T. *J Am Chem Soc*. 2002; 124:6552–6554. [PubMed: 12047173]
108. Williams RM, Herberich B. *J Am Chem Soc*. 1998; 120:10272–10273.
109. Hill GC, Wunz TP, Mackenzie NE, Gooley PR, Remers WA. *J Med Chem*. 1991; 34:2079–2088. [PubMed: 2066979]
110. (a) Garcia-Carbonero R, Supko JG, Maki RG, Manola J, Ryan DP, Harmon D, Puchalski TA, Goss G, Seiden MV, Waxman A, Quigley MT, Lopez T, Sancho MA, Limeno J, Guzman C, Demetri GD. *J Clinical Oncol*. 2005; 23:5484–5492. [PubMed: 16110008] (b) Garcia-Carbonero R, Supko JG, Manola J, Seiden MV, Harmon D, Ryan DP, Quigley MT, Merriam P, Canniff J, Goss G, Matulonis U, Maki RG, Lopez T, Puchalski TA, Sancho MA, Gomez J, Guzman C, Jimeno J, Demetri GD. *J Clinical Oncol*. 2004; 22:1480–1490. [PubMed: 15084621] (c) Hing J, Perea-Ruixo J, Stuyckens K, Soto-Matos A, Lopez-Lazaro L, Zannikos P. *Clinical Pharmacol Therapeutics*. 2008; 83:130–143.

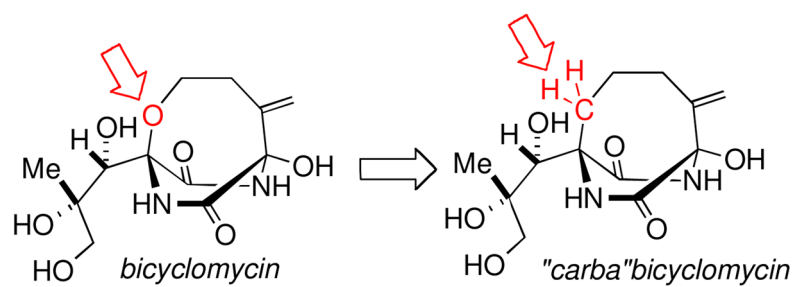
111. Cuevas C, Perez M, Martin MJ, Chicharro JL, Fernandez-Rivas C, Flores M, Francesch A, Gallego P, Zarzuelo M, de la Calle F, Garcia J, Polanco C, Rodriguez I, Manzanares I. *Org Lett.* 2000; 2:2545–2548. [PubMed: 10956543]
112. (a) Piel J, Hui D, Wen G, Butzke D, Platzer M, Fusetani N, Matsunaga S. *Proc Natl Acad Sci USA.* 2004; 101:16222–7. [PubMed: 15520376] (b) Sudek S, Lopanik NB, Waggoner LE, Hildebrand M, Anderson C, Liu H, Patel A, Sherman DH, Haygood MG. *J Nat Prod.* 2007; 70:67–74. [PubMed: 17253852]
113. Paclitaxel the generic name for Taxol<sup>®</sup>, is a registered trademark to Bristol-Myers Squibb. Due to greater familiarity with the word taxol, this will be used throughout this article and the symbol <sup>®</sup> has been deleted for the sake of clarity and brevity. For reviews see: (a) Georg GI, Ali SM, Zygmunt J, Jayasinghe LR. *Exp Opin Ther Patents.* 1994; 4:109–120.(b) Jenkins ANPR, Lawerence NJ. *Contemp Org Synth.* 1994;47–75.(c) Nicolaou KC, Dai WM, Guy RK. *Angew Chem Int Ed.* 1994; 33:15–44.(d) Guenard D, Gueritte-Voegelein F, Potier P. *Acc Chem Res.* 1993; 26:160–167.(e) Kingston DG. *Pharmac Ther.* 1991; 52:1–34.(f) Swindell CS. *Org Prep Proc Inter.* 1991; 23:465–543.*Biosynthesis of Taxol*(g)Floss HG, Mocek U, Suffness M. *Taxol: Science and Applications.* CRC PressBoca Raton, Florida1995(h) Rohr J. *Angew Chem Int Ed.* 1997; 36:2190–2195.
114. Wani MC, Tayler HL, Wall ME, Coggon P, McPhail AT. *J Am Chem Soc.* 1971; 93:2325–2327. [PubMed: 5553076]
115. For some leading references on the total synthesis of taxol and synthetic approaches, see: (a) Juo RA, Kim RR, Williams HB, Harusawa AD, Lowenthal SRE, Yogai S. *J Am Chem Soc.* 1988; 110:6558–6560.(b) Wender PA, Mucciaro TP. *J Am Chem Soc.* 1992; 114:5878–5879.(c) Nicolaou KC, Yang Z, Liu JJ, Nantermet PG, Guy RK, Claiborne CF, Renaud J, Couladouros EA, Paulvannan K, Sorensen EJ. *Nature.* 1994; 367:630–634. [PubMed: 7906395] (d) Nicolaou KC, Nantermet PG, Ueno H, Guy RK, Couladouros EA, Sorensen EJ. *J Am Chem Soc.* 1995; 117:624–633.(e) Nicolaou KC, Liu JJ, Yang Z, Ueno H, Sorensen EJ, Claiborne CF, Guy RK, Hwang CK, Nakada M, Nantermet PG. *J Am Chem Soc.* 1995; 117:634–644.(f) Yang KCZ, Liu J-J, Nantermet PG, Claiborne CF, Renaud J, Guy RK, Shibayama K. *J Am Chem Soc.* 1995; 117:645–652.(g) Nicolaou KC, Ueno H, Liu JJ, Nantermet PG, Yang Z, Renaud J, Paulvannan K, Chadha R. *J Am Chem Soc.* 1995; 117:653–659.(and references cited therein) (h) Holton RA, Somoza C, Kim HB, Liang F, Biediger J, Boatman PD, Shindo M, Smith CC, Kim S, Nadizadeh H, Suzuki Y, Tao C, Vu P, Tang S, Zhang P, Murthi KK, Gentile LN, Liu JH. *J Am Chem Soc.* 1994; 116:1597–1598.(i) idem. *J Am Chem Soc.* 1994; 116:1599–1600.(j) Masters JJ, Link JT, Snyder LB, Young WB, Danishefsky SJ. *Angew Chem Int Ed.* 1995; 34:1723–1726.(k) Wender PA, Badham NF, Conway SP, Floreancig PE, Glass TE, Granicher C, Houze JB, Janichen J, Lee D, Marquess DG, McGrane PL, Meng W, Mucciaro TP, Muhlebach M, Natchus MG, Paulsen H, Rawlins DB, Satkofsky J, Shuker AJ, Sutton JC, Taylor RE, Tomooka K. *J Am Chem Soc.* 1997; 119:2755–2756.(l) Wender PA, Badham NF, Conway SP, Floreancig PE, Glass TE, Houze JB, Krauss NE, Lee D, Marquess DG, McGrane PL, Meng W, Natchus MG, Shuker AJ, Sutton JC, Taylor RE. *J Am Chem Soc.* 1997; 119:2757–2758.(m) Morihira K, Hara R, Kawahara S, Nishimori T, Nakamura N, Kusama H, Kuwajima I. *J Am Chem Soc.* 1998; 120:12980–12981. (n) Paquette LA, Wang HL, Su Z, Zhao M. *J Am Chem Soc.* 1998; 120:5213–5225.(o) Mukaiyama T, Shiina I, Iwadare H, Saitoh M, Nishimura T, Ohkawa N, Sakoh H, Nishimura K, Tani Y, Hasegawa M, Yamada K, Saitoh K. *Chem Eur.* 1999; 5:121–161.
116. Han KH, Fleming P, Walker K, Loper M, Chilton WS, Mocek U, Gordon MP, Floss HG. *Plant Sci.* 1994; 95:187–196.
117. (a) Stierle A, Strobel G, Stierle D. *Science.* 1993; 260:214–216. [PubMed: 8097061] (b) Strobel G, Yang X, Sears J, Kramer R, Sidhu R, Hess WM. *Microbiol.* 1996; 142:435–440.(c) Strobel GA, Hess WM, Ford E, Sidhu R, Yang X. *J Ind Microbiol.* 1996; 17:417–423.(d) Strobel GA, Hess WM, Li Jia-Yao, Ford E, Sears J, Sidhu RS, Summerell B. *Australian J Botany.* 1997; 45:1073–1082.(e) Hoffman A, Khan W, Worapong J, Strobel G, Griffin D, Arbogast B, Barofsky D, Boone RB, Ning L, Zheng P, Daley L. *Spectroscopy.* 1999; 13:22–32.Bioactive Metabolites of the Endophytic Fungi of Pacific Yew, *Taxus brevifolia* (f)Stierle A, Stierle D, Strobel G, Bignami G, Grothaus P. *Taxane Anticancer Agents.* American Chemical Society1995; 6:82–97. (g) Shrestha K, Strobel GA, Shrivastava SP, Gewali MB. *Planta medica.* 2001; 67:374–376. [PubMed: 11458463] (h) Li JY, Sidhu RS, Ford EJ, Long DM, Strobel GA. *J Ind Microbiol*

- Biotech. 1998; 20:259–264.(i) Metz AM, Haddad A, Worapong J, Long DM, Ford EJ, Hess WM, Strobel GA. *Microbiol.* 2000; 146:2079–2089.
118. (a) Fleming PE, Knaggs AR, He XG, Mocek U, Floss HG. *J Am Chem Soc.* 1994; 116:4137–4138.(b) Fleming PE, Mocek U, Floss HG. *J Am Chem Soc.* 1993; 115:805–807.
119. (a) Harrison JW, Scrowston RM, Lythgoe B. *J Chem Soc (C).* 1966;1933–1945.see also: (b) Gueritte-Voegelein F, Guenard D, Potier P. *J Nat Prod.* 1987; 50:9–18. [PubMed: 2885400]
120. (a) Koepp AE, Hezari M, Zajicek J, Vogel BS, LaFever RE, Lewis NG, Croteau R. *J Biol Chem.* 1995; 270:8686–8690. [PubMed: 7721772] (b) Hezari M, Lewis NG, Croteau R. *Arch Biochem Biophys.* 1995; 322:437–444. [PubMed: 7574719] (c) Lin X, Hezari M, Koepp AE, Floss HG, Croteau R. *Biochemistry.* 1996; 35:2968–2977. [PubMed: 8608134] (d) Wildung MR, Croteau R. *J Biol Chem.* 1996; 271:9201–9204. [PubMed: 8621577] (e) Hezari M, Croteau R. *Planta Med.* 1997; 63:291–295. [PubMed: 9270370]
121. Williams DC, Caroll BJ, Jin Q, Rithner CD, Lenger SR, Floss HG, Coates RA, Williams RM, Croteau R. *Chem Biol.* 2000; 7:969–977. [PubMed: 11137819]
122. (a) Rubenstein SM, Williams RM. *J Org Chem.* 1995; 60:7215–7223.(b) Rubenstein, SM. PhD dissertation. Colorado State University; 1996. Elucidating the Biosynthetic Pathway to Taxol. (c) Vazquez A, Williams RM. *J Org Chem.* 2000; 65:7865–7869. [PubMed: 11073592]
123. (a) Hefner J, Rubenstein SM, Ketchum REB, Gibson DM, Williams RM, Croteau R. *Chem Biol.* 1996; 3:479–489. [PubMed: 8807878] see also: (b)Borman SCEN. Researchers Probe steps of Taxol Biosynthesis. 1996 July 1.:27–29.
124. (a) Walker K, Ketchum REB, Hezari M, Gatfield D, Goleniowski M, Barthol A, Croteau R. *Arch Biochem Biophys.* 1999; 364:273–279. [PubMed: 10190984] (b) Walker K, Croteau R. *Proc Natl Acad Sci USA.* 2000; 97:583–587. [PubMed: 10639122] (c) Walker K, Schoendorf A, Croteau R. *Arch Biochem Biophys.* 2000; 374:371–380. [PubMed: 10666320]
125. For leading references, see: (a)Herbert BA. The Biosynthesis of Secondary Metabolites. Chapman and HallLondon1981(b)Nakanishi K, Goto T, Ito S, Nozoe S. Natural Products Chemistry. IKodansha, LtdTokyo1974; (c)Towers GHN, Stafford HA. Recent Advances in Phytochemistry Vol. 24: Biochemistry of the Mevalonic Acid Pathway to Terpenoids. Plenum PressNew York1990(d)Luckner M. Secondary Metabolism in Microorganisms, Plants and Animals. Springer-VerlagBerlin1990
126. Jennewein S, Long RM, Williams RM, Croteau R. *Chem Biol.* 2004; 11:379–387. [PubMed: 15123267]
127. (a) Horiguchi T, Rithner CD, Croteau R, Williams RM. *Tetrahedron.* 2003; 59:267–273.(b) Rubenstein SM, Vazquez A, Williams RM. *J Labeled Cmpd Radiopharm.* 2000; 43:481–491.(c) Horiguchi T, Rithner CD, Croteau R, Williams RM. *J Org Chem.* 2002; 67:4901–4903. [PubMed: 12098303] (d) Horiguchi T, Li H, Croteau R, Williams RM. *Tetrahedron.* 2008; 64:6561–6567. [PubMed: 19122848] (e) Tohru Horiguchi T, Rithner CD, Croteau R, Williams RM. *J Labeled Cmpd Radiopharm.* 2008; 51:325–328.
128. Chau M, Croteau R. *Arch Biochem Biophys.* 2004; 427:48–57. [PubMed: 15178487]
129. Chau M, Jennewein S, Walker K, Croteau R. *Chem Biol.* 2004; 11:663–672. [PubMed: 15157877]
130. Croteau R. unpublished results.
131. Schoendorf A, Rithner CD, Williams RM, Croteau R. *Proc Natl Acad Sci USA.* 2001; 98:1501–1506. [PubMed: 11171980]
132. Jennewein S, Rithner CD, Williams RM, Croteau R. *Proc Natl Acad Sci USA.* 2001; 98:13595–13600. [PubMed: 11707604]
133. Kaspera R, Croteau R. *Phytochem Rev.* 2006; 5:433–444. [PubMed: 20622990]
134. (a) Ketchum REB, Croteau R. Plant Metabolomics (in Biotechnology in Agriculture and Forestry). 2006; 57:291–309.(b) Ketchum REB, Horiguchi T, Qiu D, Williams RM, Croteau R. *Phytochem.* 2007; 68:335–341.
135. (a) Uchida I, Takase S, Kayakiri H, Kiyoto S, Hashimoto M, Tada T, Koda S, Morimoto Y. *J Am Chem Soc.* 1987; 109:4108–4109.(b) Iwami M, Kiyoto S, Terano H, Kohsaka M, Aoki H, Imanaka H. *J Antibiotics.* 1987; 40:589–593. [PubMed: 3610817] (c) Kiyoto S, Shibata T, Yamashita M, Komori T, Okuhara M, Terano H, Kohsaka M, Aoki H, Imanaka H. *J Antibiotics.*

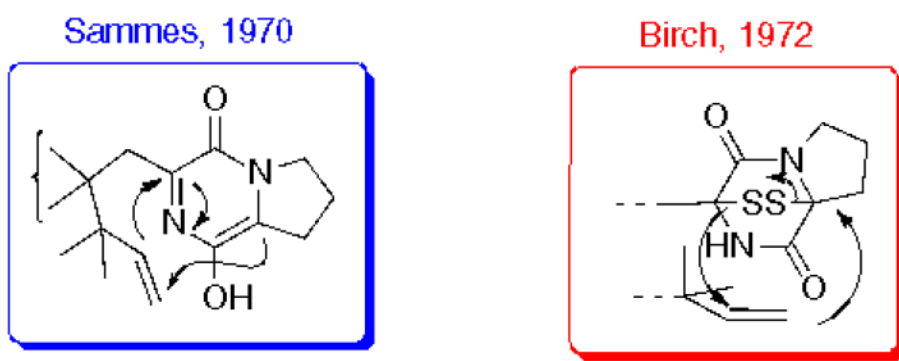
- 1987; 40:594–599. [PubMed: 3610818] (d) Fujita T, Takase S, Otsuka T, Terano H, Kohsaka M. *J Antibiotics*. 1988; 41:392–394. [PubMed: 3366695]
136. (a) Shimomura K, Hirai O, Mizota T, Matsumoto S, Mori J, Shibayama F, Kikuchi H. *J Antibiot*. 1987; 40:600–606. [PubMed: 3610819] (b) Hirai O, Shimomura K, Mizota T, Matsumoto S, Mori J, Kikuchi H. *J Antibiot*. 1987; 40:607–611. [PubMed: 3112079] (c) Shimomura K, Manda T, Mukumoto S, Masuda K, Nakamura T, Mizota T, Matsumoto S, Nishigaki F, Oku T, More J, Shibayama F. *Cancer Res*. 1988; 48:1116–1172.(d) Masuda K, Makamura T, Shimomura K, Shibata T, Terano H, Kohsaka M. *J Antibiot*. 1988; 41:1497–1499. [PubMed: 3192500] (e) Masuda K, Nakamura T, Mizota T, Mori J, Shimomura K. *Cancer Res*. 1988; 48:5172–5177. [PubMed: 3409243] (f) Nakamura T, Masada K, Matsumoto S, Oku T, Manda T, Mori J, Shimomura K. *Jpn J Pharmacol*. 1989; 49:317–324. [PubMed: 2501546]
137. (a) Naoe Y, Inami M, Matsumoto S, Nishigaki F, Tsujimoto S, Kawamura I, Miyayasu K, Manda T, Shimomura K. *Cancer Chemother Pharmacol*. 1998; 42:31–36. [PubMed: 9619755] (b) Naoe Y, Inami M, Kawamura I, Nishigaki F, Tsujimoto S, Matsumoto S, Manda T, Shimomura K. *Jpn J Cancer Res*. 1998; 89:666–672. [PubMed: 9703365] (c) Naoe Y, Inami M, Takagaki S, Matsumoto S, Kawamura I, Nishigaki F, Tsujimoto S, Manda T, Shimomura K. *Jpn J Cancer Res*. 1998; 89:1047–1054. [PubMed: 9849584] (d) Naoe Y, Inami M, Matsumoto S, Takagaki S, Fujiwara T, Yamazaki S, Kawamura I, Nishigaki F, Tsujimoto S, Manda T, Shimomura K. *Jpn J Cancer Res*. 1998; 89:1306–1317. [PubMed: 10081492] (e) Naoe Y, Kawamura I, Inami M, Matsumoto S, Nishigaki F, Tsujimoto S, Manda T, Shimomura K. *Jpn J Cancer Res*. 1998; 89:1318–1325. [PubMed: 10081493] (f) Furuse K, Hasegawa K, Kudo S, Niitaru H. Proceedings of the American Society of Clinical Oncology. 1999; 18:179a, abstract #689.(g) Ravandi F, Wenske C, Royca M, Hoff P, Brito R, Zukowski T, Mekki Q, Pazdur R. *Proc Am Soc Clinical Onc*. 1999; 18:225a, abstract #867.
138. (a) Beijnen JH, Lingeman H, Underberg WJM, Vanmunster HA. *J Pharm Biomed Anal*. 1986; 4:275. [PubMed: 16867594] (b) Tomasz M. *Chem Biol*. 1995; 2:575–579. [PubMed: 9383461]
139. For a comprehensive review on DNA cross-linking agents, see: (a) Rajski SR, Williams RM. *Chem Rev*. 1998; 98:2723–2796. [PubMed: 11848977] for an excellent review of oxyl radical-based damage to DNA, see: (b) Breen AP, Murphy JA. *Free Radical Biol Med*. 1995; 18:1033–1076. [PubMed: 7628729]
140. (a) Baluna R, Rizo J, Gordon BE, Ghetie V, Vitetta E. *Proc Natl Acad Sci USA*. 1999; 96:3957–3962. [PubMed: 10097145] (b) Rafi-Janajreh AQ, Chen Dawai, Schmits Rudolf, Mak TW, Grayson RL, Sponenberg DP, Nagarkatti M, Nagarkatti PS. *J Immunol*. 1999; 163:1619–1627. [PubMed: 10415067] (c) Baluna R, Vitetta E. *Immunopharmacol*. 2001; 37:117–132.(d) Teelucksingh S, Padfield PL, Edwards CRWQ. *J Med*. 1990; 75:515–524.(e) Barnadas MA, Cisteros A, Dolors S, Pascual E, Puig X, de Moragas JM. *J Am Acad Dermatol*. 1995; 32:364–366. [PubMed: 7829741]
141. (a) Williams RM, Rajski SR, Rollins SB. *Chem Biol*. 1997; 4:127–137. [PubMed: 9190287] (b) Huang H, Rajski SR, Williams RM, Hopkins PB. *Tetrahedron Lett*. 1994; 35:9669–9672.
142. (a) Fukuyama T, Xu L, Goto S. *J Am Chem Soc*. 1992; 114:383–385.(b) Schkeryantz JM, Danishefsky SJ. *J Am Chem Soc*. 1995; 117:4722–4723.(c) Katoh T, Itoh E, Yoshino T, Terashima S. *Tetrahedron Lett*. 1996; 37:3471–3474.(d) Yoshino T, Nagata Y, Itoh E, Hashimoto M, Katoh T, Terashima S. *Tetrahedron Lett*. 1996; 37:3475–3478.(e) Katoh T, Yoshino T, Nagata Y, Nakatani S, Terashima S. *Tetrahedron Lett*. 1996; 37:3479–3482.(f) Katoh T, Itoh E, Yoshino T, Terashima S. *Tetrahedron*. 1997; 53:10229–10238.(g) Yoshino T, Nagata Y, Itoh E, Hashimoto M, Katoh T, Terashima S. *Tetrahedron*. 1997; 53:10239–10252.(h) Katoh T, Nagata Y, Yoshino T, Nakatani S, Terashima S. *Tetrahedron*. 1997; 53:10253–10270.(i) Katoh T, Terashima S. *J Synth Org Chem Jpn*. 1997; 55:946–957.(j) Fellows IM, Kaelin DE Jr, Martin SF. *J Am Chem Soc*. 2000; 122:10781–10787.(k) Ducray R, Ciufolini MA. *Angew Chem Int Ed*. 2002; 41:4688–4691.(l) Suzuki M, Kambe M, Tokuyama H, Fukuyama T. *Angew Chem Int Ed*. 2002; 41:4686–4688.(m) Paleo MR, Aurrecochea N, Jung KY, Rapoport H. *J Org Chem*. 2003; 68:130–138. [PubMed: 12515471] (n) Trost BM, O'Boyle BM. *Org Lett*. 2008; 10:1369–1372. [PubMed: 18318539]
143. Judd T, Williams RM. *Angew Chem Int Ed*. 2002; 41:4683–4685.

144. (a) Rollins SB, Williams RM. *Tetrahedron Lett.* 1997; 38:4033–4036.(b) Williams RM, Rollins SB, Judd TC. *Tetrahedron*. 2000; 56:521–532.(c) Judd T, Williams RM. *Org Lett.* 2002; 4:3711–3714. [PubMed: 12375925]
145. (a) Tepe JJ, Williams RM. *Angew Chem Int Ed*. 1999; 38:3501–3503.(b) Tepe JJ, Kosogof C, Williams RM. *Tetrahedron*. 2002; 58:3553–3559.
146. Williams RM, Tepe J. *J Am Chem Soc.* 1999; 121:2951–2955.(b) Kosogof C, Tepe JJ, Williams RM. *Tetrahedron Lett.* 2001; 42:6641–6643.
147. Subramanian V, Ducept P, Williams RM, Luger K. *Chem Biol.* 2007; 14:553–563. [PubMed: 17524986]
148. (a) Beckerbauer L, Tepe J, Cullison J, Reeves R, Williams RM. *Chem Biol.* 2000; 7:805–812. [PubMed: 11033083] (b) Beckerbauer L, Tepe JJ, Eastman RA, Mixter P, Williams RM, Reeves R. *Chem Biol.* 2002; 8:427–441. [PubMed: 11983332]
149. (a) Mao Y, Varoglu M, Sherman DH. *Chem Biol.* 1999; 6:251–263. [PubMed: 10099135] (b) Varoglu M, Mao Y, Sherman DH. *J Am Chem Soc.* 2001; 123:6712–6713. [PubMed: 11439066] (c) Sheldon PR, Mao Y, He M, Sherman DH. *J Bacteriol.* 1999; 181:2199–2208. [PubMed: 10094699] (d) Belcourt MF, Penketh PG, Hodnick WF, Johnson DA, Sherman DH, Rockwell S, Sartorelli AC. *Proc Natl Acad Sci USA.* 1999; 96:10489–10494. [PubMed: 10468636] (e) He M, Sheldon P, Sherman DH. *Proc Natl Acad Sci USA.* 2001; 98:926–931. [PubMed: 11158572] (f) Martin TWZ, Dauter Y, Devedjev P, Sheffield M, He M, Sherman DH, Derewenda ZS, Derewenda U. *Structure.* 2002; 10:933–942. [PubMed: 12121648]
150. Chamberland S, Sherman DH, Williams RM. *Org Lett.* 2009; 11:791–794. [PubMed: 19161340]
151. Taunton J, Hassig CA, Schreiber SL. *Science.* 1996; 272:408–11. [PubMed: 8602529]
152. Grozinger CM, Hassig CA, Schreiber SL. *Proc Natl Acad Sci, USA.* 1999; 96:4868–4873. [PubMed: 10220385]
153. Minucci S, Pelicci PG. *Nature Rev Cancer.* 2006; 6:38–51. [PubMed: 16397526]
154. Johnstone RW. *Nature Rev Drug Discovery.* 2002; 1:287–299.
155. McLaughlin F, La Thangue NB. *Current Drug Targets: Inflammation & Allergy.* 2004; 3:213–219. [PubMed: 15180476]
156. Lin HS, Hu CY, Chan HY, Liew YY, Huang HP, Lepescheux L, Bastianelli E, Baron R, Rawadi G, Clement-Lacroix P. *British J Pharmacol.* 2007; 150:862–872.
157. Avila AM, Burnett BG, Taye AA, Gabanella F, Knight MA, Hartenstein P, Cizman Z, Di Prospero NA, Pellizzoni L, Fischbeck KH, Sumner CJ. *J Clinical Investig.* 2007; 117:659–671. [PubMed: 17318264]
158. Cao H, Stamatoyannopoulos G. *Am J Hematol.* 2006; 81:981–983. [PubMed: 16888791]
159. Hockly E, Richon VM, Woodman B, Smith DL, Zhou X, Rosa E, Sathasivam K, Ghazi-Noori S, Mahal A, Lowden PAS, Steffan JS, Marsh JL, Thompson LM, Lewis CM, Marks PA, Bates GP. *Proc Natl Acad Sci, USA.* 2003; 100:2041–2046. [PubMed: 12576549]
160. Meinke PT, Liberator P. *Curr Med Chem.* 2001; 8:211–235. [PubMed: 11172676]
161. Rodriguez M, Aquino M, Bruno I, De Martino G, Taddei M, Gomez-Paloma L. *Curr Med Chem.* 2006; 13:1119–1139. [PubMed: 16719774]
162. Piekarz RL, Frye AR, Wright JJ, Steinberg SM, Liewehr DJ, Rosing DR, Sachdev V, Fojo T, Bates SE. *Clinl Cancer Res.* 2006; 12:3762–3773.
163. Shah MH, Binkley P, Chan K, Xiao J, Arbogast D, Collamore M, Farra Y, Young D, Grever M. *Clin Cancer Res.* 2006; 12:3997–4003. [PubMed: 16818698]
164. (a) Curtin M, Glaser K. *Curr Med Chem.* 2003; 10:2373–2392. [PubMed: 14529480] (b) Remiszewski SW. *Curr Med Chem.* 2003; 10:2393–2402. [PubMed: 14529481]
165. (a) Xu WS, Parmigiani RB, Marks PA. *Oncogene.* 2007; 26:5541–5552. [PubMed: 17694093] (b) Kelly WK, Marks PA. *Nature Clin Practice Oncol.* 2005; 2:150–157.(c) Glozak MA, Seto E. *Oncogene.* 2007; 26:5420–5432. [PubMed: 17694083] (d) Yang XJ, Gregoire S. *Mol Cell Biol.* 2005; 25:2873–2884. [PubMed: 15798178] (e) Grozinger CM, Schreiber SL. *Chem Biol.* 2002; 9:3–16. [PubMed: 11841934]
166. Li KW, Wu J, Xing W, Simon JA. *J Am Chem Soc.* 1996; 118:7237–7238.

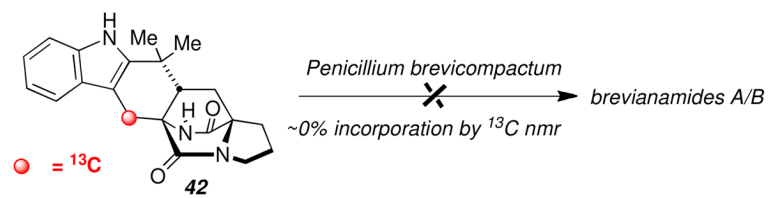
167. Johns DM, Greshock TJ, Noguchi Y, Williams RM. Org Lett. 2008; 10:613–616. [PubMed: 18205373]
168. (a) Taori K, Paul VJ, Luesch H. J Am Chem Soc. 2008; 130:1806–1807. [PubMed: 18205365] (b) Taori K, Paul VJ, Luesch H. J Am Chem Soc. 2008; 130:13506–13506.
169. Bowers A, West N, Taunton J, Schreiber SL, Bradner JE, Williams RM. J Am Chem Soc. 2008; 130:11219–11222. [PubMed: 18642817]
170. (a) Ying Y, Taori K, Kim H, Hong J, Luesch H. J Am Chem Soc. 2008; 130:8455–8459. [PubMed: 18507379] (b) Chen F, Gao AH, Li J, Nan FJ. Chem Med Chem. 2010; 53:4654–4667. (c) Ying Y, Liu Y, Byeon SR, Kim H, Luesch H, Hong J. Org Lett. 2009; 10:4021–4024. [PubMed: 18707106] (d) Numajiri Y, Takahashi T, Takagi M, Shin-ya K, Doi T. SynLett. 2008;2483–2486.(e) Ghosh A, Kulkarni S. Org Lett. 2008; 10:3907–3909. [PubMed: 18662003] (f) Seiser T, Kamena F, Cramer N. Angew Chem Int Ed. 2008; 47:6483–6485.(g) Seiser T, Cramer N. Chimia. 2009; 63:19–22.(h) Nasveschuk CG, Ungermannova D, Liu X, Phillips AJ. Org Lett. 2008; 10:3595–3598. [PubMed: 18616341] (i) Ren Q, Dai L, Zhang H, Tan W, Xu Z, Ye T. Syn Lett. 2008;2379–2383.
171. Greshock TJ, Noguchi Y, West N, Schreiber SL, Wiest O, Bradner JE, Williams RM. J Am Chem Soc. 2009; 131:2900–2905. [PubMed: 19193120]
172. Bowers AL, West N, Newkirk TL, Troutman-Youngman AE, Schreiber SL, Wiest O, Bradner JE, Williams RM. Org Lett. 2009; 11:1301–1304. [PubMed: 19239241]



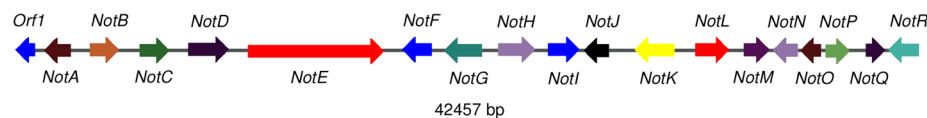
**Figure 1.**  
Design of isosteric “carba”bicyclomycin analog.



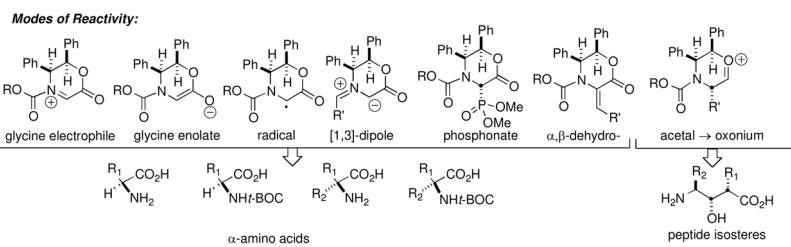
**Figure 2.**  
Sammes and Birch proposals for the construction of the bicyclo[2.2.2]diazaoctane core structure.

**Figure 3.**

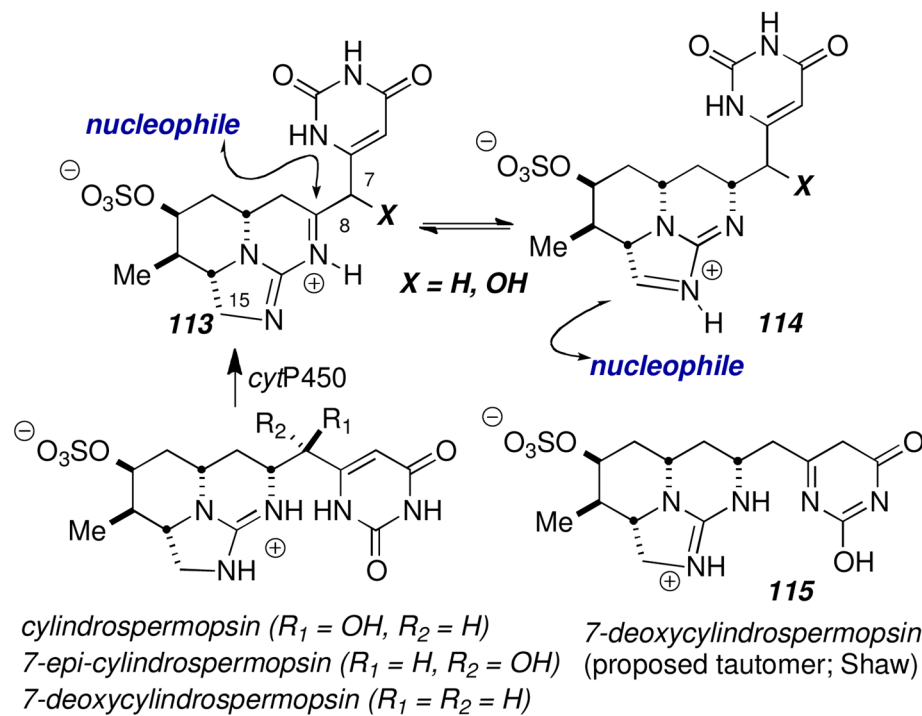
Attempted precursor incorporation experiment with racemic cycloadduct **42**.



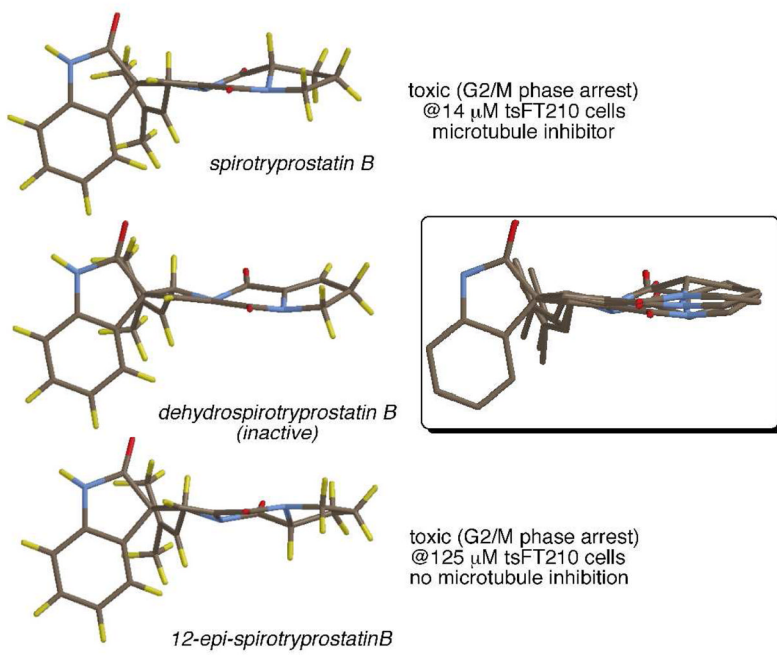
**Figure 4.**  
The notoamide (*not*) biosynthetic gene cluster.



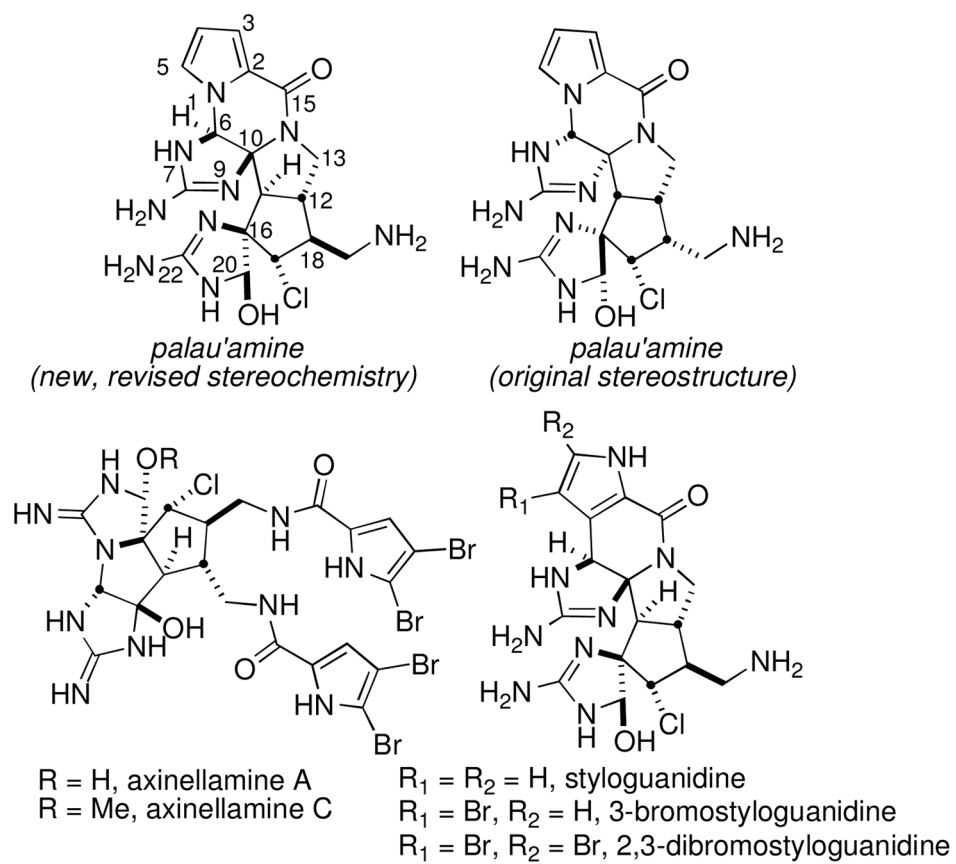
**Figure 5.**  
Various modes of reactivity accessible to the diphenyloxazinones.



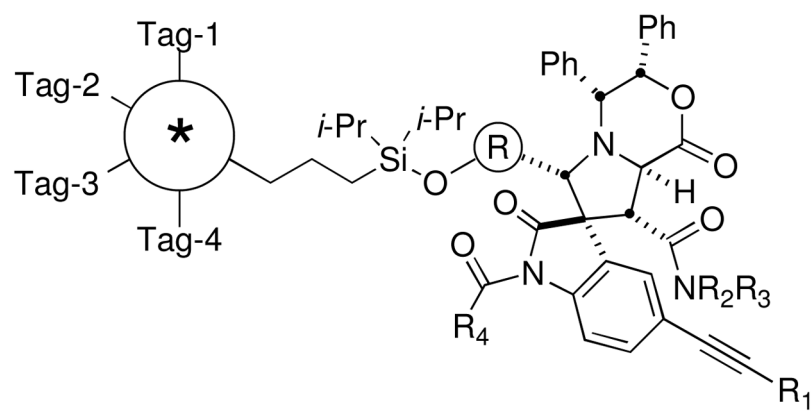
**Figure 6.**  
Biomechanistic queries on the cylindrospermopsins.



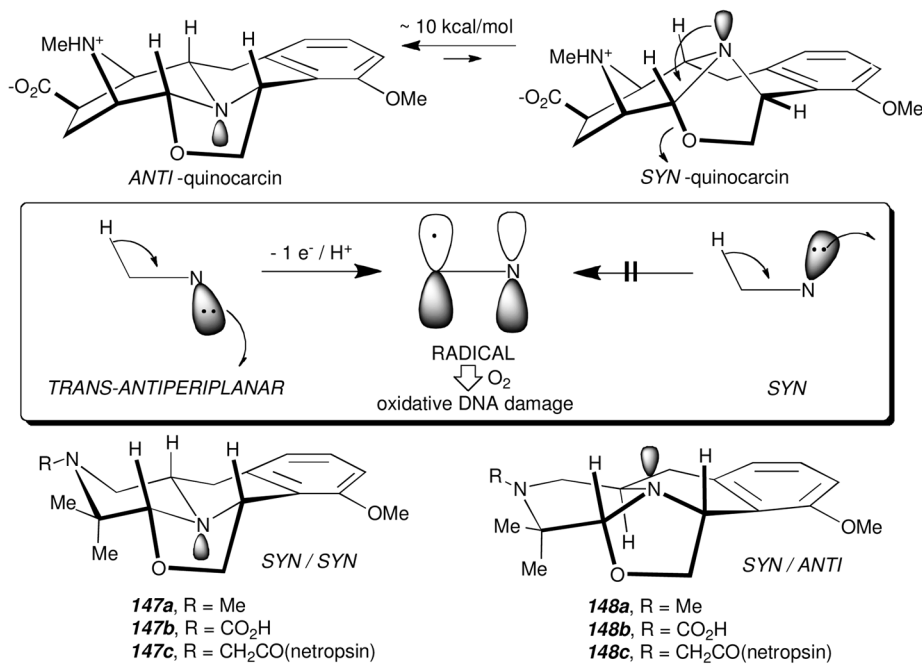
**Figure 7.**  
Overlay of spirotryprostatin B, C-12-*epi*-spirotryprostatin B and dehydrospirotryprostatin B.



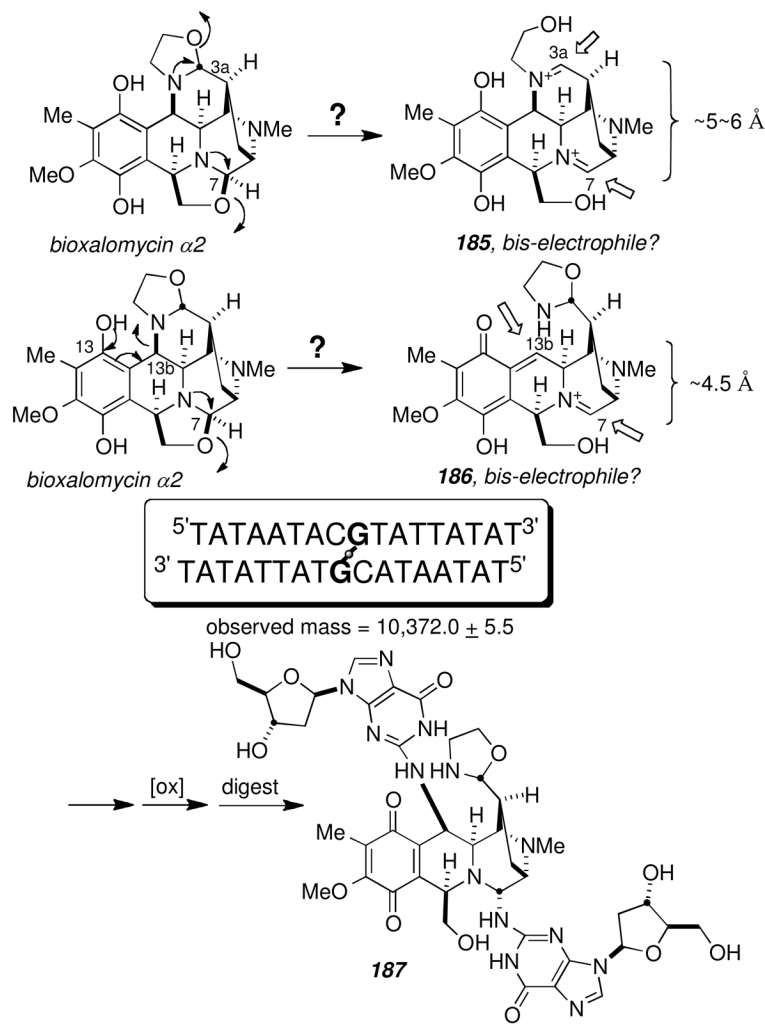
**Figure 8.**  
Structures of palau'amine and congeners.



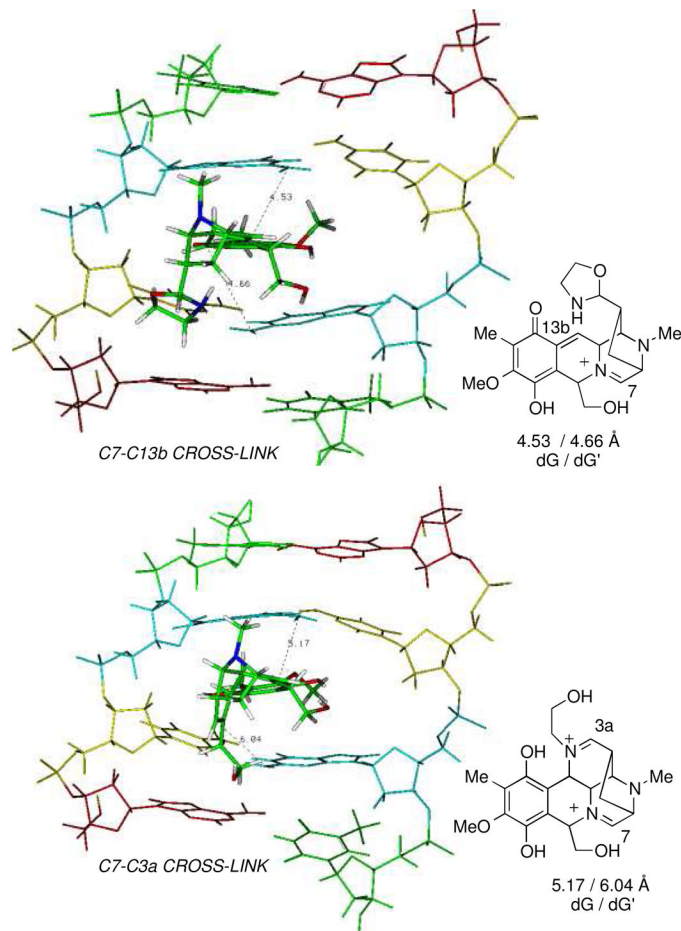
**Figure 9.**  
Schreiber's spirooxindole library.



**Figure 10.**  
Stereoelectronic control of redox disproportionation.

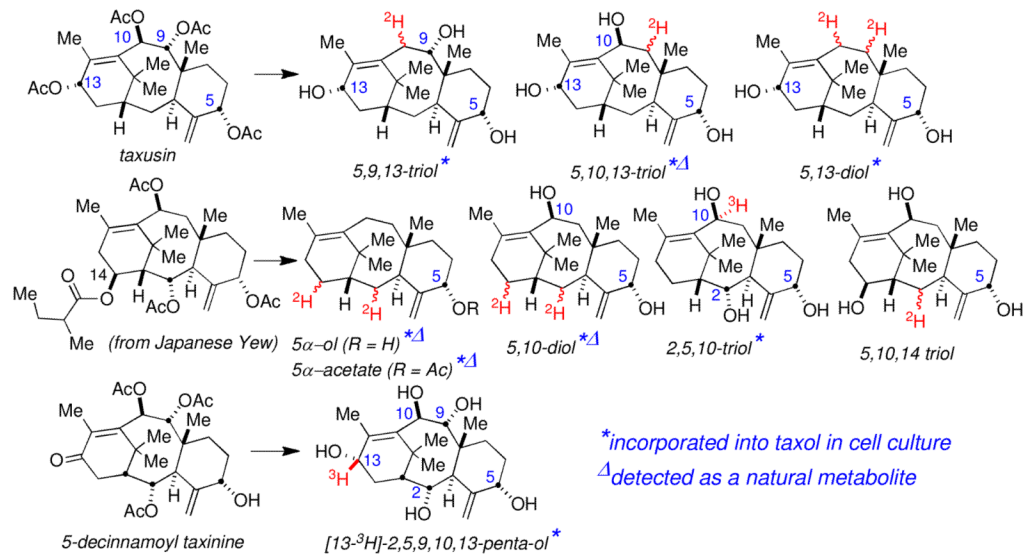
**Figure 11.**

Proposed mechanism and structure of the bioxalomycin-induced covalent interstrand DNA cross-link.

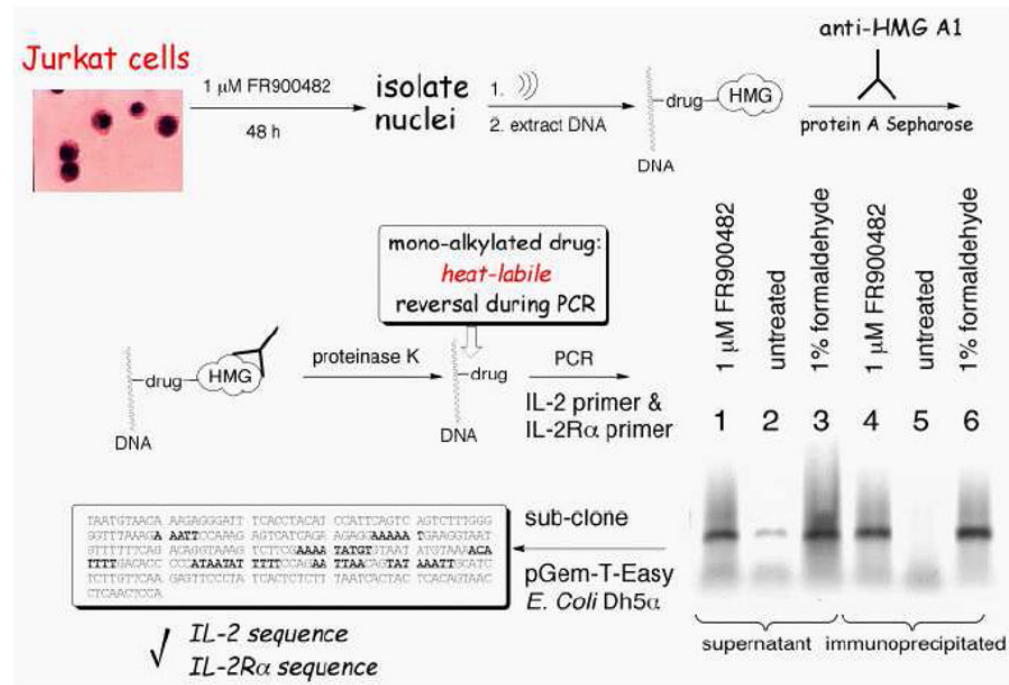


**Figure 12.**

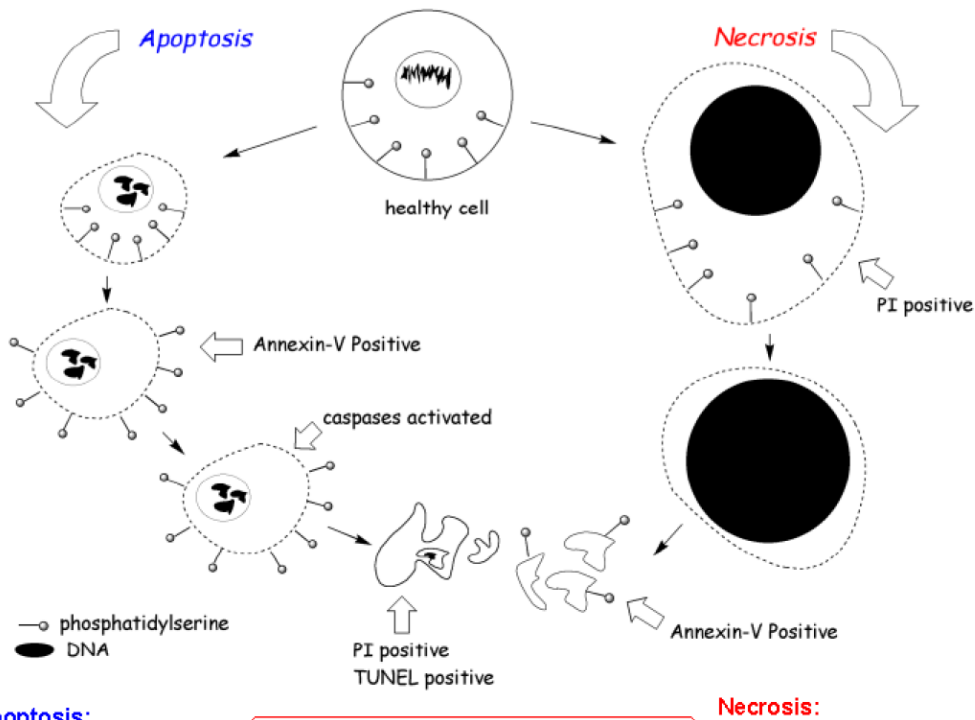
Molecular modeling of the two most reasonable modes for interstrand cross-link formation by bioxalomycin  $\alpha 2$ .



**Figure 13.**  
Semi-synthesis of lightly oxygenated taxoids

**Figure 14.**

ChIP assay used to demonstrate the cross-linking of FR900482 to HMG-A1 bound to chromosomal DNA in Jurkat cells.

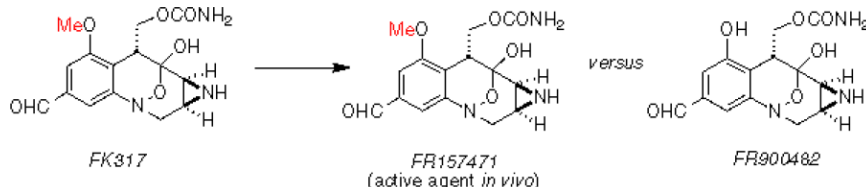
**Apoptosis:**

Cytoplasmic shrinkage  
Changes in Ca<sup>+2</sup>, ATP  
Caspases activated  
Fragmentation of DNA  
Phosphatidylserine flips early  
Phagocytosis of apoptotic bodies

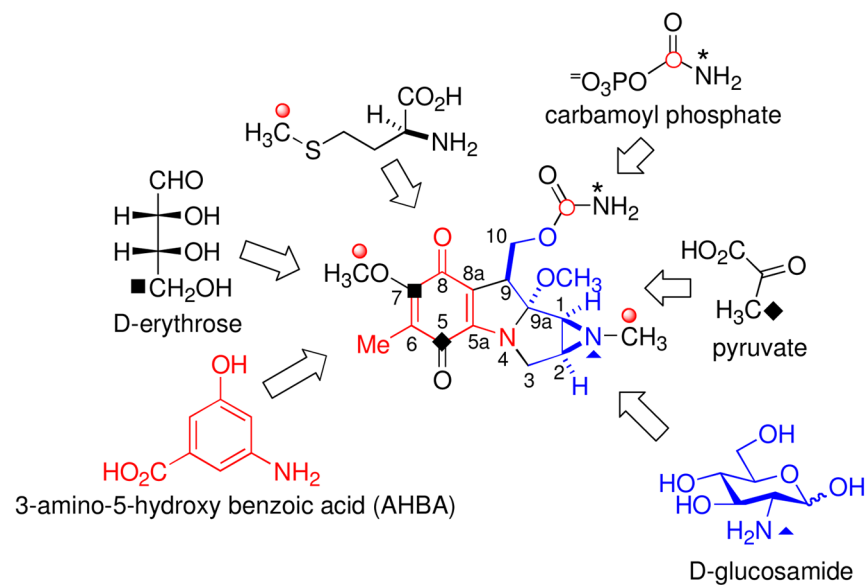
**FR900482:** necrosis at all concentrations  
**FK317:** necrosis at low concentrations  
switching to apoptosis above 1 μM!

**Necrosis:**

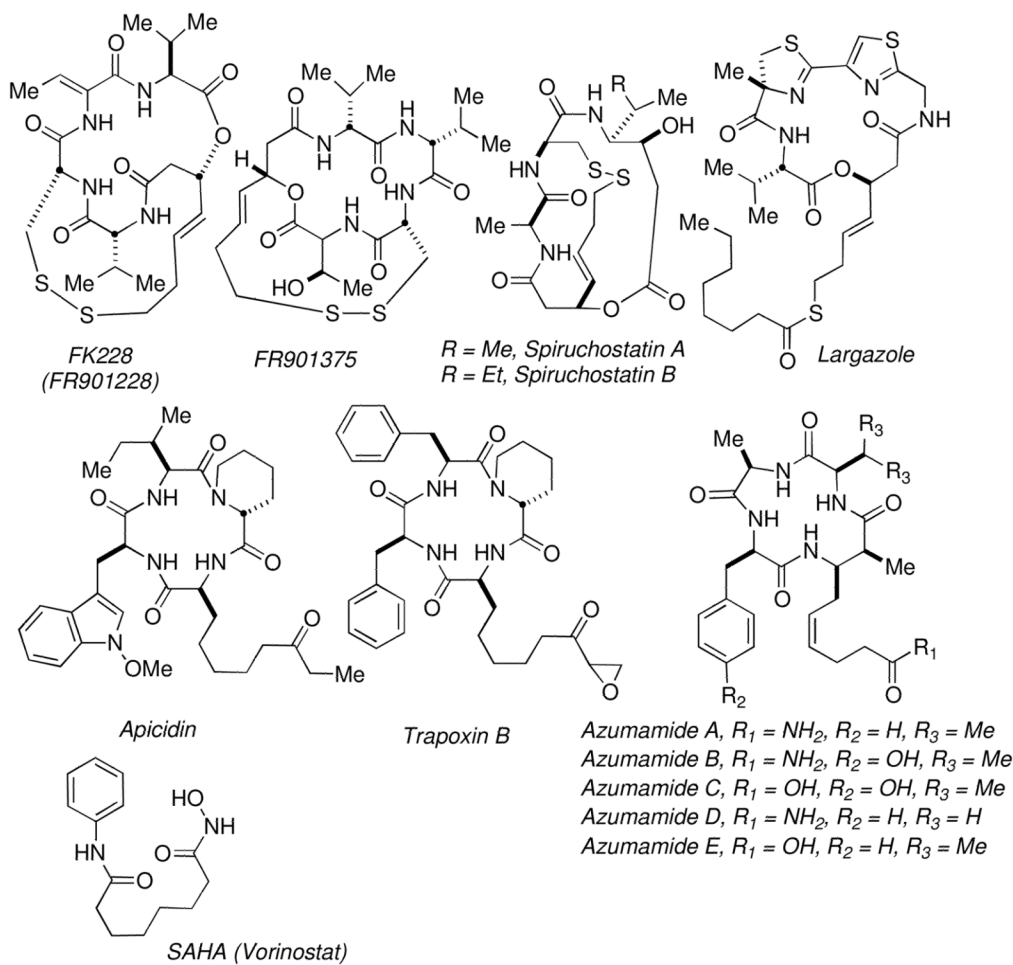
Cytoplasmic enlargement  
Nuclear enlargement  
Chromatin condensation  
Cytoplasmic leakage  
Phosphatidylserine flips late  
Inflammatory response

**Figure 15.**

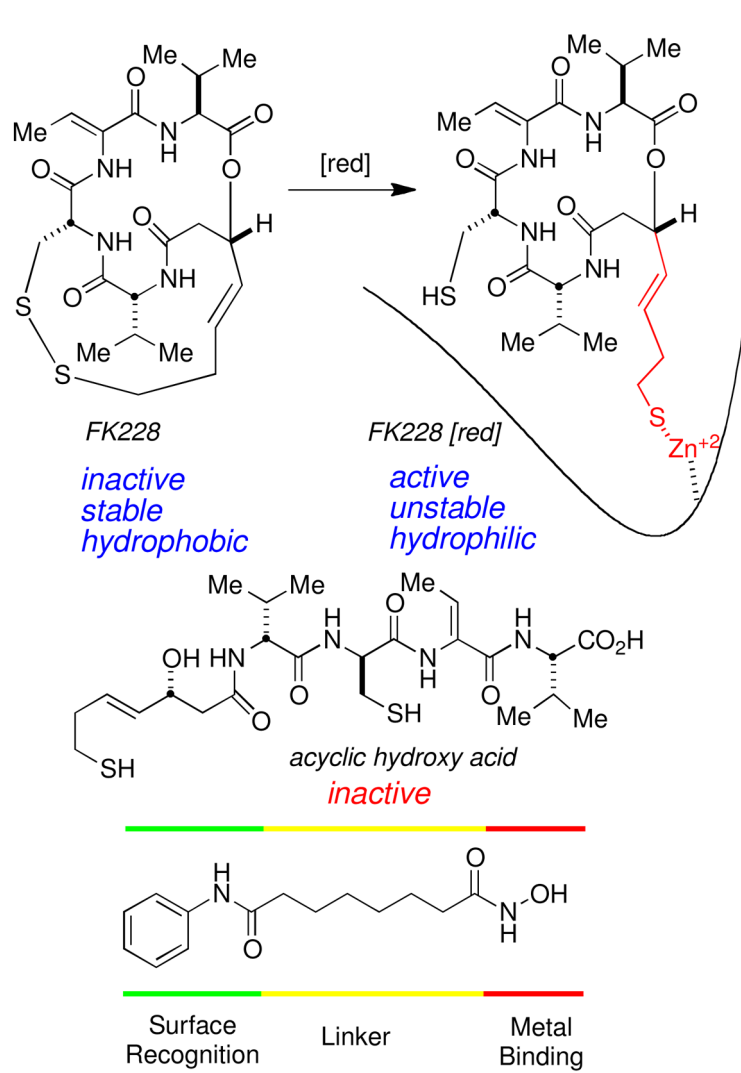
Apoptotic *versus* necrotic cell death mediated by FR900482 and FK317.

**Figure 16.**

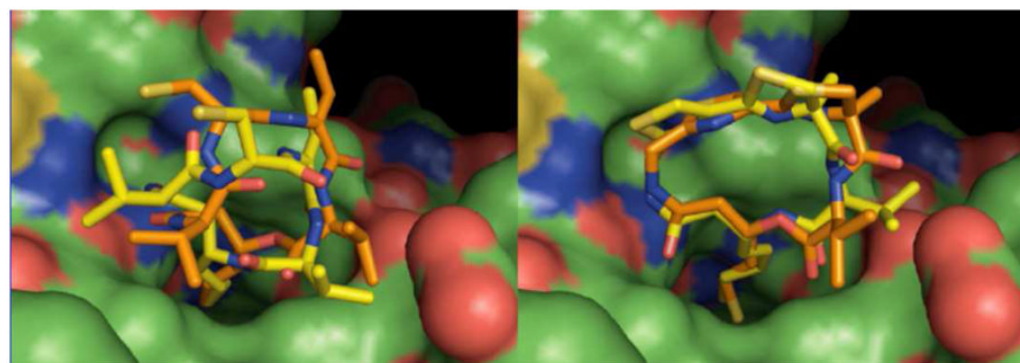
Radiolabeled precursor incorporation studies on the mitomycins.



**Figure 17.**  
Structures of some known HDAC inhibitors.

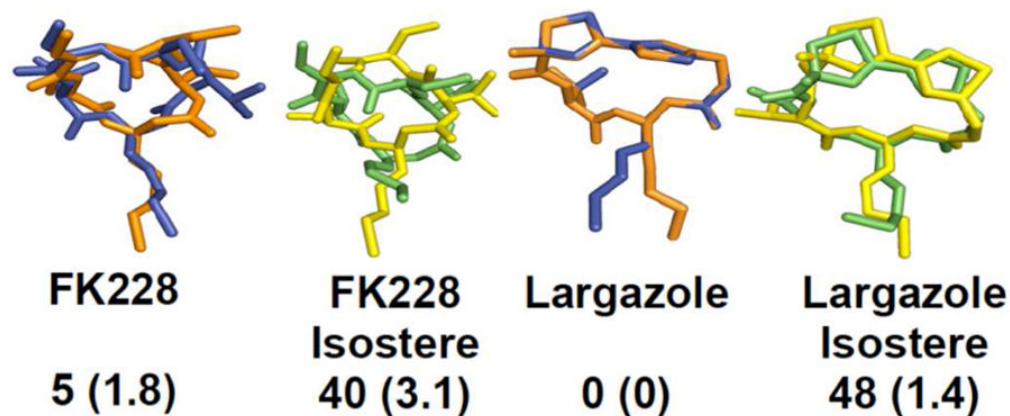


**Figure 18.**  
Mechanism of activation of FK228 and HDACi model.



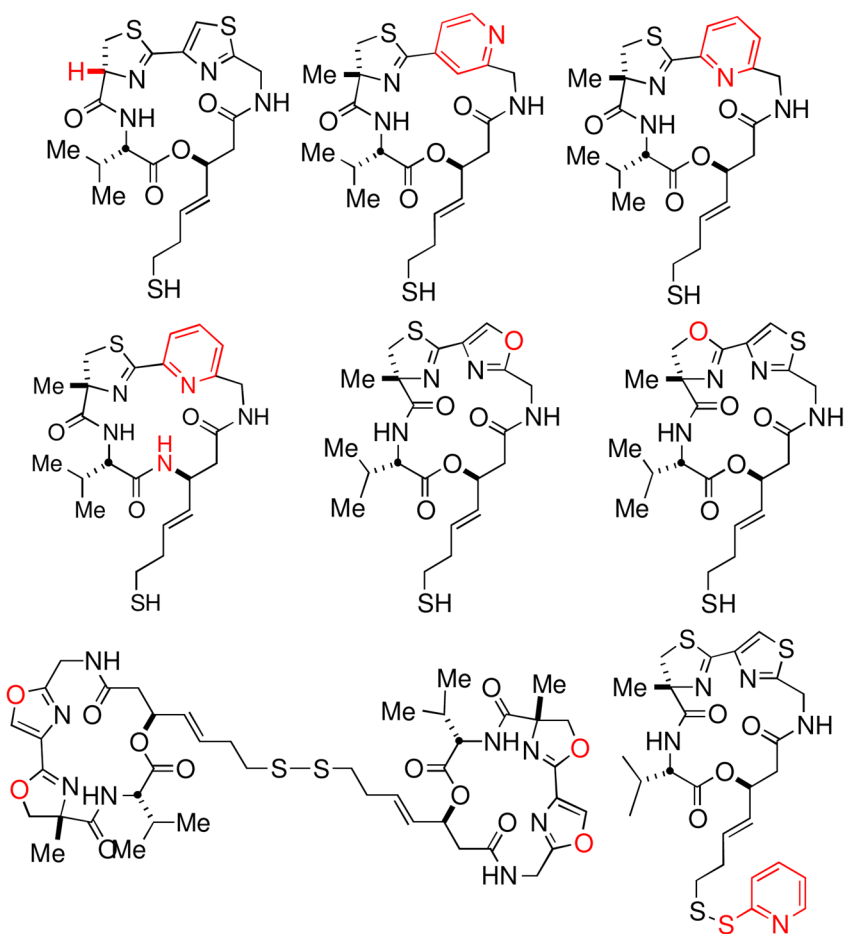
**Figure 19.**

Coordination mode of FK228 (left) and largazole thiol (right) to the HDAC1 active site.  
Depsipeptides are shown in orange and amide isosteres are shown in yellow.

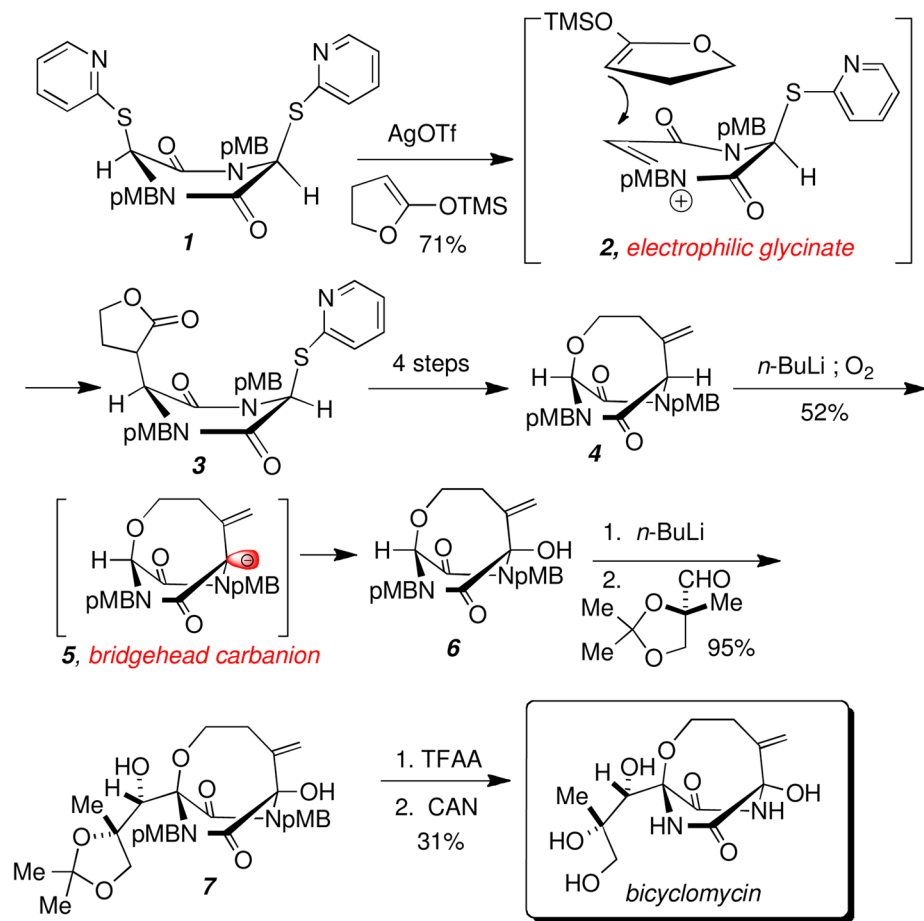


**Figure 20.**

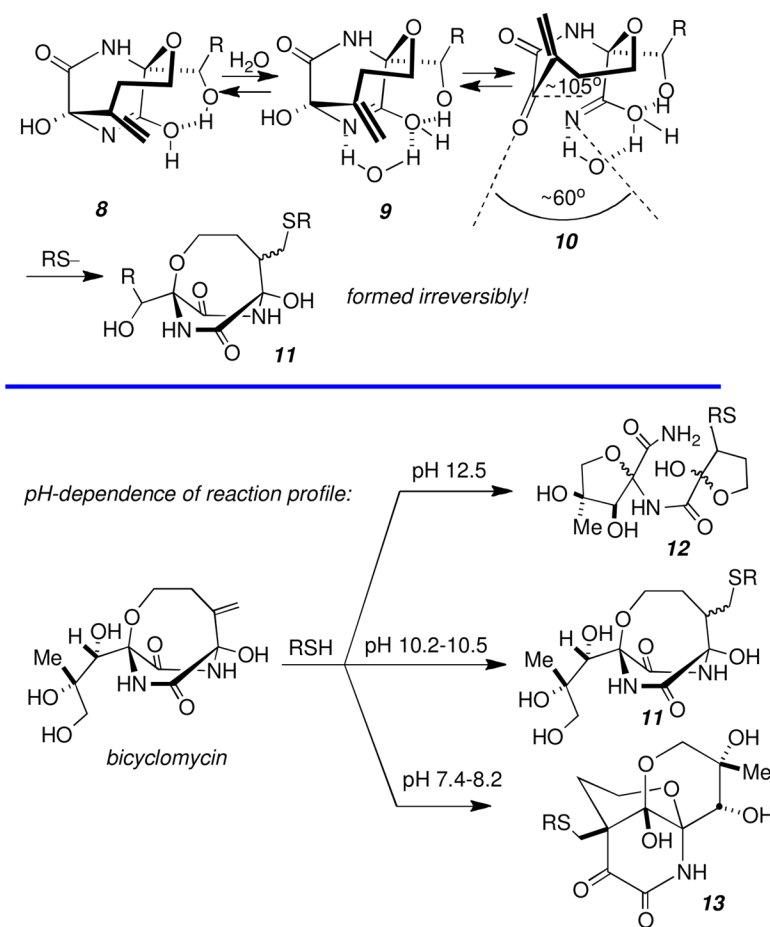
Superimposed lowest and binding conformations of FK228 and largazole as well as their peptide isosteres.

**Figure 21.**

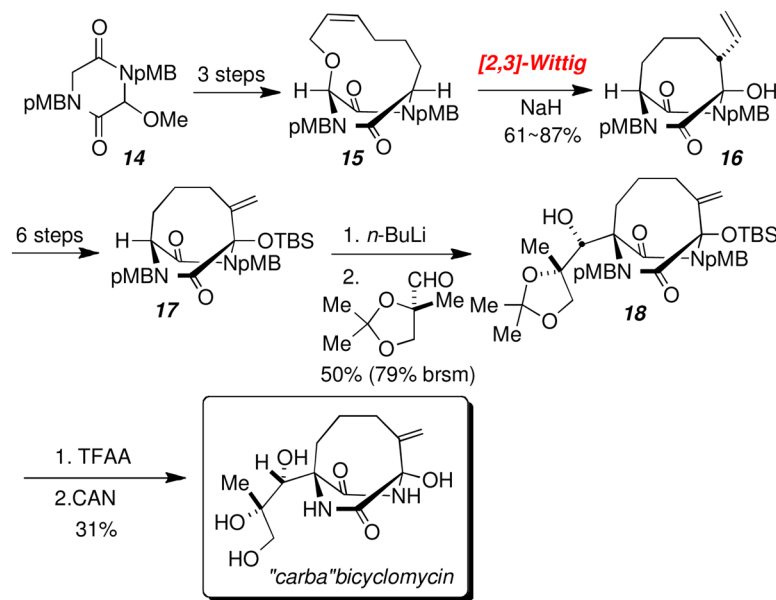
Sampling of synthetic largazole analogs that displayed potent Class I HDACi activity.



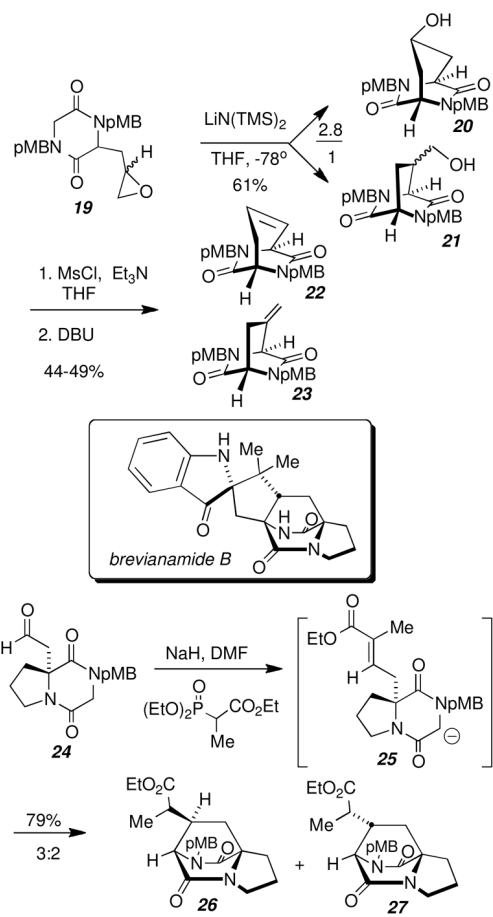
**Scheme 1.**  
Total Synthesis of Bicyclomycin.



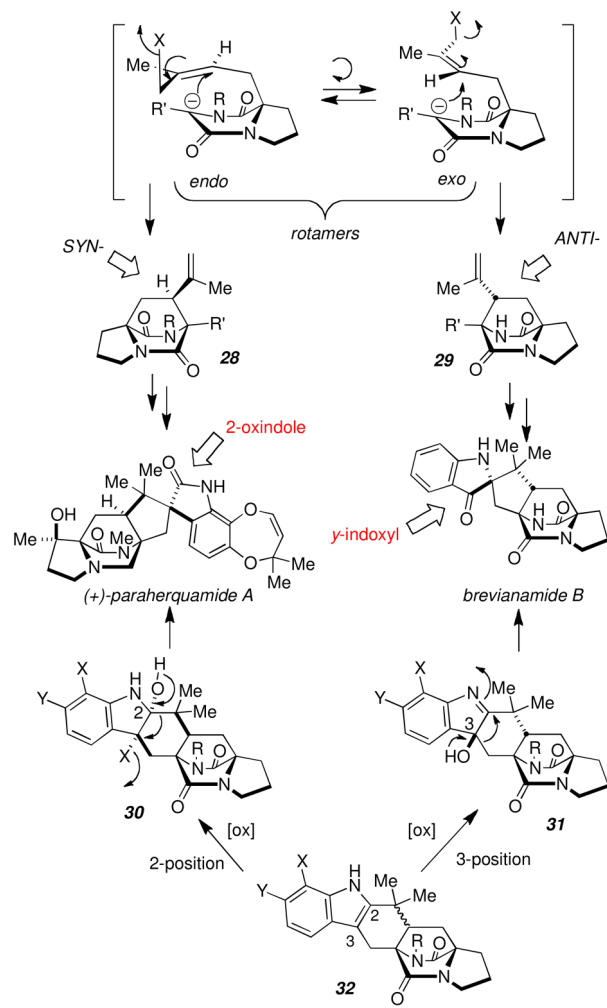
**Scheme 2.**  
Bicyclomycin: a latent Michael-acceptor and pH-dependence.



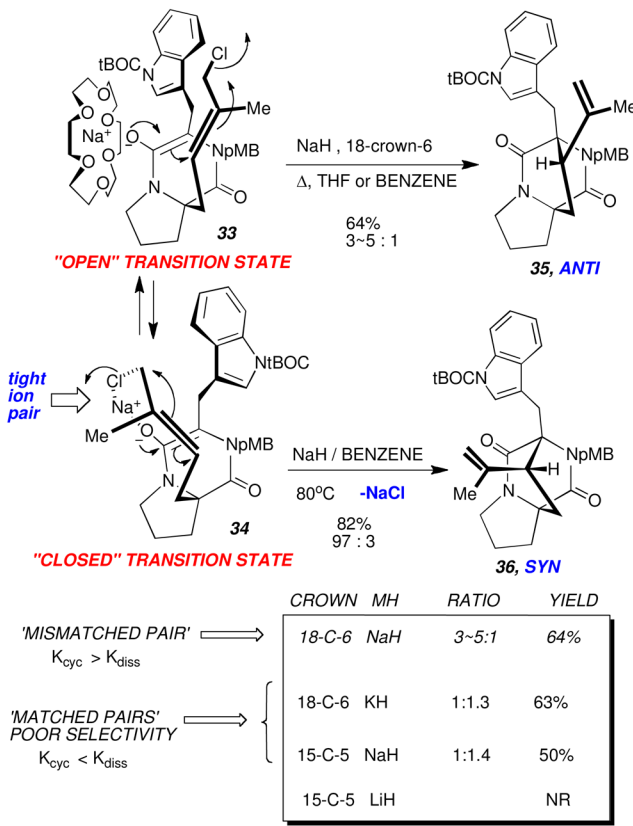
**Scheme 3.**  
Synthesis of “carba”bicyclomycin.

**Scheme 4.**

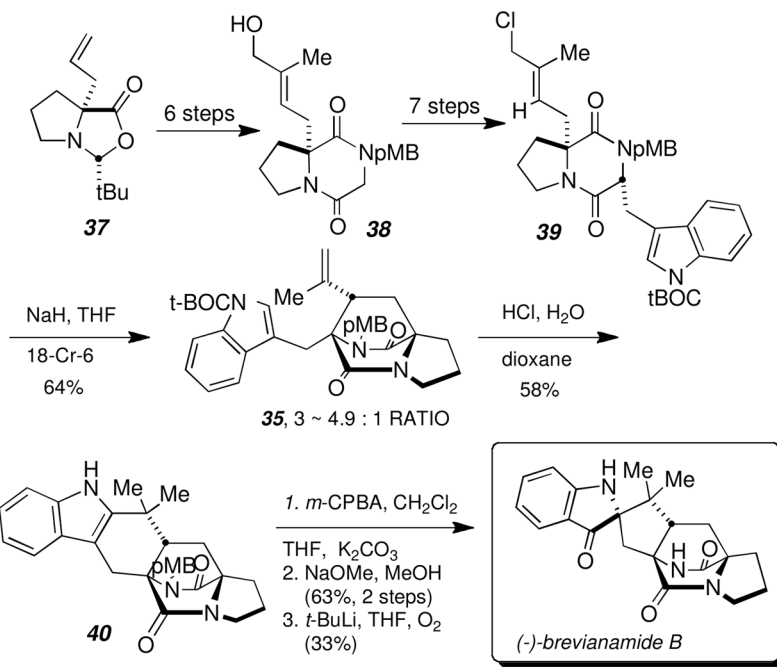
Early synthetic studies on bicyclo[2.2.2]diazaoctanes.

**Scheme 5.**

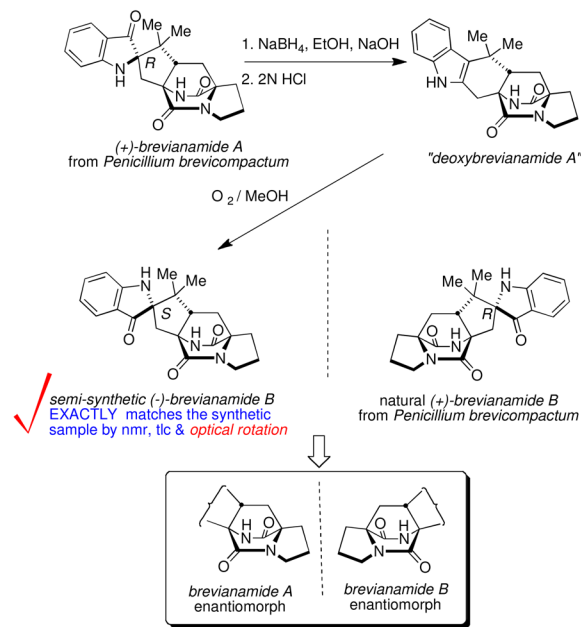
A “unified” retrosynthesis for the brevianamides and paraherquamides.



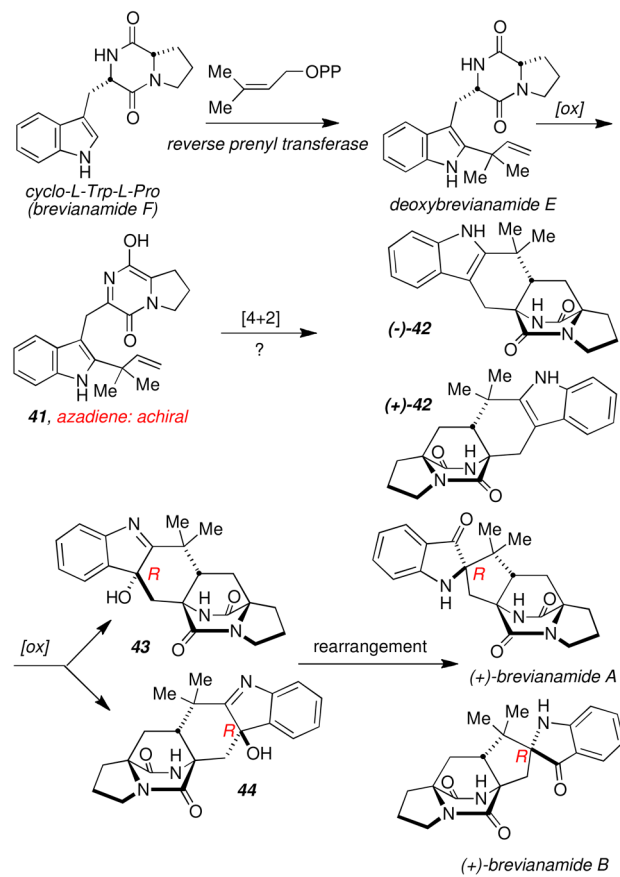
**Scheme 6.**  
Diastereoselective intramolecular  $S_N2'$  cyclization reactions.



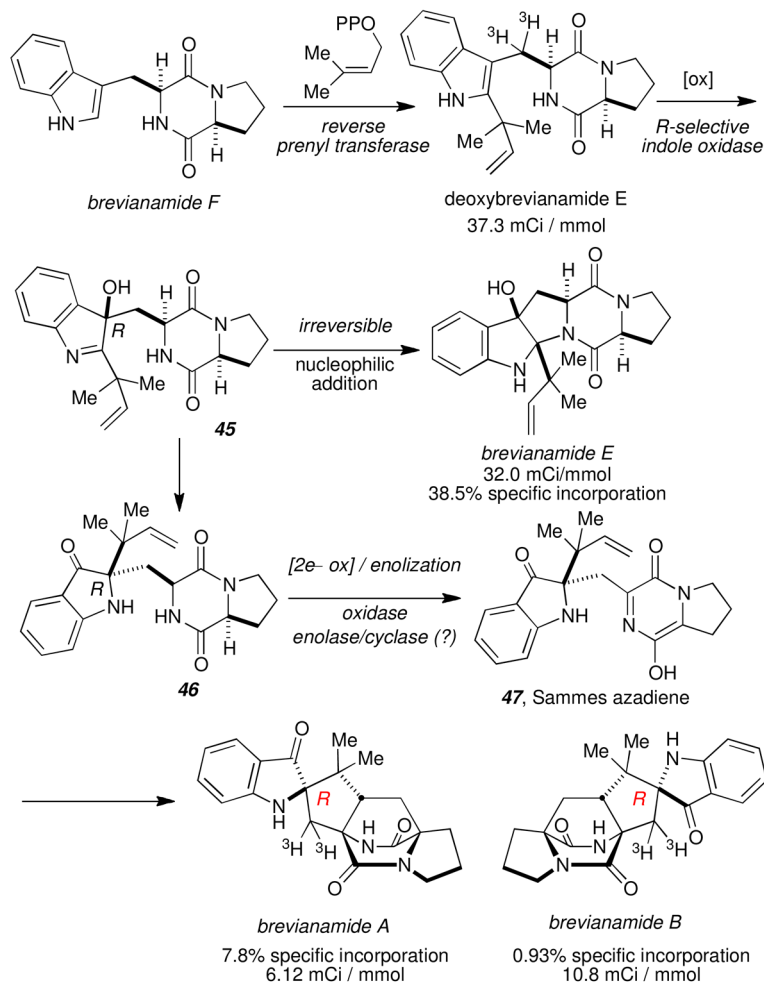
**Scheme 7.**  
Asymmetric synthesis of (*-*)-brevianamide B.



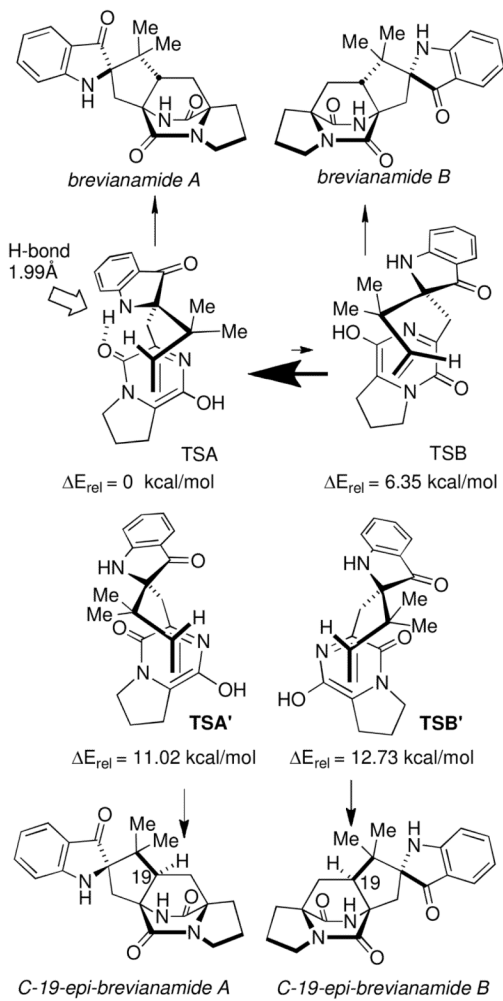
**Scheme 8.**  
Discovery of the enantio-divergent biogenesis of brevianamides A and B.

**Scheme 9.**

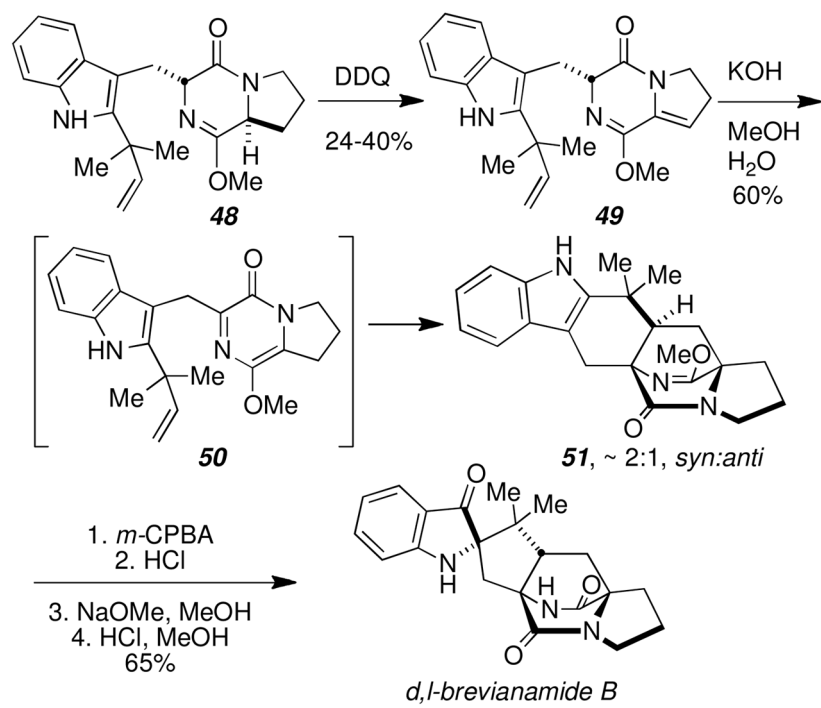
Modified biogenetic proposal to accommodate the natural stereochemistries of brevianamides A and B.

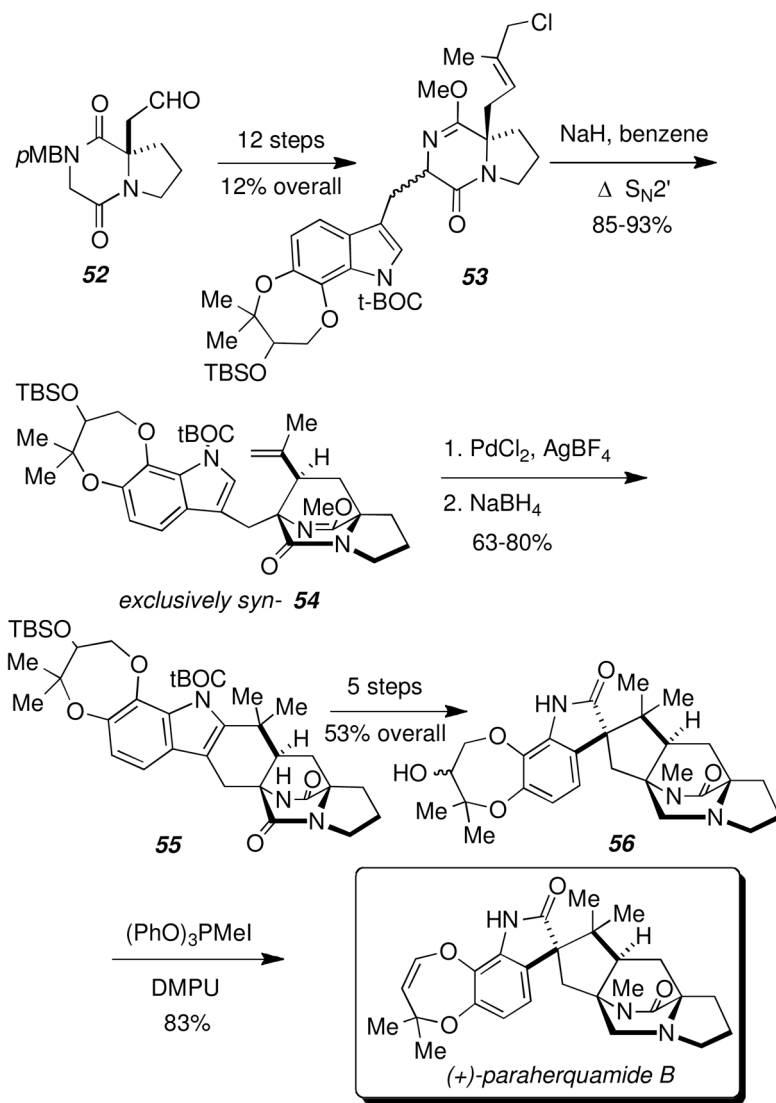


**Scheme 10.**  
Alternative biogenetic pathway.

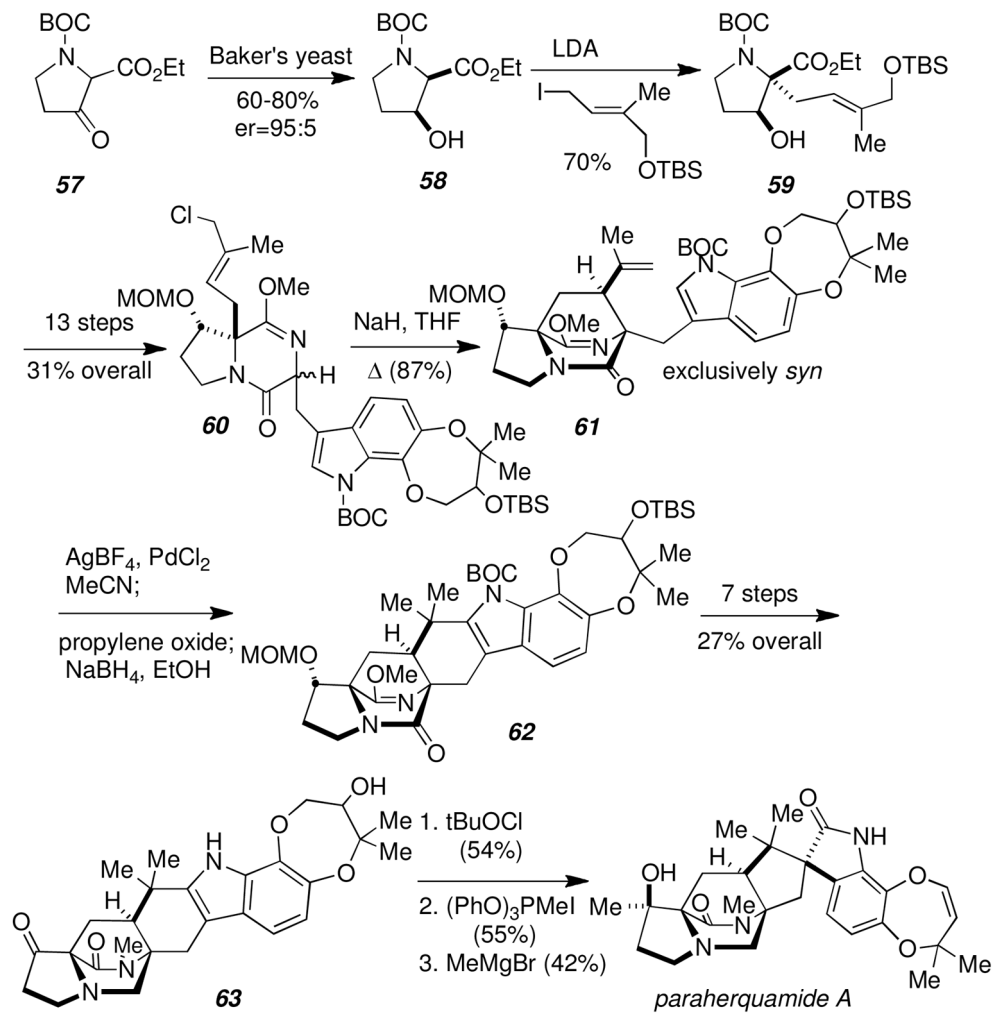
**Scheme 11.**

*Ab initio* calculations on the putative Diels-Alder cycloadditions by Domingo, et al.<sup>19</sup>

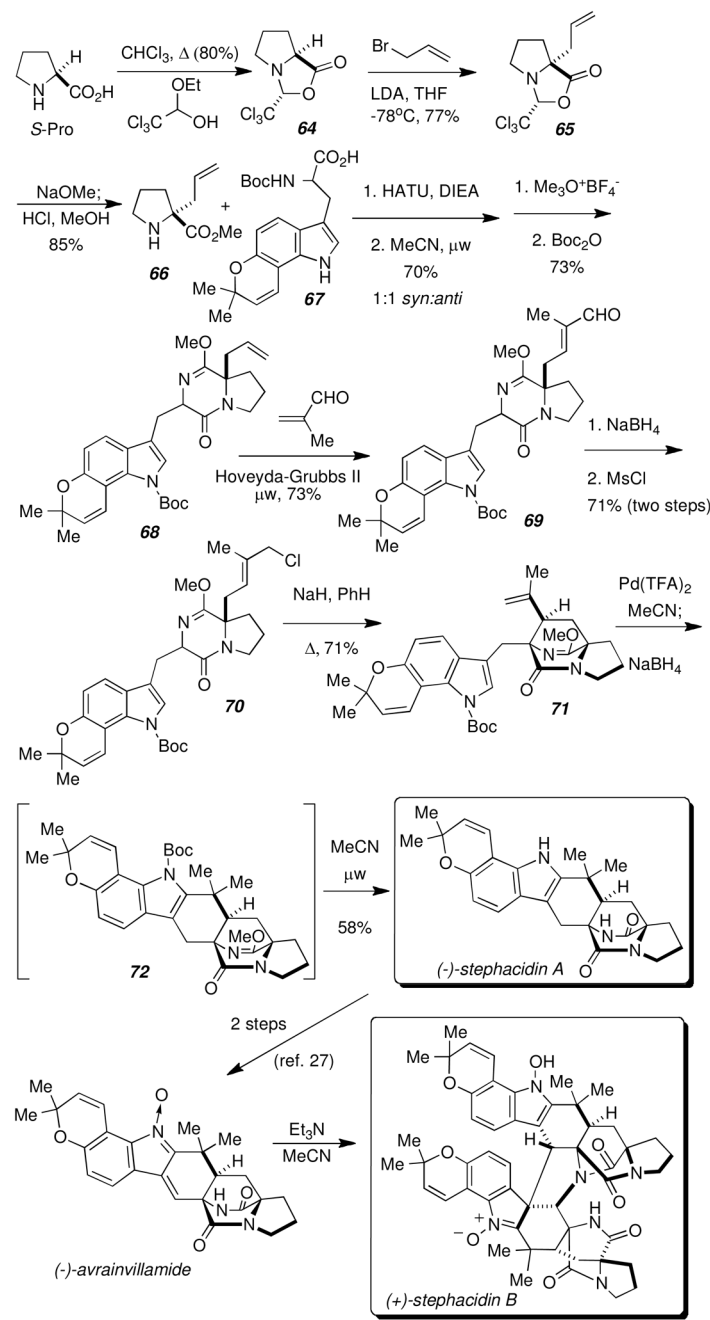
**Scheme 12.**Biomimetic synthesis of *d, l*-brevianamide B.



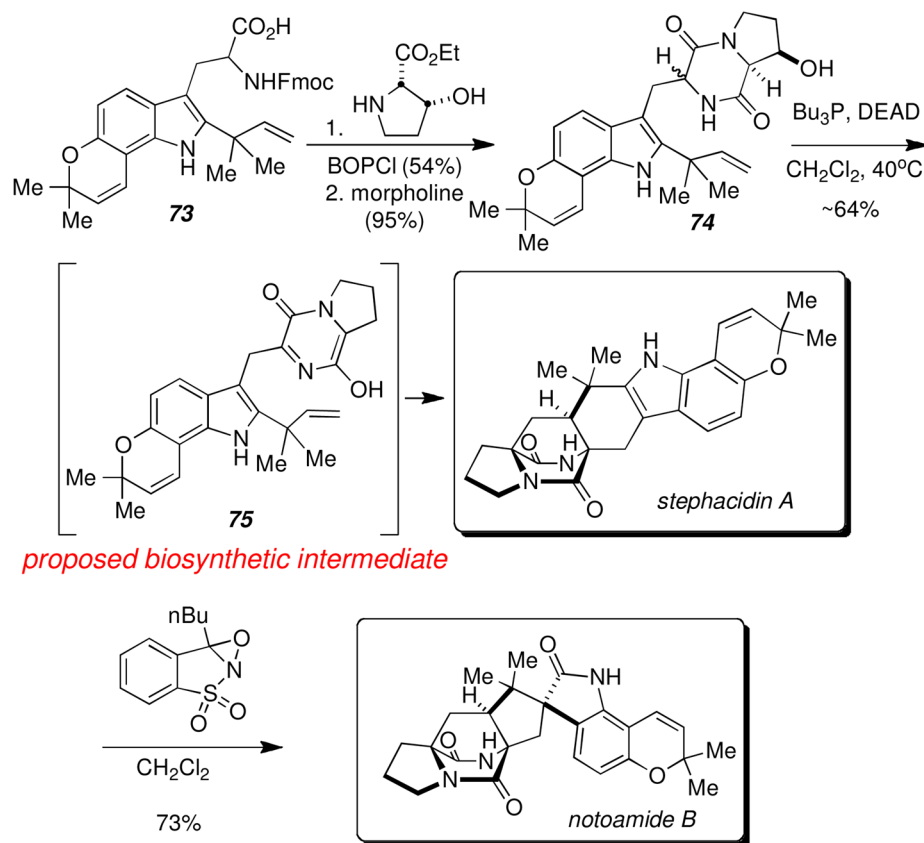
**Scheme 13.**  
Asymmetric synthesis of *(+)*-paraherquamide B.<sup>21</sup>



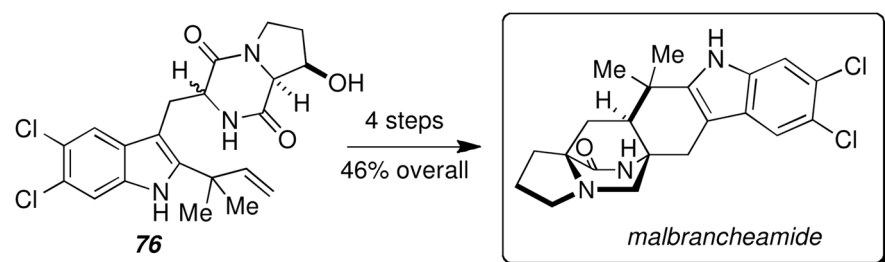
**Scheme 14.**  
Asymmetric synthesis of (*-*)-paraherquamide A.<sup>22</sup>

**Scheme 15.**

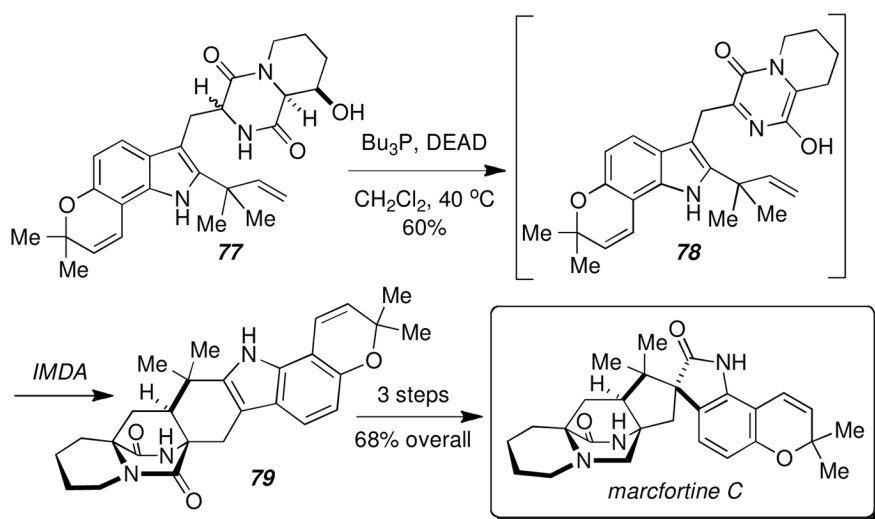
Asymmetric total synthesis of (-)-stephacidin A and (+)-notoamide B.

**Scheme 16.**

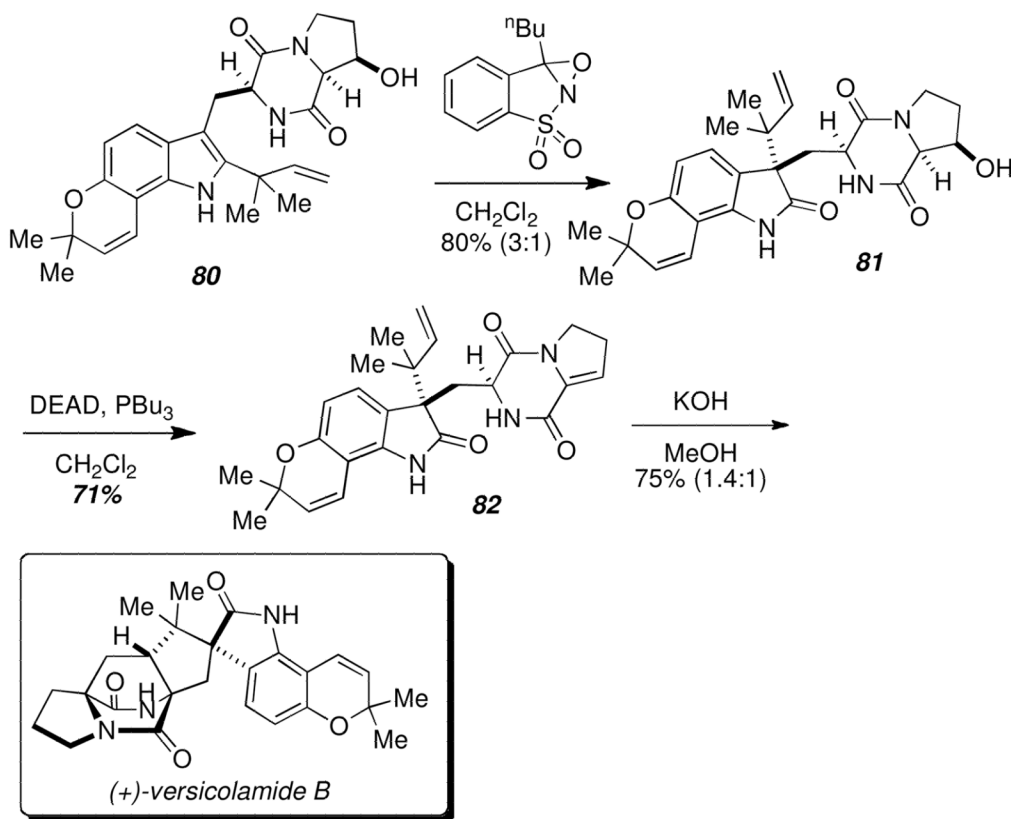
Biomimetic total synthesis of *D, L*-stephacidin A and *D, L*-notoamide B.



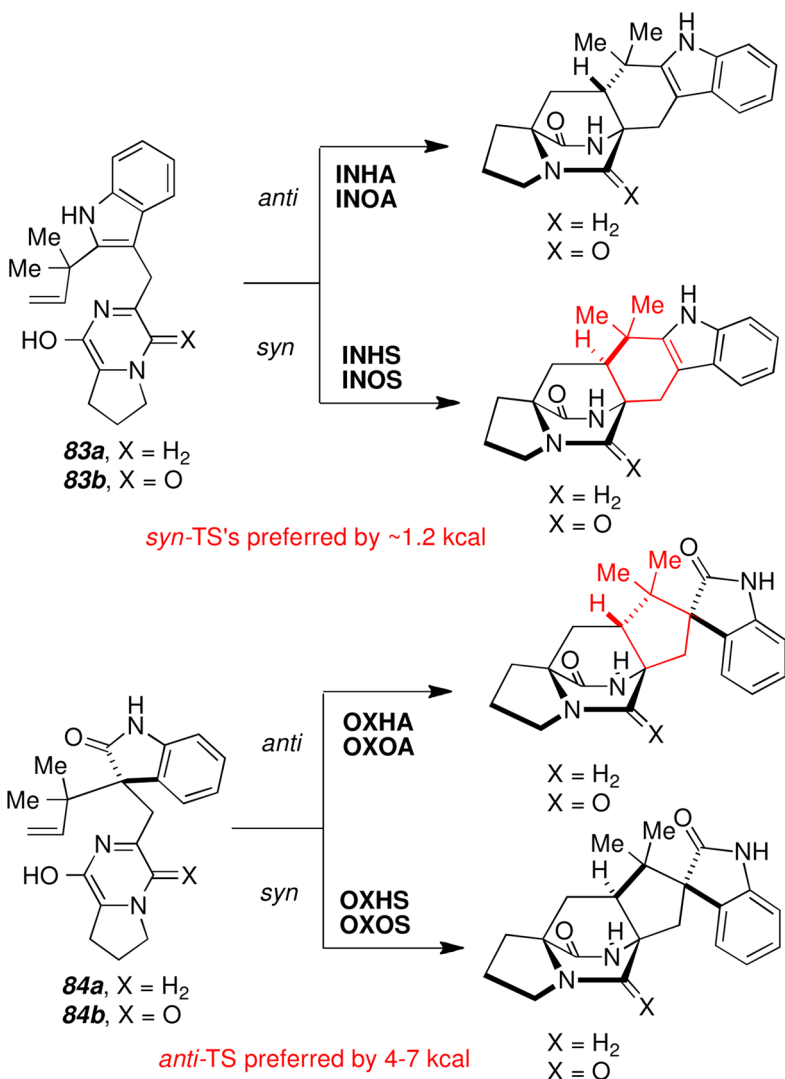
**Scheme 17.**  
Biomimetic total synthesis of malbrancheamide.<sup>33</sup>

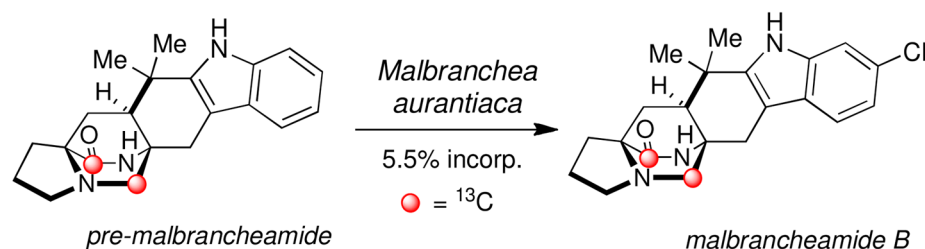


**Scheme 18.**  
Biomimetic total synthesis of marcfortine C.<sup>34</sup>



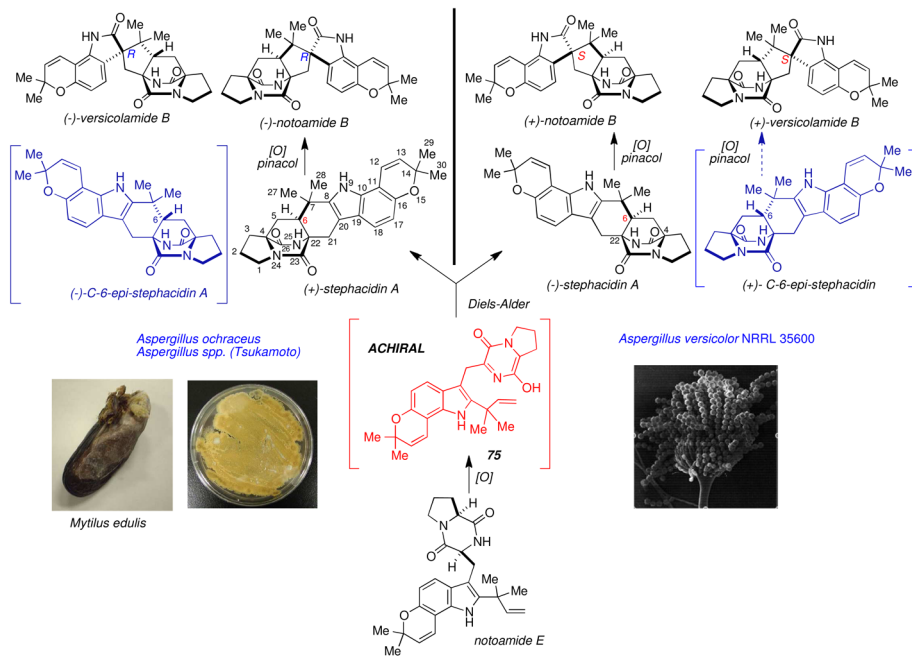
**Scheme 19.**  
Synthesis of (+)-versicolamide B.<sup>35</sup>



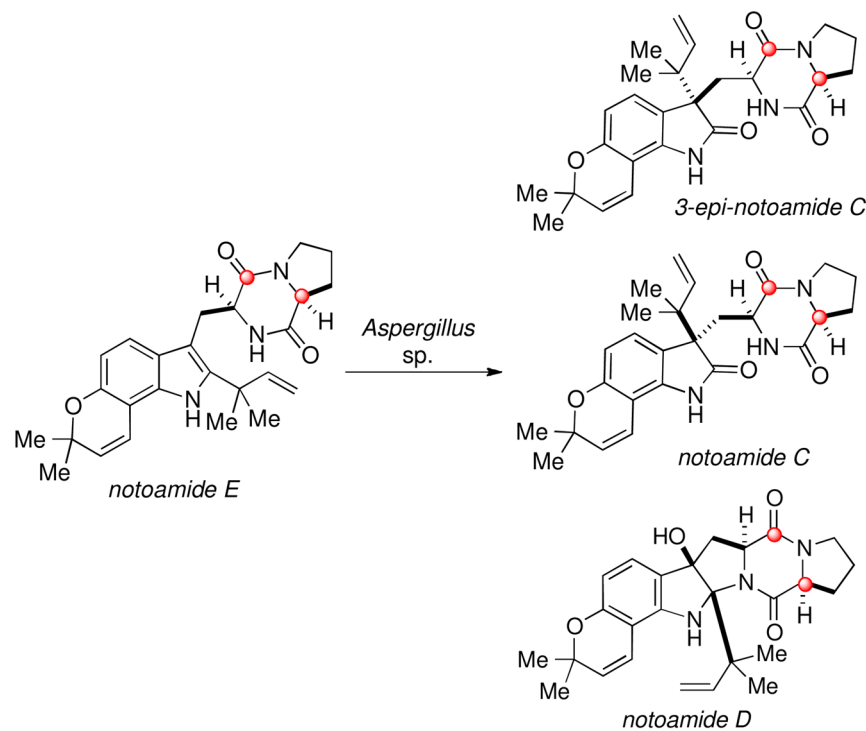


**Scheme 21.**

Biosynthetic incorporation of pre-malbrancheamide into malbrancheamide B.<sup>33b</sup>

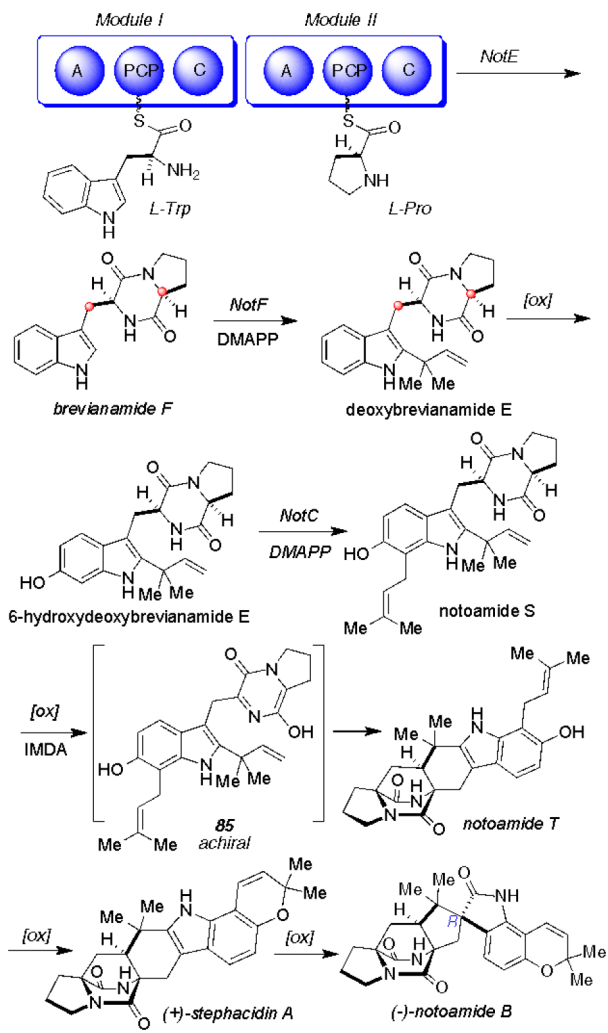
**Scheme 22.**

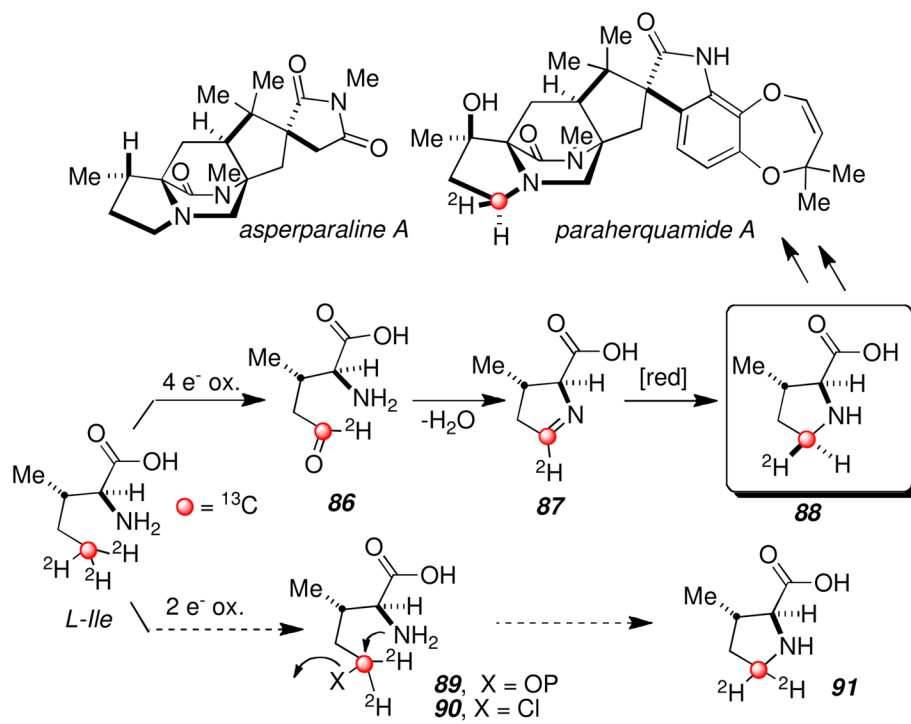
Initial biogenetic hypothesis to accommodate enantio-divergent production of stephacidin A, notoamide B and versicolamide B.



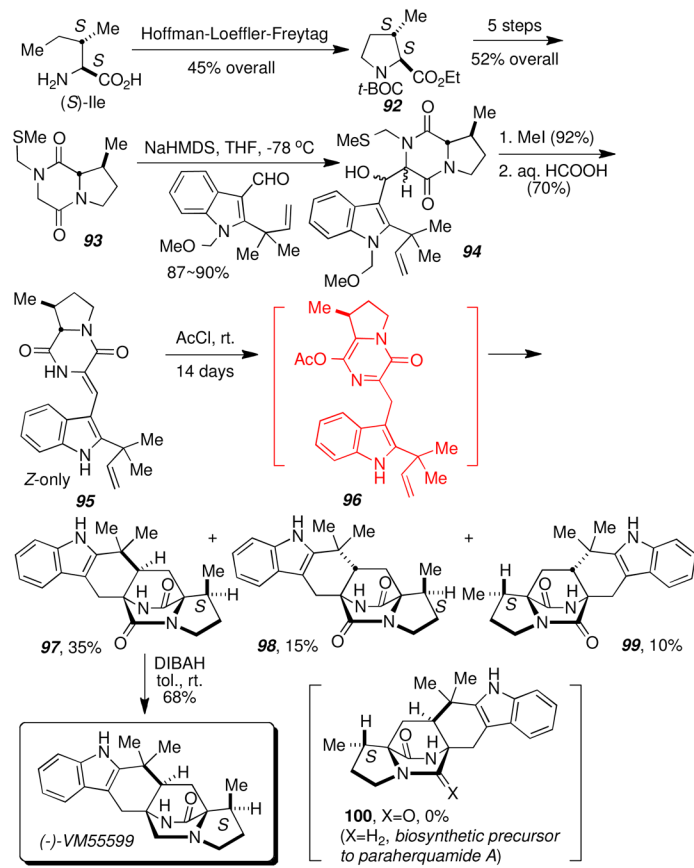
**Scheme 23.**

Biosynthetic transformation of notoamide E into notoamides C, D and 3-*epi*-notoamide C.

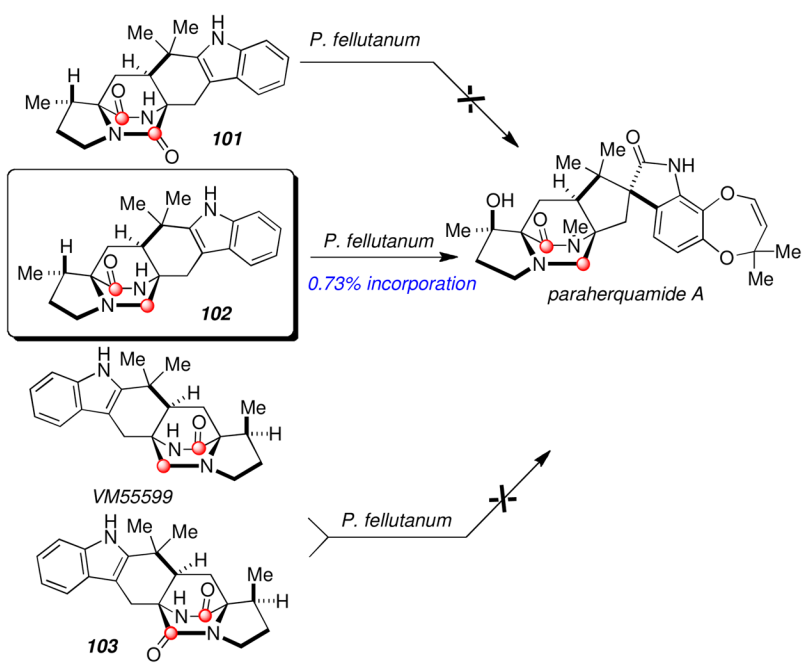
**Scheme 24.**Current biogenetic proposal for stephacidin A (marine-derived *Aspergillus* sp.).

**Scheme 25.**

Origin of the  $\beta$ -methylproline ring in paraherquamide and asperparaline biosynthesis.

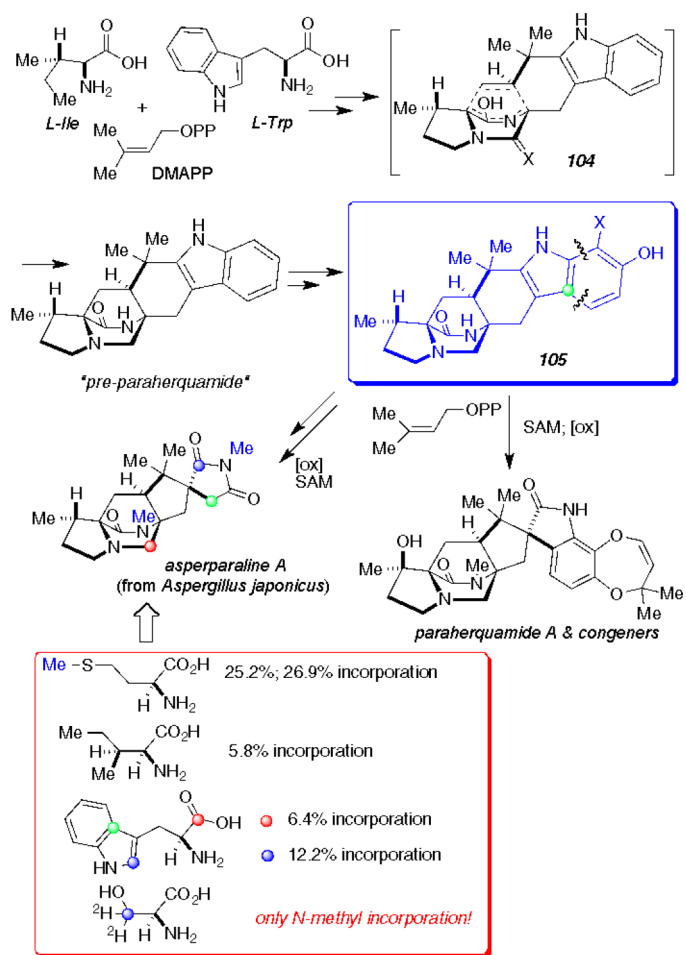


### Scheme 26.

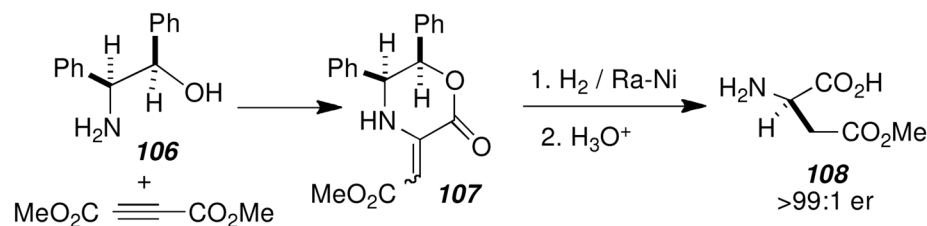


Scheme 27.

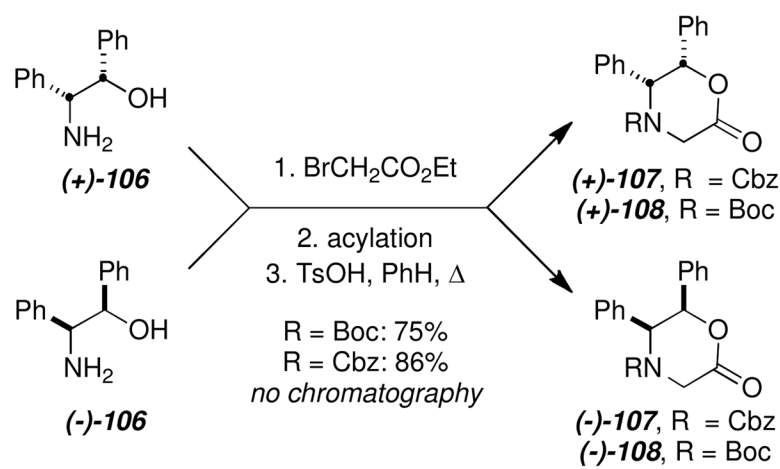
Discovery and incorporation of “pre-paraherquamide”.

**Scheme 28.**

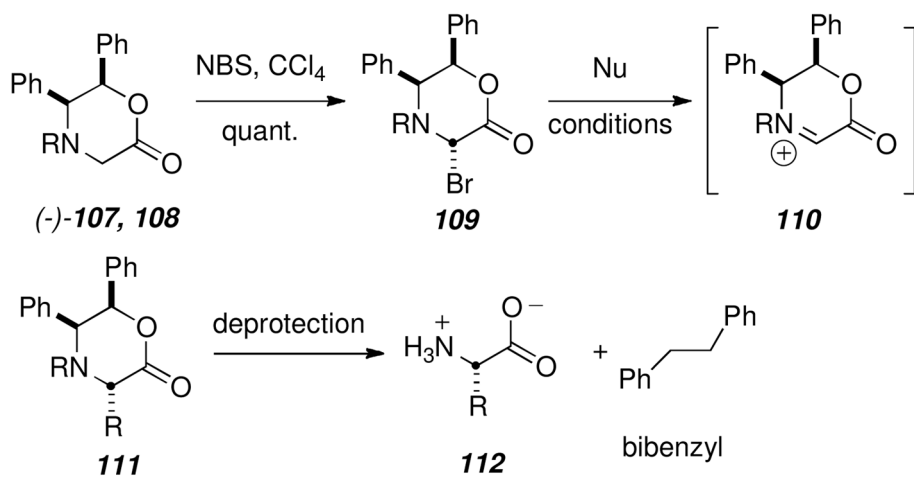
A “unified” biogenetic hypothesis for the paraherquamides and asperparalines.



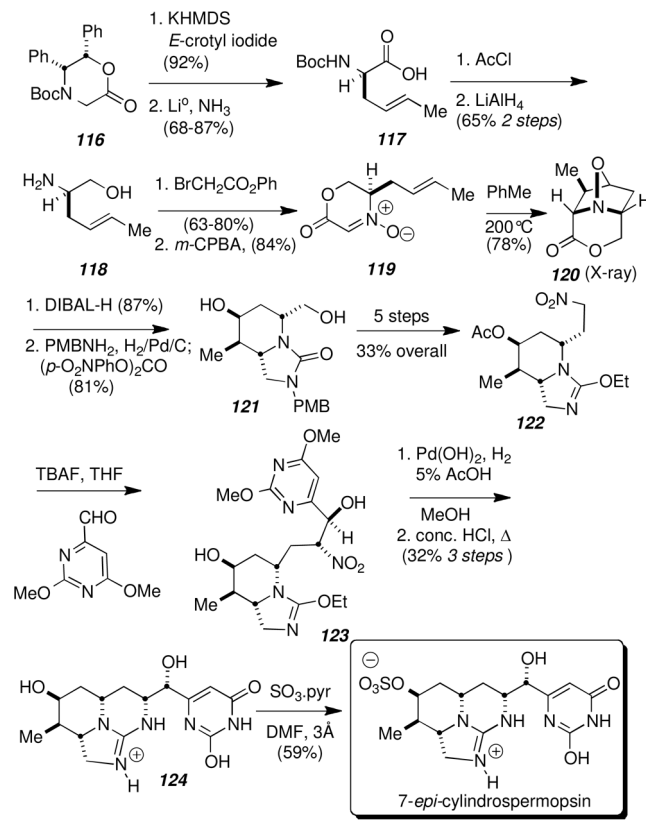
**Scheme 29.**  
Kagan's aspartic acid synthesis.<sup>47</sup>

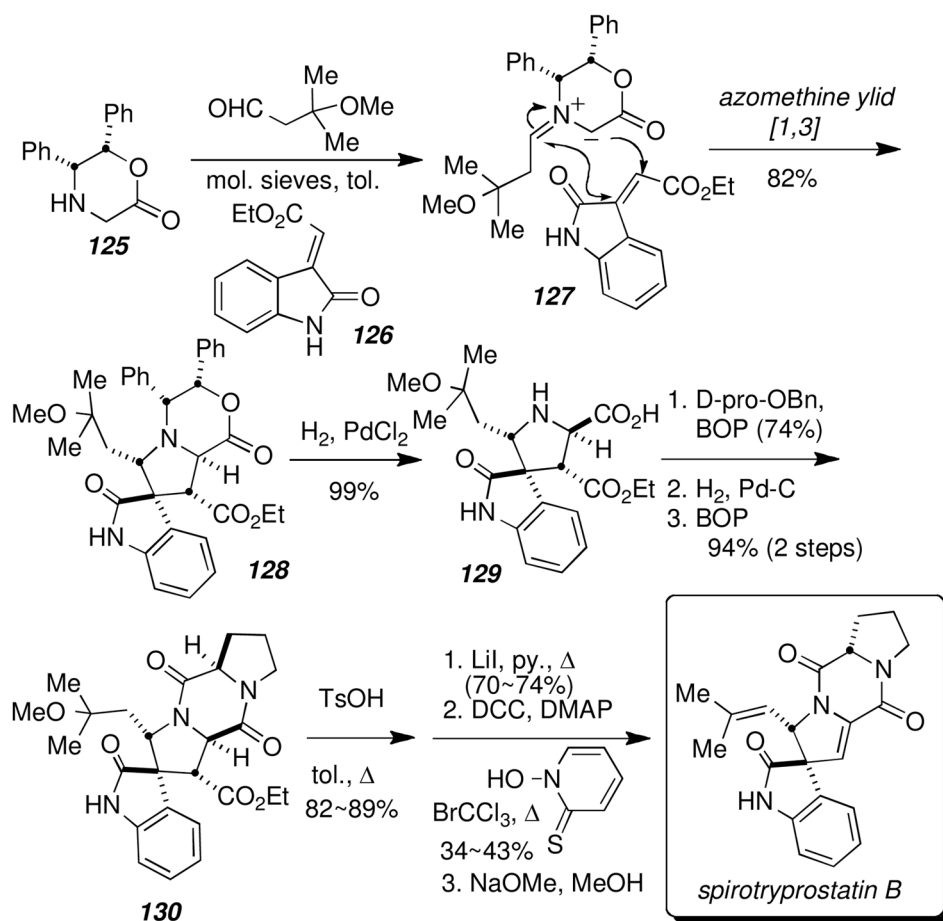
**Scheme 30.**

Preparation of the diphenyloxazinones.

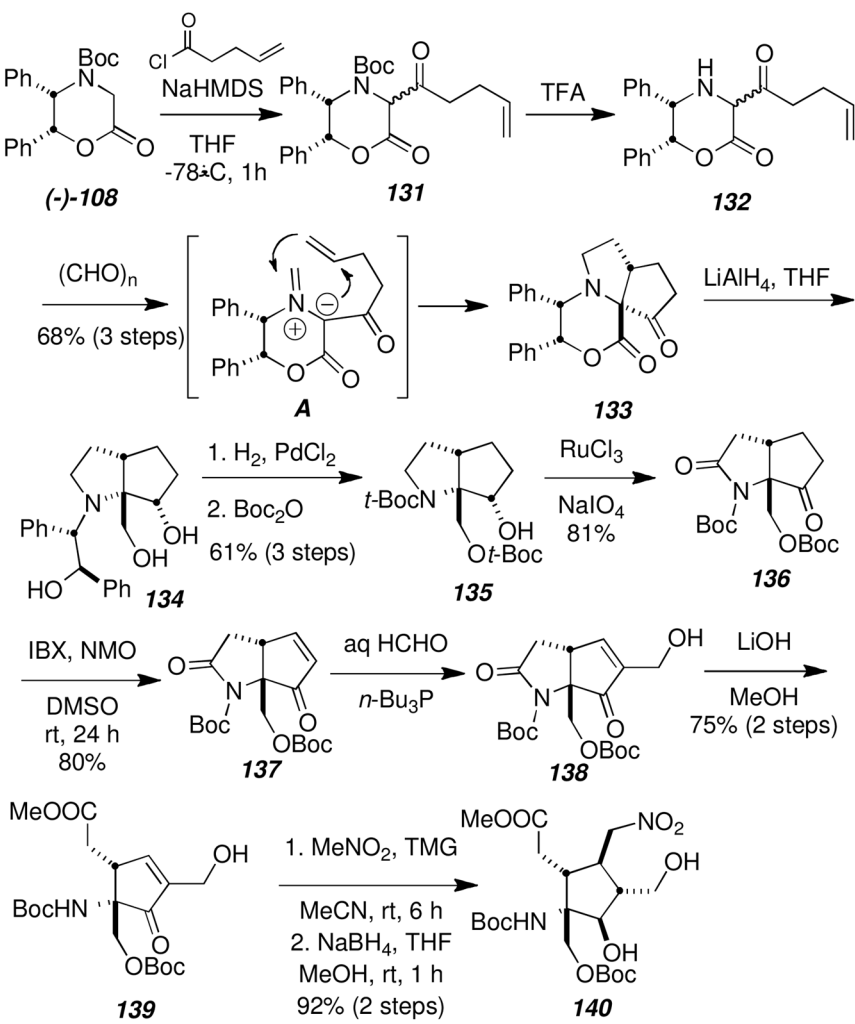


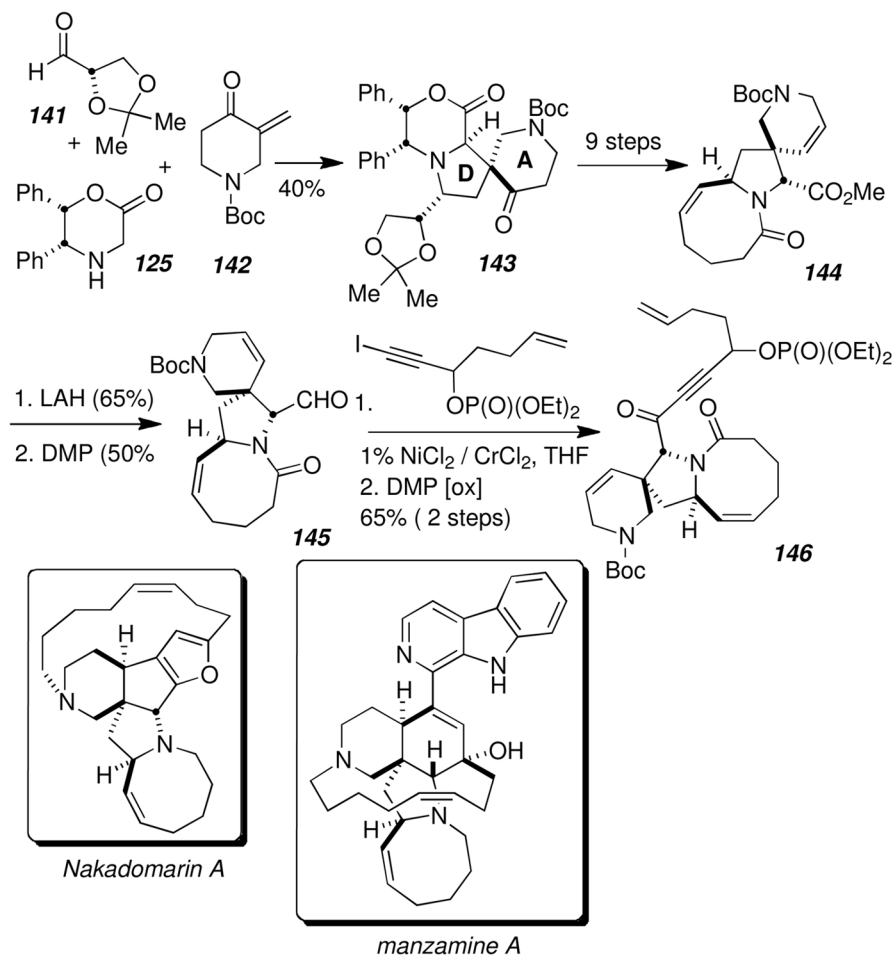
**Scheme 31.**  
Electrophilic glycinate methodology.

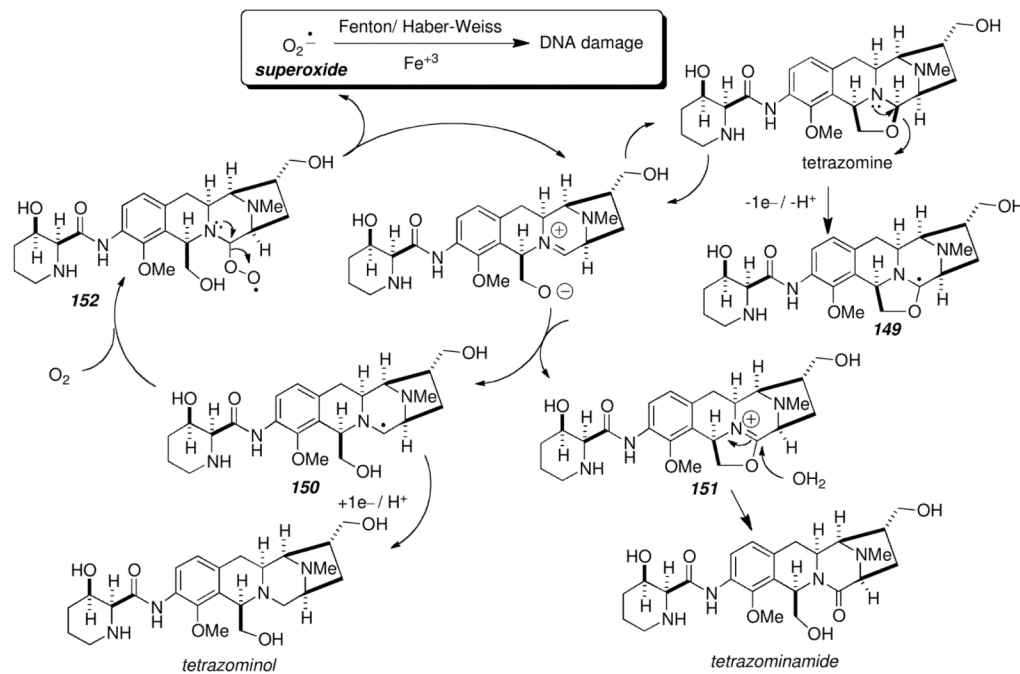
**Scheme 32.**The asymmetric synthesis of natural 7-*epi*-cylindrospermopsin.

**Scheme 33.**

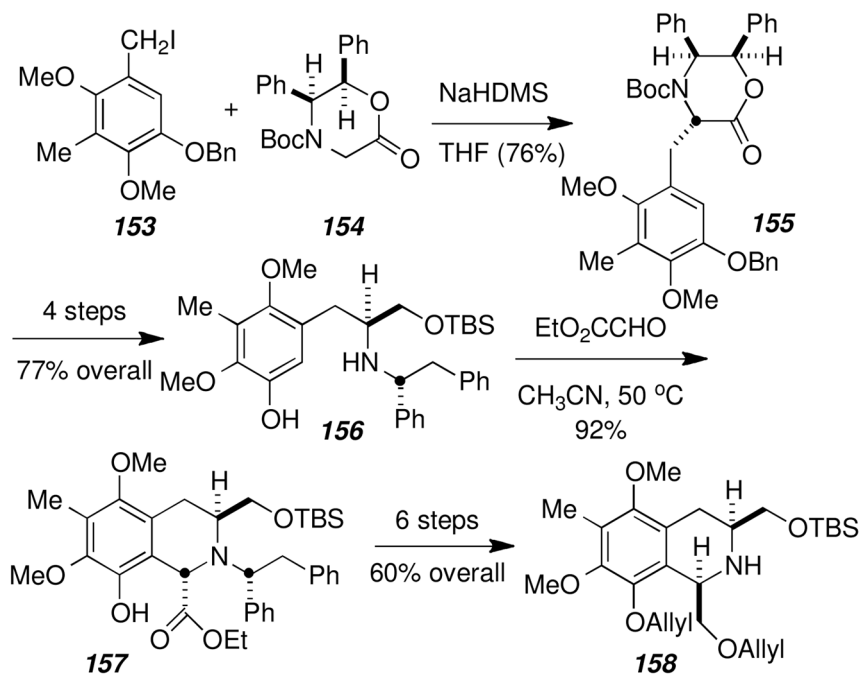
Asymmetric synthesis of spirotryprostatin B via an azomethine ylide cycloaddition.

**Scheme 34.**Asymmetric synthesis of the cyclopentane core of palau'amine (**140**).<sup>92a</sup>

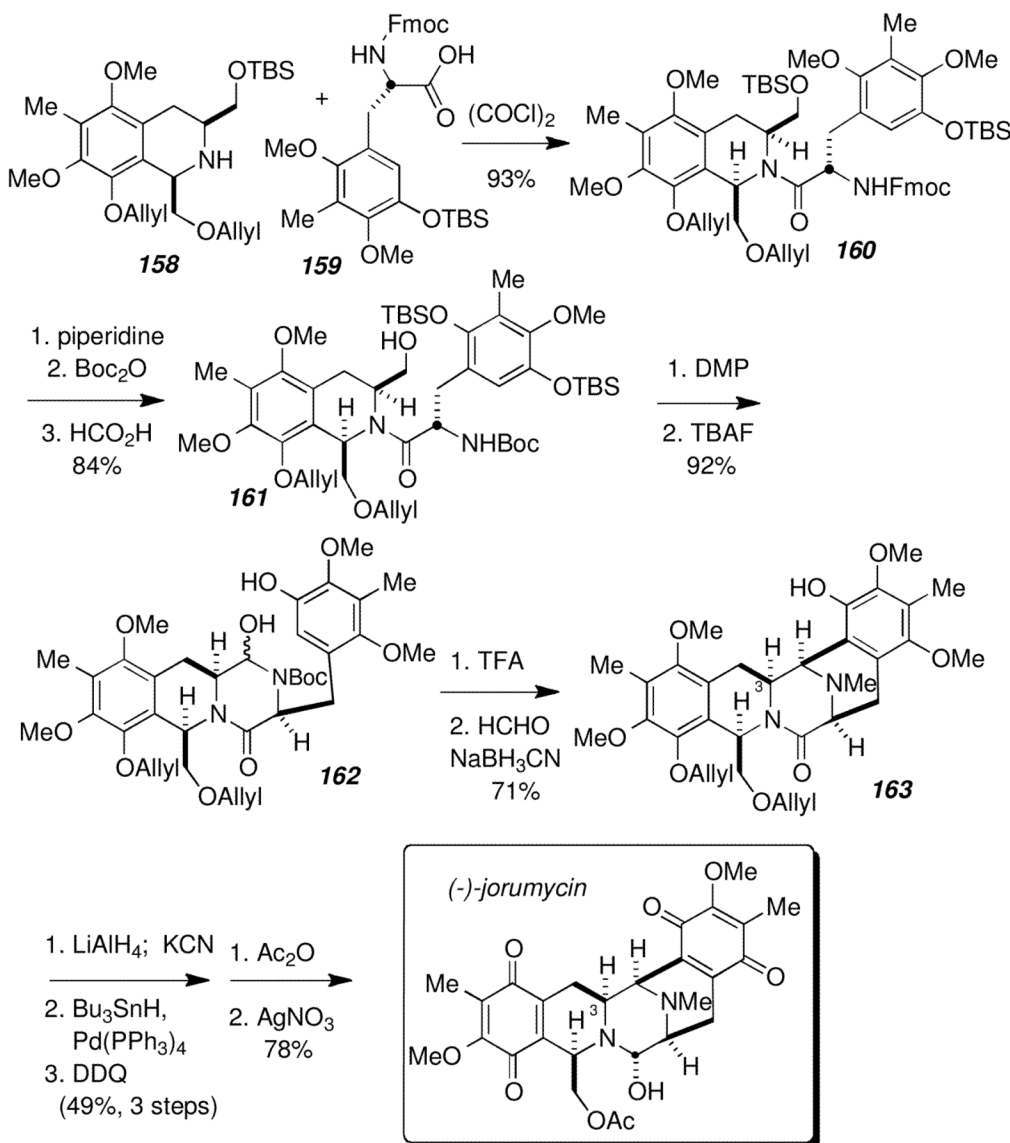
**Scheme 35.**Dipolar cycloaddition approach to nakadomarin.<sup>97</sup>

**Scheme 36.**

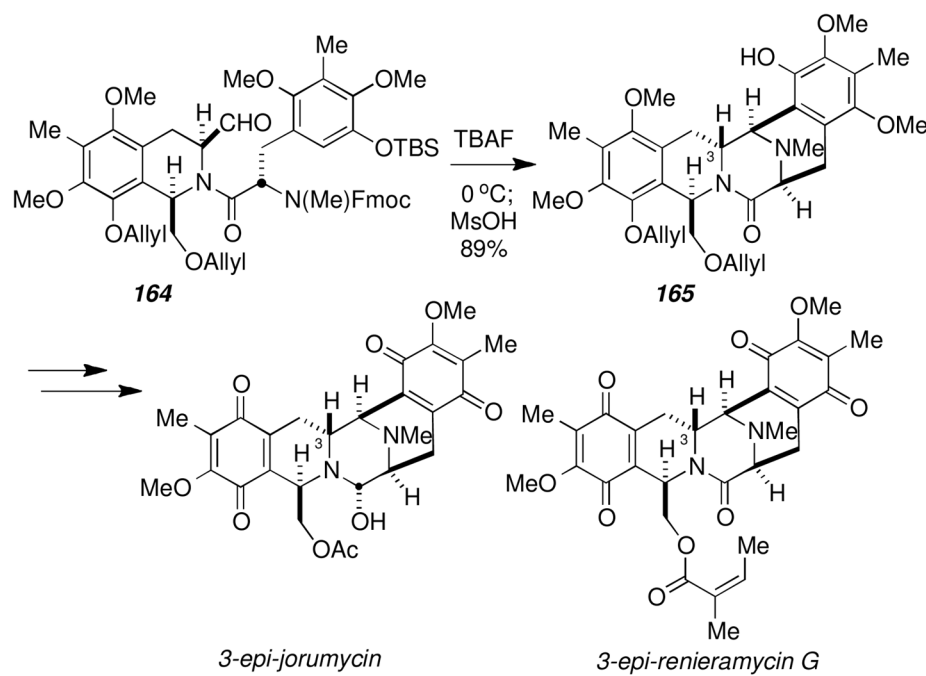
Autoredox disproportionation of tetrazomine.

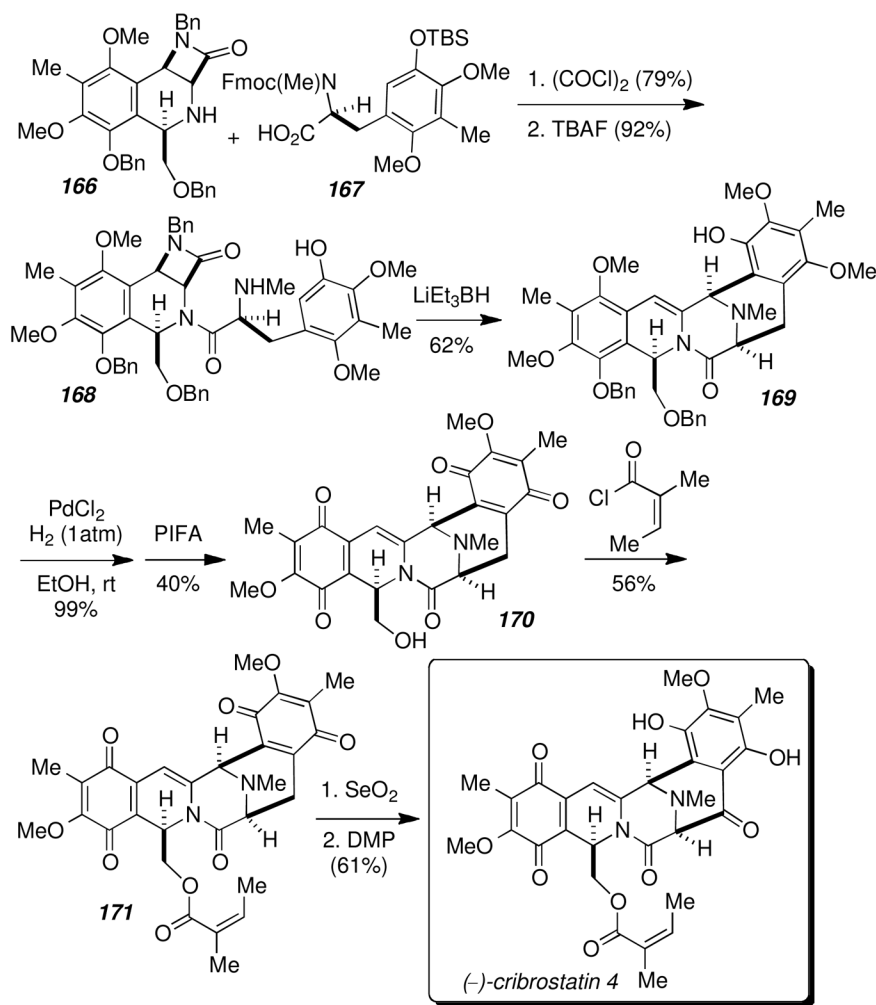


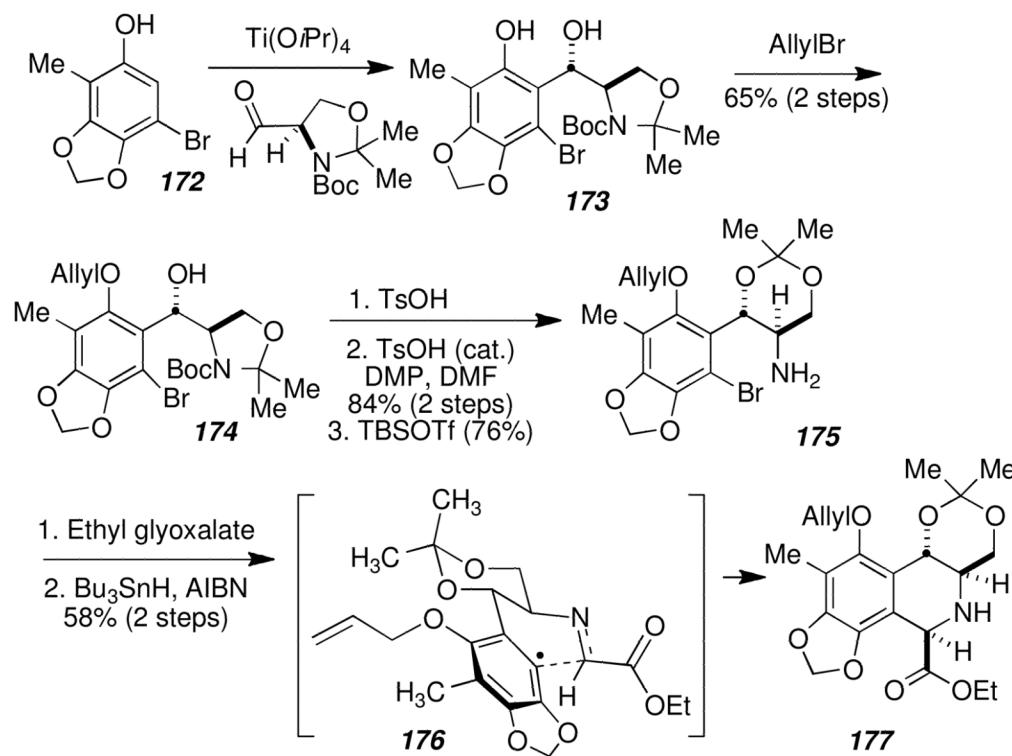
**Scheme 37.**  
Synthesis of a versatile THIQ.



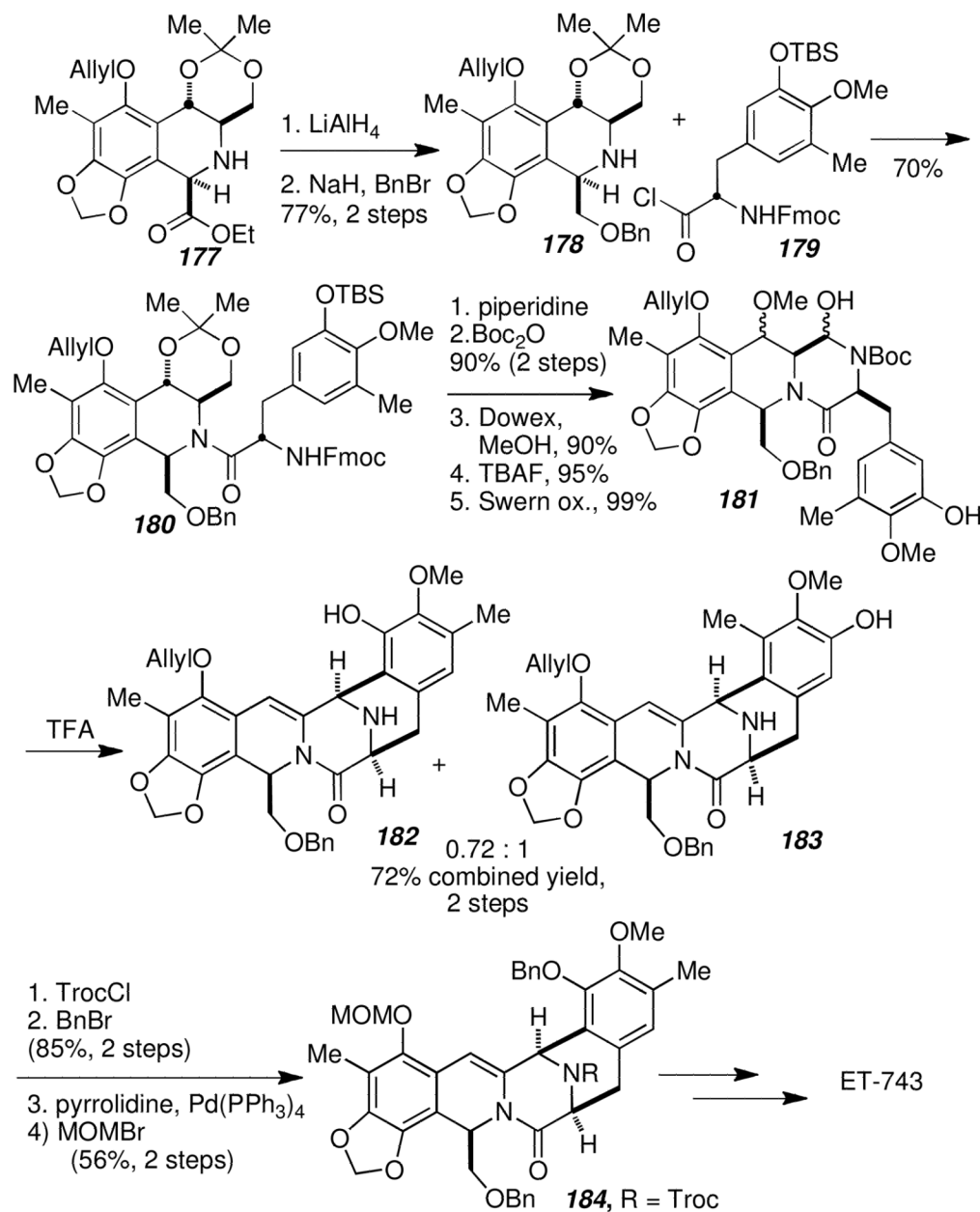
**Scheme 38.**  
Asymmetric synthesis of *(-)*-jorumycin.

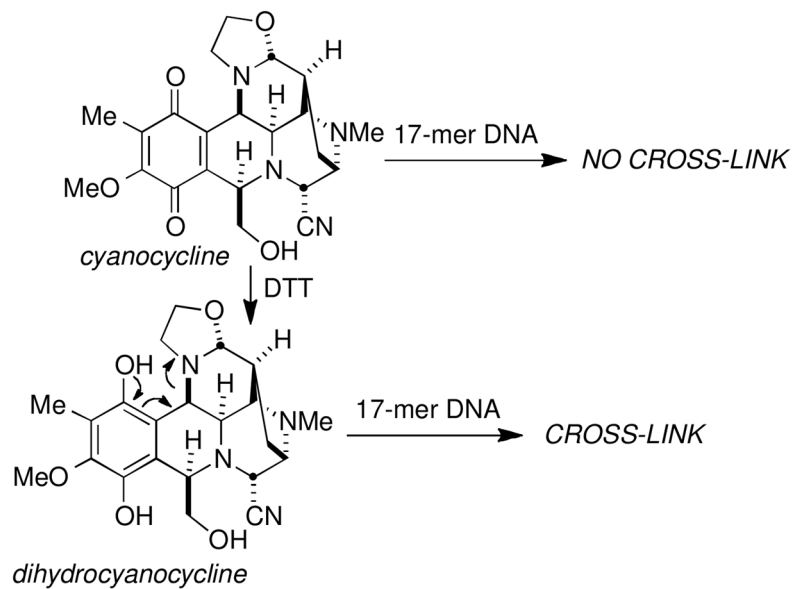
**Scheme 39.**Preparation of 3-*epi*-jorumycin and 3-*epi*-renieramycin G.

**Scheme 40.**Asymmetric synthesis of *(-)*-cribrostatin 4.

**Scheme 41.**

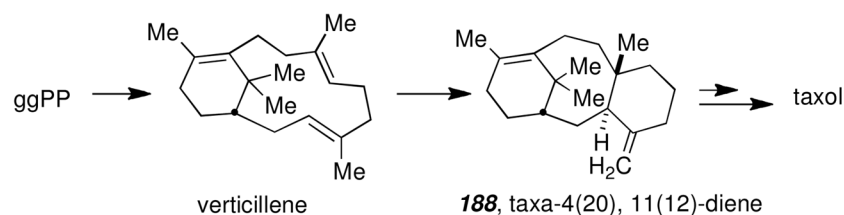
Diastereoselective tetrahydroisoquinolone construction for Et-743.

**Scheme 42.**Formal total synthesis of Et-743.<sup>104</sup>



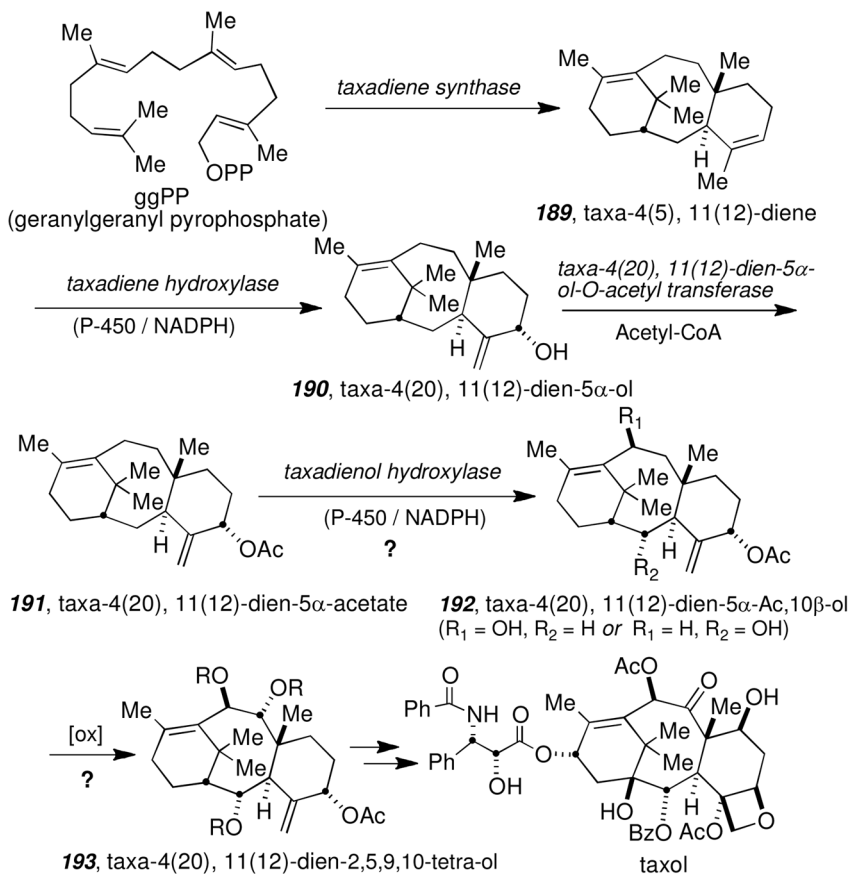
**Scheme 43.**

Cyanocycline requires reduction to dihydrocyanocycline to cross-link DNA.

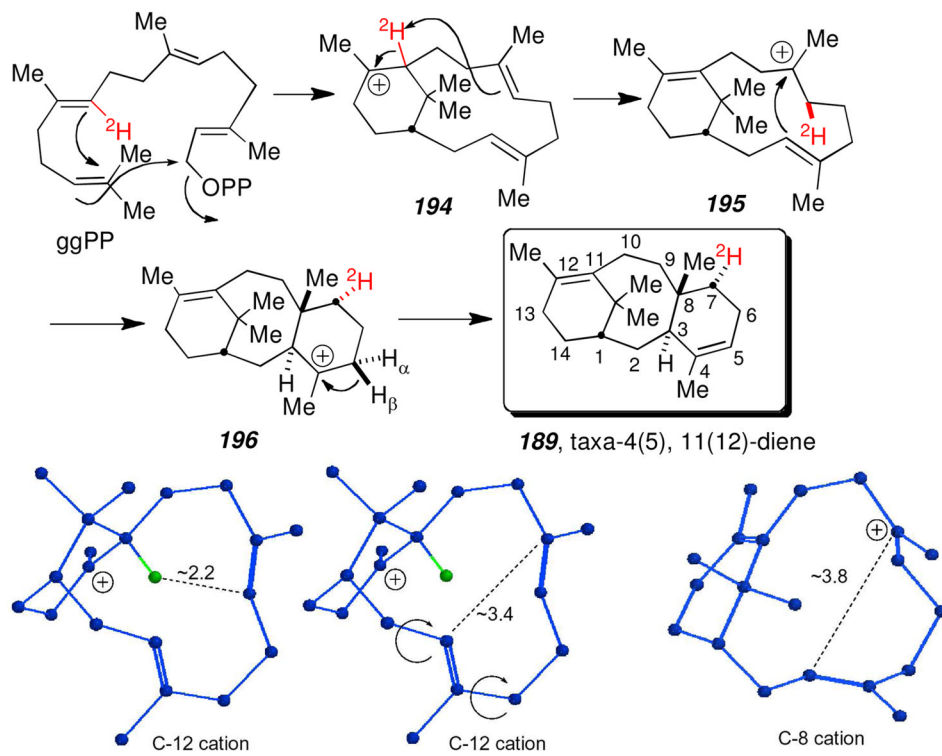


**Scheme 44.**

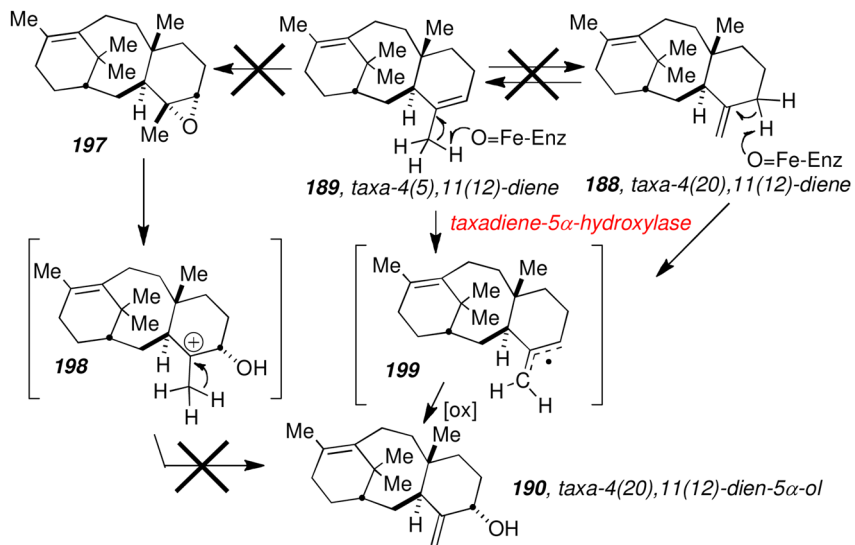
Early biosynthetic proposal from ggPP to taxol.

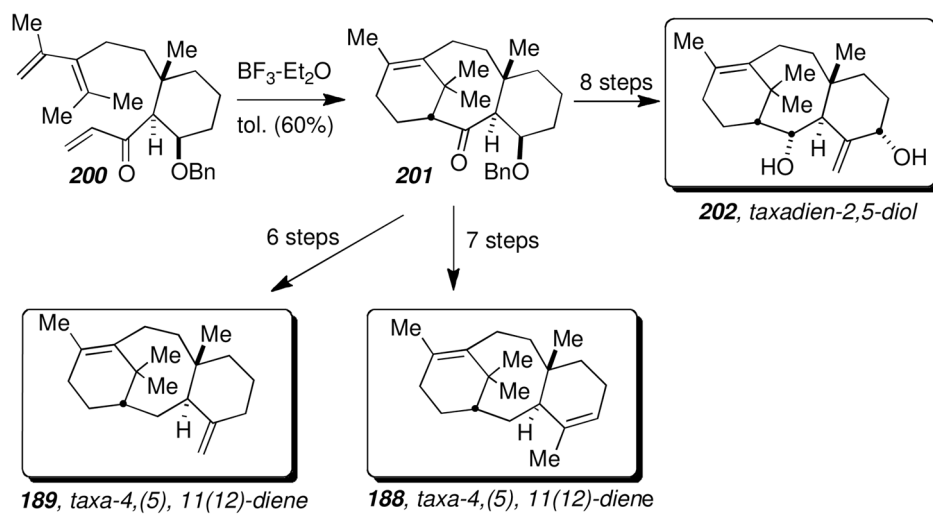


**Scheme 45.**  
Croteau-Williams biogenesis of taxol.<sup>120–123</sup>

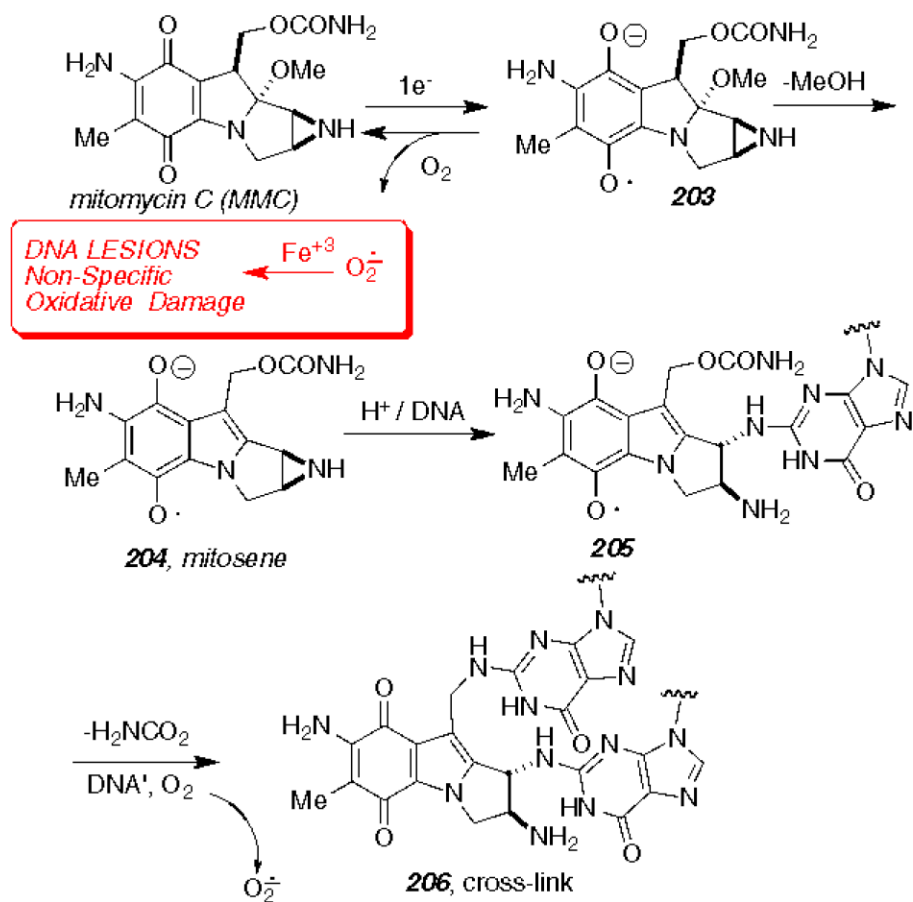


**Scheme 46.**  
Mechanism of taxadiene synthase.<sup>120,121</sup>

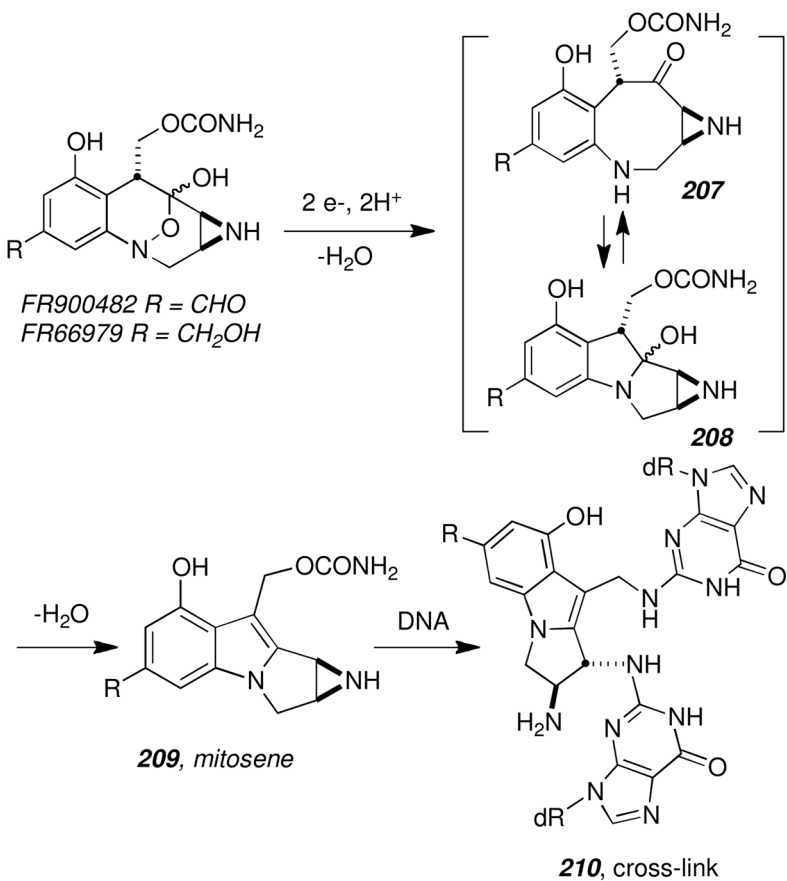
**Scheme 47.**Mechanism of taxadiene hydroxylase.<sup>126</sup>



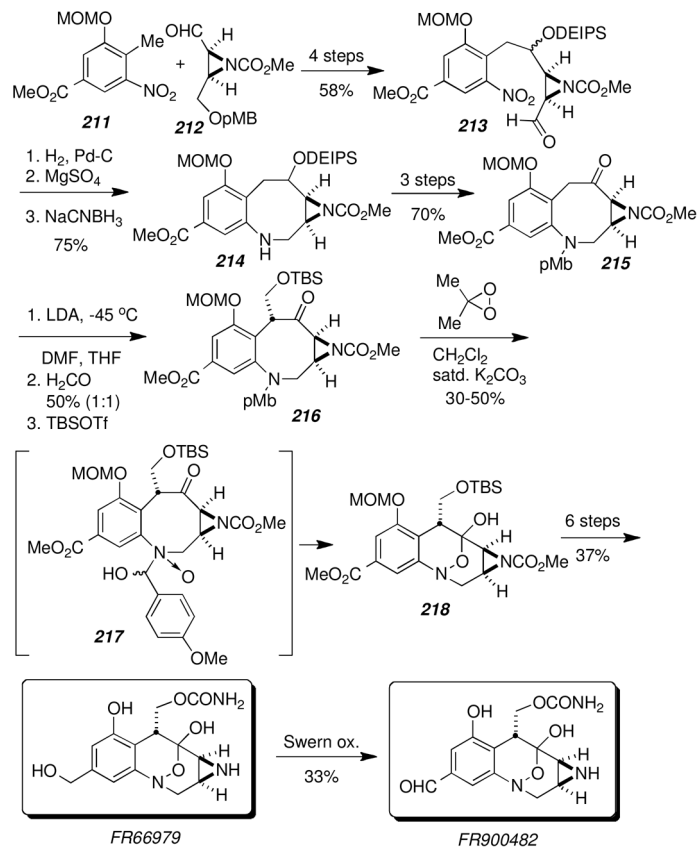
**Scheme 48.**  
IMDA-based synthesis of taxadienes.<sup>122</sup>

**Scheme 49.**

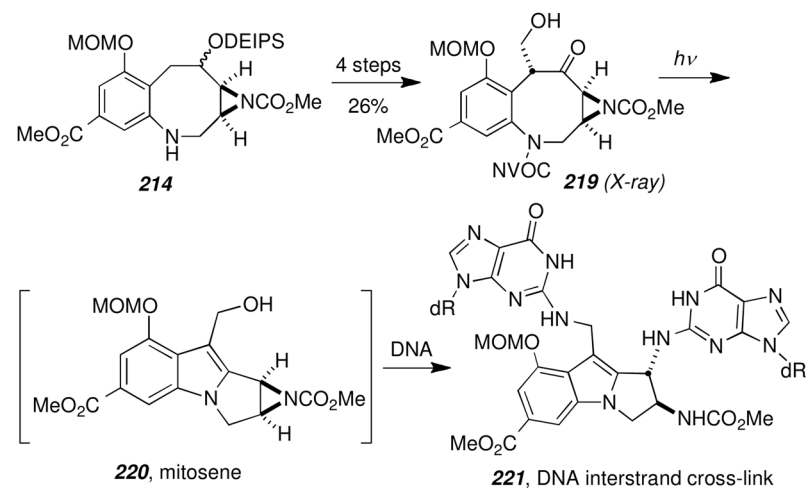
Mechanism of Activation and DNA Interstrand Cross-linking by Mitomycin C.

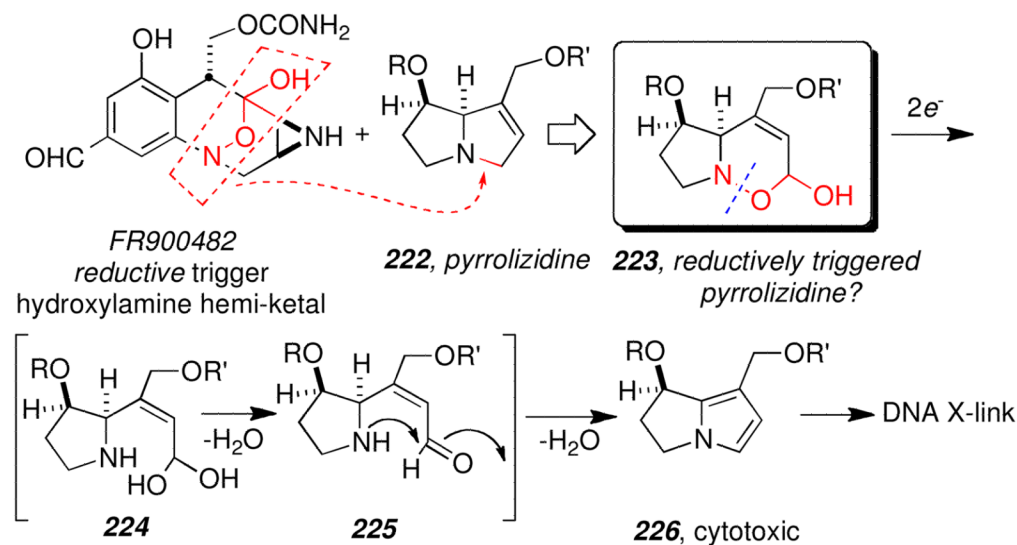
**Scheme 50.**

Mechanism of Reductive Activation of FR900482 and FR66979.

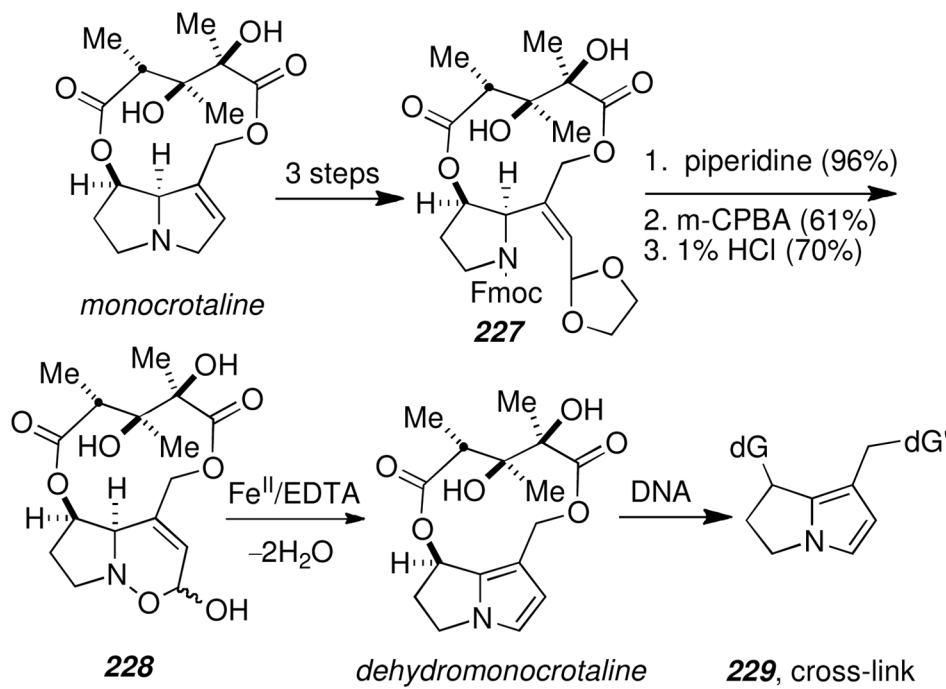
**Scheme 51.**

Asymmetric synthesis of FR66979 and FR900482

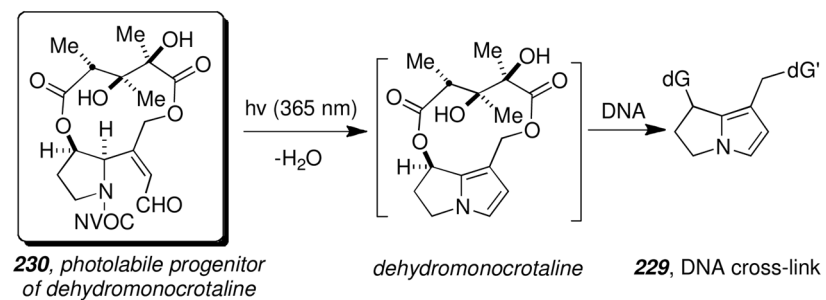
**Scheme 52.**Synthesis of a photo-activated pro-mitosene.<sup>144</sup>

**Scheme 53.**

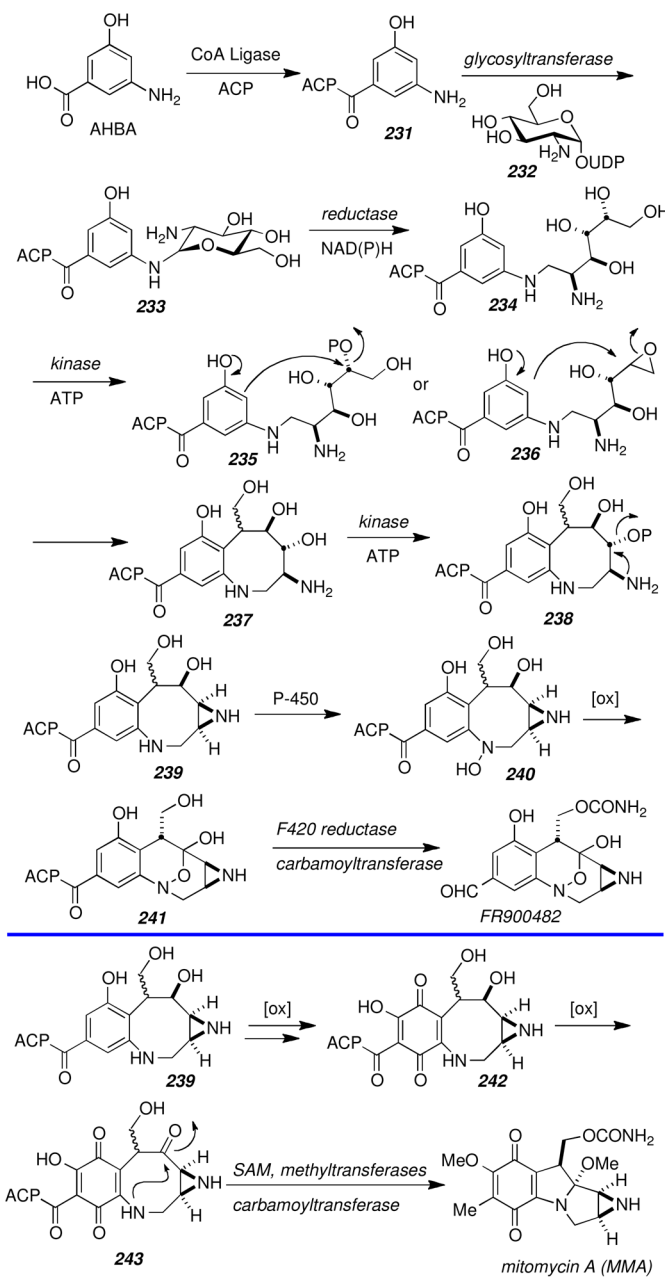
Design of a “chimeric” FR900482-pyrrolizidine alkaloid hybrid.

**Scheme 54.**

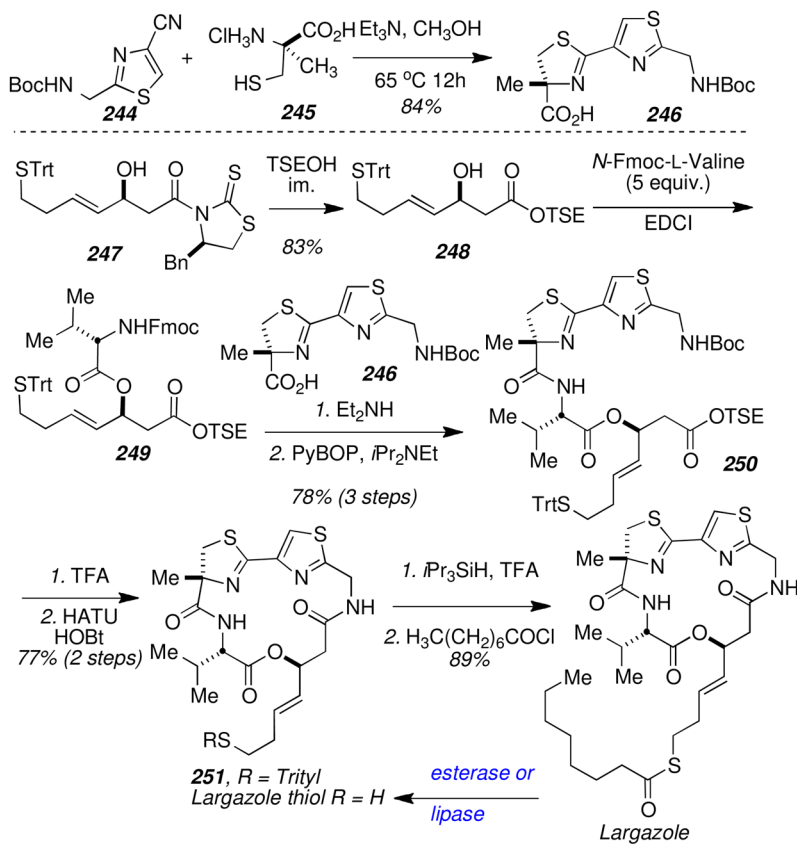
Synthesis and activation of a reductively activated pyrrolizidine alkaloid.

**Scheme 55.**

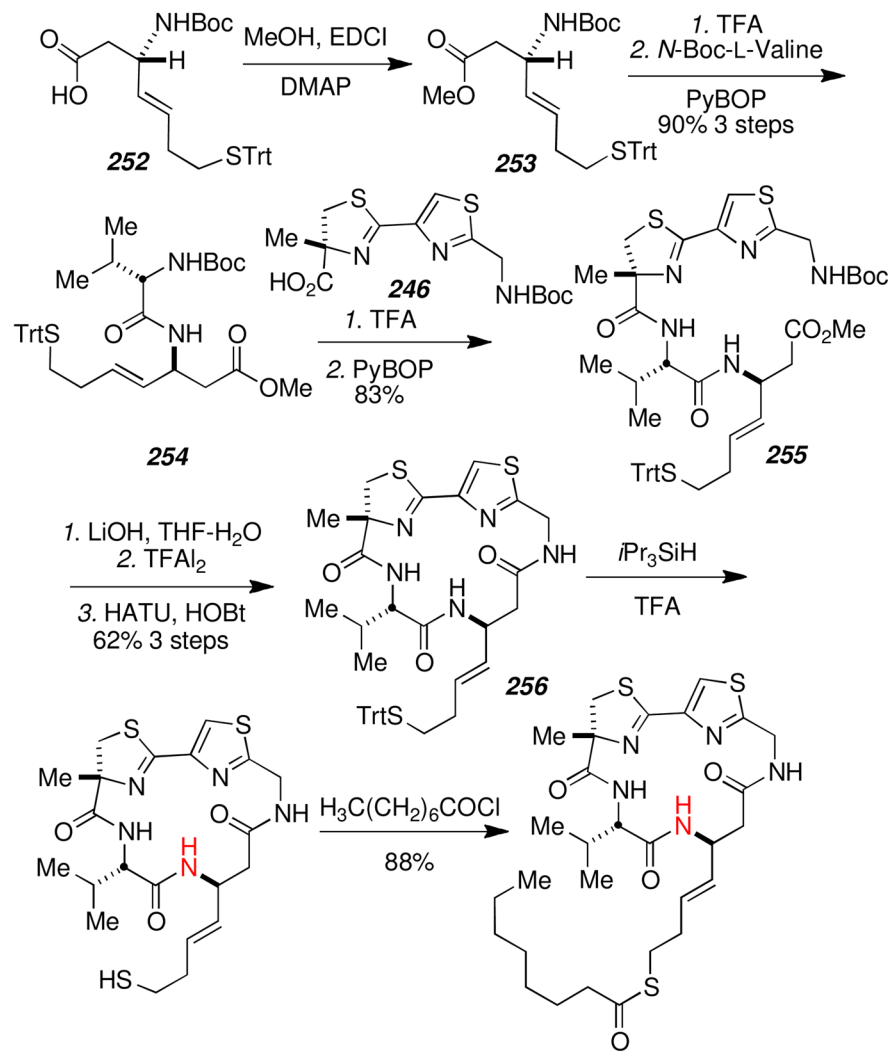
The first photolabile progenitor of dehydromonocrotaline.



**Scheme 56.**  
Proposed unified biogenesis of FR900482 and MMC.



**Scheme 57.**  
Total synthesis of largazole.<sup>169</sup>



**257, largazole peptide isostere thiol      258, largazole peptide isostere**

**Scheme 58.**  
Synthesis of the largazole peptide isostere.

**Table 1**

Calculated potential energy barriers and relative energies (kcal/mol) fro TSA, TSB, TSA' and TSB'.<sup>19</sup>

	3-21G/3-21G		6-31G*/3-21G	
	$\Delta E_a$	$\Delta E_{rel}$	$\Delta E_a$	$\Delta E_{rel}$
TSA	31.81	0.00	38.68	0.00
TSB	39.42	7.61	45.03	6.35
TSA'	44.17	12.36	49.71	11.02
TSB'	47.07	15.26	51.41	12.73

**Table 2**

Modes of reactivity and classes of amino acids

Mode of Reactivity	Classes of Amino Acids
<i>Electrophilic Glycinate</i>	simple aliphatic $\alpha$ -amino acids $\gamma$ $\delta$ -unsaturated $\alpha$ -amino acids <i>E</i> - $\beta$ , $\gamma$ -unsaturated $\alpha$ -amino acids arylglycines biarylglycines
<i>Glycine Enolate</i>	simple aliphatic $\alpha$ -amino acids $\alpha$ $\alpha$ -disubstituted $\alpha$ -amino acids $\gamma$ $\gamma$ -unsaturated $\alpha$ -amino acids 2,6-diaminopimelic acids cyclic amino acids <i>anti</i> - $\beta$ -hydroxy $\alpha$ -amino acids <i>syn</i> - $\beta$ -amino $\alpha$ -amino acids
<i>Azomethine Ylide</i>	di- and tri-substituted pyrrolidine carboxylic acids
$\alpha$ $\beta$ - <i>Dehydro/phosphonate</i>	<i>E</i> -1-aminocyclopropanecarboxylic acids
$\alpha$ $\beta$ - <i>Dehydro</i>	pyrrolidine-2-amino-2-carboxylic acids cyclohexenyl-4-amino-4-carboxylic acids
<i>C-1 Oxocarbenium ion</i>	peptide isosteres

**Table 3**

## Antiproliferative activities

compound	Cell Line	
	A549	HCT-116
3- <i>epi</i> -jorumycin	4.64	0.61
(−)-jorumycin	0.02	0.002
3- <i>epi</i> -renieramycin G	10.1	1.4
(−)-renieramycin G	12.9	3.87

<sup>a</sup>Values reported are GI<sub>50</sub> in μM

**Table 4**HDAC inhibitory activity ( $IC_{50}$ ; nM)

Compound	HDAC1	HDAC2	HDAC3	HDAC6
FK228	0.2	1	3	200
FK228 isostere	10	80	70	>3000
Largazole thiol	0.1	0.8	1	40
Largazole isostere thiol	0.9	4	4	1500
Largazole isostere	>3000	>3000	>3000	>3000
SAHA	10	40	30	30